

**Understory Transpiration Rates Following Stand Density Reduction  
in a Coast Redwood Forest**

A Thesis

SUBMITTED TO THE FACULTY OF THE UNIVERSITY OF  
MINNESOTA BY

**Shelby Hammerschmidt**

IN PARTIAL FULFILLMENT OF THE REQUIREMENTS FOR THE  
DEGREE OF  
MASTER OF WATER RESOURCES SCIENCE

Dr. Salli Dymond

August, 2020

Copyright © 2020

Shelby Hammerschmidt

## **Acknowledgements**

First and foremost, I would like to thank my advisor, Dr. Salli Dymond. Salli, thank you for pushing me to grow as a scientist while always being understanding and patient. The climate you've created in your lab is so supportive and wonderful, and I have learned so much from you.

Thank you to the National Science Foundation, CAL FIRE, and to the Forest Service for funding this research. I would also like to gratefully acknowledge the support I've received from the Fort Bragg CAL FIRE and Forest Service, both in the field and in my research. Thank you to Liz Keppeler and Lynn Webb, for taking me under your wing while I was in Fort Bragg, lending a helping hand when needed, and for providing me a home at the JDSF Forest Learning Center.

I would like to thank my committee members, Dr. Xue Feng and Dr. Jessica Savage, whose knowledge was invaluable in my experimental design and literature search. I would also like to thank Dr. Tedy Ozersky, whose statistics and R expertise helped me out of many slumps.

Thank you to the Department of Earth and Environmental Sciences and the Water Resources Program for funding, facilities, and for the incredible opportunities during my time as a graduate student.

To my fellow WaTER lab members: Emma Burgeson, Hannah Behar, Julia Petreshen, Mitch Ihllang, and Erin Bergen, thank you for your constant emotional support, your proofreading, and your consultation. A special thanks is in order to Julia, for being the best fieldwork partner I could ask for and for being by my side through many a crisis.

I have been blessed with the most wonderful friends, who during my time as a graduate student have provided me with housing, quiet company while I write, an audience for practice presentations, and an escape during difficult days. Pavana Reddy said “somedays I am the flower, somedays I am the rain.” Over the past two years, my family and friends have graciously been the rain. Thank you to my fiancé Andrew, for letting me be the flower even though you’ve had a full plate of your own. Thank you for believing in me, encouraging me, and being my person. Thank you to my mom for being such a huge support, even from 4 hours away, and for encouraging my sense of adventure. And thank you to my brother and sisters, who believe in me more than anyone I know.

## **Dedication**

For my dad, whose love and respect of nature inspired mine.

## ABSTRACT

In forests where the overstory canopy has been disturbed, evapotranspiration (ET) by the understory may be the main flux of water back to the atmosphere. The ability to take field measurements of water use by understory plants, therefore, is vital for a complete ecosystem water budget. However, little research has been apportioned to directly measuring understory water use, and the technology to do so is thus limited. Portable ET chambers have been used to measure ET rates in agricultural fields, grasslands, and deserts, but not in a forest understory. Thus, a portable rapid chamber which can be easily deployed and collect quick ET measurements of single plants was developed for measuring understory plant water use in logged watersheds in coastal California. Mean understory ET rate was highest in the watershed with the lowest residual basal area ( $\mu = 87 \pm 56$  mm/day) and lowest in the control watershed ( $\mu = 31 \pm 19$  mm/day). Multiple regression modeling indicates that the difference in ET rate between watersheds is caused by freed soil water as a result of overstory tree removal. These results imply that understory water use is likely significant in harvested watersheds, and should be quantified at the landscape scale.

# Table of Contents

<b>ABSTRACT .....</b>	<b>IV</b>
<b>LIST OF TABLES .....</b>	<b>VII</b>
<b>LIST OF FIGURES .....</b>	<b>VIII</b>
<b>LIST OF ABBREVIATIONS.....</b>	<b>IX</b>
<b>INTRODUCTION .....</b>	<b>1</b>
<b>BACKGROUND.....</b>	<b>3</b>
<b>EVAPOTRANSPIRATION.....</b>	<b>3</b>
<i>Evapotranspiration Models .....</i>	<i>7</i>
<i>Lysimeters .....</i>	<i>8</i>
<i>Sap Flow .....</i>	<i>9</i>
<i>Eddy Covariance .....</i>	<i>10</i>
<i>Transpiration Chambers.....</i>	<i>12</i>
<b>PLANT WATER RELATIONS IN COAST REDWOOD FORESTS .....</b>	<b>15</b>
<b>HYDROLOGICAL AND ECOLOGICAL IMPACTS OF DISTURBANCE.....</b>	<b>18</b>
<b>CALIFORNIA FOREST PRACTICE ACT AND RIPARIAN ZONE PROTECTION .....</b>	<b>24</b>
<b>WATER SOURCE APPORTIONMENT .....</b>	<b>ERROR! BOOKMARK NOT DEFINED.</b>
<b>SITE DESCRIPTION .....</b>	<b>28</b>
<b>METHODS.....</b>	<b>34</b>
<b>FIELD PROCEDURES .....</b>	<b>34</b>
<i>Sampling Scheme .....</i>	<i>34</i>
<i>Evapotranspiration Measurements.....</i>	<i>35</i>
<i>Effect of Chamber on Light Intensity.....</i>	<i>39</i>
<b>DATA ANALYSIS .....</b>	<b>40</b>
<i>Diversity, Richness, and Evenness.....</i>	<i>40</i>

<i>Evapotranspiration Calculations</i> .....	41
<i>Measuring Plant Leaf Area and Biomass</i> .....	42
<i>Evapotranspiration Rate Statistics</i> .....	44
<i>Multiple Regression Models</i> .....	45
<b>RESULTS</b> .....	<b>49</b>
<i>Watershed Vegetation</i> .....	49
<i>Basal Area Reduction by Plot</i> .....	52
<i>Evapotranspiration Rate by Watershed</i> .....	54
<i>Evapotranspiration Rate as a Function of Basal Area</i> .....	56
<i>Variation in Evapotranspiration Rate along the Hillslope</i> .....	58
<i>Environmental Controls on Evapotranspiration</i> .....	63
<i>Multiple Regression Models</i> .....	68
<b>DISCUSSION</b> .....	<b>78</b>
<i>Evapotranspiration Rate Across Watersheds</i> .....	80
<i>Topography, Basal Area, and Soil Water Relations</i> .....	82
<i>Environmental and Climactic Controls on Evapotranspiration</i> .....	84
<i>Density and Diversity</i> .....	88
<b>CONCLUSION</b> .....	<b>88</b>
<b>BIBLIOGRAPHY</b> .....	<b>90</b>
<b>APPENDIX A: COMMON AND SCIENTIFIC SPECIES NAMES</b> .....	<b>100</b>
<b>APPENDIX B: SUPPLEMENTAL TABLES</b> .....	<b>101</b>



## LIST OF TABLES

Table 1: Elevation, aspect, and Slope of Study Plots _____	33
Table 2: Regression Equations for Calculating Fern Biomass by Species _____	44
Table 3: Variables Considered in Full Model _____	47
Table 4: Diversity of Understory Vegetation by Watershed _____	50
Table 5: Basal Area of Plots Before and After Harvesting _____	52
Table 6: Mean ET Rate of Understory Vegetation by Watershed _____	56
Table 7: Mean and Standard Deviation of ET Rate by Topographic Position _____	60
Table 8: Mean ET Rate at Each Plot by Sampling Period _____	63
Table 9: Mean Light Intensity by Month and Watershed _____	64
Table 10: Mean Light Intensity of Plots by Month _____	64
Table 11: Mean Soil VWC (%) by Plot _____	66
Table 12: Percent Change in ET Rate, VWC, and LI from June to July _____	67
Table 13: Best-Approximating Model Intercepts for each Sprout Species _____	69
Table 14: Variables that were Significantly Correlated with Sprout Evapotranspiration Rate within each Watershed _____	69
Table 15: Best-Approximating Models for Sprout Evapotranspiration Rate by Watershed _____	72
Table 16: Variables that were Significantly Correlated with Fern Evapotranspiration Rate within each Watershed _____	75
Table 17: Best-Approximating Models for Fern Evapotranspiration Rate by Watershed _____	75

## LIST OF FIGURES

Figure 1: Images of Stump-Sprouting Vegetation _____	23
Figure 2: Caspar Creek Experimental Watershed Map _____	29
Figure 3: Map of Watersheds and Study Sites _____	31
Figure 4: Schematic Showing Topographic Positioning of Study Plots _____	32
Figure 5: Layout of Study Plots _____	35
Figure 6: Schematic of Chamber Setup with Sensors and Fans _____	36
Figure 7: Example Time Series Produced by ET Chamber Measurement _____	37
Figure 8: Species Richness and Stem Density of Understory Vegetation by Watershed	50
Figure 9: Number of Individuals of Each Understory Species by Watershed _____	51
Figure 10: Mean Residual Basal Area by Topographic Position Across all Four Watersheds _____	53
Figure 11: Boxplot of Understory Plant ET Rates by (A) Watershed and (B) Sampling Period _____	55
Figure 12: ET Rate vs. Basal Area Reduction _____	57
Figure 13: ET Rate vs. Residual Basal Area With Regression Line _____	58
Figure 14: Boxplot of ET Rate by Topographic Position _____	59
Figure 15: ET Rate of Understory Vegetation by Plot for June, July, and for All Data _	61
Figure 16: ET Rate vs. Light Intensity by Watershed _____	65
Figure 17: ET rate vs VWC by Watershed _____	67
Figure 18: Marginal Effects of Several Predictor Variables on Sprout ET Rate _____	71
Figure 19: Marginal Effects of Several Predictor Variables on Fern ET Rate _____	77

## LIST OF ABBREVIATIONS

<b>Abbreviation</b>	<b>Definition</b>
AET	Actual Evapotranspiration
AIC	Akaike Information Criterion
ANOVA	Analysis of Variance
BA	Basal Area
BMP	Best Management Practices
CAL FIRE	California Division of Forestry and Fire Protection
CI	Confidence Interval
DBH	Diameter at Breast Height
DF	Degrees of Freedom
DPS	Distinct Population Segment
EL	Elevation
ESA	Endangered Species Act
ESU	Ecological Significance Unit
ET	Evapotranspiration
FPA	Forest Practice Act
FPR	Forest Practice Rules
GMWL	Global Meteoric Water Line
HSD	Honestly Significant Difference
LA	Leaf Area
LAF	Average Frond Length
LI	Light Intensity
NFR	Number of Fronds
PH	Percent Harvest (Reduction in Basal Area)
PET	Potential Evapotranspiration
PSW	Pacific Southwest Research Station
RH	Relative Humidity
SD	Standard Deviation
SP	Species

SSE	Sum of Squares Error
SSR	Sum of Squares Regression
SST	Sum of Squares Total
T	Temperature
TMDL	Total Maximum Daily Load
TO	
TRE	Treat Watershed - 35% Harvest
UQL	Uqlidisi Watershed - 55% Harvest
USDA	United States Department of Agriculture
USFS	United States Department of Agriculture Forest Service
USGS	United States Geological Survey
VIF	Variance Inflation Factor
VPD	Vapor Pressure Deficit
VWC	Volumetric Water Content
WIL	Williams Watershed - Control
WLPZ	Watercourse and Lake Protection Zones
ZIE	Ziemer Watershed - 75% Harvest

## INTRODUCTION

A significant proportion of precipitation falling on natural watersheds is returned to the atmosphere via plant transpiration and evaporation from the surface of leaves (Jasechko *et al.*, 2013). Decades of paired watershed studies have shown us that removing vegetation via timber harvesting causes significant changes in the hydrology of a forested watershed, especially by increasing streamflow (Stednick, 1996). Since the first official paired watershed study in 1909 (Bates and Henry, 1928), the effects of overstory tree removal on various ecological, biogeochemical, geological, and hydrological processes have been well studied. One topic that has lacked much attention, however, is the effect of overstory harvest on the forest understory. Evapotranspiration (ET) by the understory may be a significant component of the hydrologic budget, especially in forests where the overstory canopy has been disturbed (Greenwood *et al.*, 1985; Kelliher *et al.*, 1990; Köstner, 2001; Delzon and Loustau, 2005). The ability to take field measurements of water use by understory plants, therefore, is vital for a complete ecosystem water budget. Studies have shown that removing the understory but leaving the overstory intact is sufficient to significantly increase streamflow (Johnson and Kovner, 1956) or increase overstory ET rates (Kelliher *et al.*, 1986). Other studies have measured understory water use in an undisturbed forest and speculated that increased ET from the understory may counteract decreased ET from the overstory as a result of timber harvesting (Greenwood *et al.*, 1985). However, very few studies have attempted to quantify understory ET after overstory harvest or along a range of thinning treatments. Furthermore, since little research has been apportioned to directly measuring understory water use, the technology to do so is limited. Portable ET chambers have been used to

measure ET rates in agricultural fields, grasslands, and deserts, but not in a forest understory. Thus, a portable, rapid chamber which can be easily deployed and collect quick ET measurements of single plants was developed for measuring understory plant water use in logged watersheds in coastal California.

This study was conducted at the USDA Forest Service (USFS) Caspar Creek Experimental Watersheds in tandem with a large forest harvesting experiment. Several small watersheds within the South Fork Caspar Creek watershed have been harvested to varying degrees of intensity. This provides the USFS and the California Department of Forestry and Fire Protection (CAL FIRE) with the unique opportunity to observe the threshold at which harvesting impacts forest regeneration, streamflow, sediment yield, and water source partitioning. This study takes advantage of ongoing research in the South Fork Caspar Creek experimental watershed by utilizing pre-established study plots in order to investigate the effects of stand basal area reduction on understory water use, which is to be measured using a homemade, portable ET chamber. Additionally, the effect of climactic variables on ET rate and their variation across watersheds were investigated using multiple regression modeling. Understory water use is likely to be greater in watersheds with a greater reduction in overstory basal area due to decreased competition and increased availability of energy and water.

## **BACKGROUND**

### **EVAPOTRANSPIRATION**

In order to facilitate photosynthetic gas exchange, plants must open pores on leaf cell surfaces, called stomata. Stomatal aperture is necessary for carbon capture, but comes at the cost of water loss via evapotranspiration (ET). ET is defined as the combined processes of water loss by plant transpiration and evaporation from plant and soil surfaces (Kramer and Boyer, 1995). Transpiration is the movement of liquid water from the plant roots to the leaf cells and through the stomata, which is driven by a negative water potential gradient between plant cells and the air. When water is transpired through the stomata, cohesion between water molecules causes a continuous pull of water up through the xylem and into plant leaves via capillary action. Water on the leaf surface then evaporates if the vapor pressure in the air is lower than the vapor pressure in the leaf. This difference in vapor pressure is termed the vapor pressure deficit (VPD). Since water potential and vapor pressure are typically lower in the air than in plant cells, water tends to move unidirectionally from roots to leaves to the atmosphere.

Transpiration is regulated by resistances and conductances along the pathway from the soil to the atmosphere (Kramer and Boyer, 1995). In the canopy, transpiration is controlled by leaf area, leaf cuticle, and stomatal characteristics. Stomatal density and size (Meinzer *et al.*, 1995; Ewers *et al.*, 2005; Daley and Phillips, 2006), leaf characteristics (Scott, 1966; Norris and Bukovak, 1968; Schönherr and Schmidt, 1979; Meinzer *et al.*, 1995), and sensitivity to hormones which increase stomatal aperture (Little and Eidt, 1968; Farber, Attia and Weiss, 2016) may vary from species to species, as can other strategies which help to maximize carbon uptake while minimizing water

loss. In general, stomatal aperture increases in high light, warm temperatures, and low VPD. In turn, these environmental controls on transpiration may be influenced by wind, aspect, weather, time of day, and elevation.

Light is needed for photoreactions in the plant, which draw water to the leaves, as well as to drive evaporation from plant surfaces. This response is not linear – the rate of transpiration in response to light decreases when the stomata are fully open (Taiz and Zeiger, 2002). In excessively high light, plants are unable to convert all incoming radiation into usable energy, and free electrons create harmful reactive oxygen compounds which damage plant cells via oxidation (Taiz and Zeiger, 2002). Similarly, temperature is positively correlated with transpiration at low temperatures, but as it does with light, levels off when another factor becomes limiting (Taiz and Zeiger, 2002). Transpiration helps keep plant surfaces cool at high temperatures. However, if a plant is stressed for water, high temperatures may decrease stomatal aperture to prevent excessive water loss (Schulze *et al.*, 1973). Finally, a vapor pressure deficit is needed to pull water from the soil to the leaves. However, stomatal aperture may decrease to conserve water if VPD is too high. *S. sempervirens* relies on coastal fog to suppress transpiration and supplement moisture input during the dry months of summer (Dawson, 1998; Burgess and Dawson, 2004; Limm *et al.*, 2009; Simonin, Santiago and Dawson, 2009). It has been suggested that the shape and arrangement of redwood needles are specialized to maximize fog water interception (Dawson, 1998; Simonin, Santiago and Dawson, 2009).

In the stem, transpiration is regulated by plant hydraulics and water availability. Water moves from the roots to the leaves through the xylem tissue, which consists of



cells called tracheary elements that are specialized for water transport (Taiz and Zeiger, 2002). Maximum hydraulic conductance, or the maximum bulk flow of water through the xylem, is dictated by the size of the tracheary elements. However, dry soil may limit water transport to less than its maximum conductance. Soil water may be further influenced by slope, aspect, and soil properties.

When water stress is too high, vapor bubbles can interrupt water transport by forming embolisms in the tracheary elements in a process known as cavitation (Holbrook and Zwieniecki, 2005). Tracheary elements often have a pitted texture to help prevent embolism formation (Holbrook and Zwieniecki, 2005). Xylem morphology, including pit structure and element size, vary by species (Heath, Kerstiens and Tyree, 1997; Ewers *et al.*, 2002). Some species prioritize protection by housing smaller tracheary elements that are less prone to cavitation, while others have large tracheary elements that can transport a larger volume of water (Holbrook and Zwieniecki, 2005). If an embolism is severe enough, it may stop transport through an entire column of tracheary elements (Holbrook and Zwieniecki, 2005). Thus, hydraulic conductance may decrease as an individual plant ages.

A decline in water use with age has also been observed at the stand scale as a result of declining leaf area and hydraulic conductance (Vertessy, Watson and O'Sullivan, 2001; Delzon and Loustau, 2005; Ewers *et al.*, 2005). Delzon and Loustau (2005) observed an age-related decrease in transpiration per unit leaf area in maritime pine (*Pinus pinaster*) stands of south-western France. However, total stand ET, as calculated using a water-balance approach, was not different between stand ages. This led the authors to speculate that the ratio of understory transpiration to overstory transpiration

was higher in the older stands. In the 32 year old stand, they estimated that overstory transpiration accounted for about half of total stand transpiration.

While research generally agrees with the idea that transpiration is an important component of the hydrologic budget, few studies partition ET into its components. Canopy and subcanopy transpiration are usually lumped together, or subcanopy transpiration is neglected altogether. Though the ET rate of a shrub may be very low in comparison to a large tree, the shrub layer represents a significant fraction of basal area in many forests (Johnson and Kovner, 1956; Greenwood *et al.*, 1985). Thus, any model of total forest ET that includes only overstory trees as a factor will be an underestimate. This is especially important to consider in forests that have been recently disturbed by a fire or logging, when the understory may be the main flux of water back to the atmosphere. Partitioning ET into canopy and subcanopy components allows for the prediction of changing water fluxes before harvesting.

The complex and varied mechanisms controlling ET make it impossible to precisely measure for a community. For this reason, models are widely used for estimating ET at a landscape scale. Of the experimental methods, those available for measuring transpiration rates in situ are limited and many are specialized for use in crop fields. Some of the most common experimental methods are lysimeters, eddy covariance, sap flow and transpiration chambers. These techniques vary considerably in their applicability, and one must consider both scale and landscape when determining which method is appropriate. Research on models and experimental methods is ongoing in plant physiology, agriculture, and hydrology.

### ***Evapotranspiration Models***

Current models for estimating ET at the watershed scale are based on theory of (1) mass transfer, (2) energy balance, (3) empirical relationship to measured data, or (4) a combination of these. There are many models available, including Blaney and Criddle (1942), Penman-Monteith FAO 56 (1998), ASCE standardized Penman-Monteith (2005), Priestley and Taylor (1972), Thornthwaite (1948) and Hargreaves-Samani 1985. The Penman-Monteith method has been shown to estimate ET to a similar degree of accuracy as a weighing lysimeter (Van Zyl and De Jager, 1987). It is thus used frequently as a standard method for estimation of ET and for validation of other models (Mohan *et al.*, 1996; Allen, Pereira and Smith, 1998).

The most common modeling approach, developed by Penman in 1948, is to calculate potential evapotranspiration (PET) of a system based on vegetation and climate conditions. PET is calculated by assuming an unlimited supply of water. Thus, the model must scale PET to estimated actual ET based on available soil water. PET may be calculated based on ET by a reference crop such as alfalfa or grass (reference-surface ET) or a specific land surface (surface-dependent ET).

Many of these models were developed for application to crop fields, but some may be modified for forests. For example, a 2005 study compared several common ET models, including those by Shuttleworth and Wallace (1985), Penman and Monteith (1965), Priestley and Taylor (1972), McNaughton and Black (1973), and Penman (1948) for estimation of PET in a coniferous forest plantation in the Sierra Nevada mountains (Fisher *et al.*). The authors found that a modification of Priestley and Taylor combined

with a soil moisture function produced an estimation for canopy AET similar to that measured by eddy covariance.

While these models may be useful for predicting whole stand ET, they do not allow for partitioning of ET into canopy and subcanopy components without additional field measurements. Furthermore, forests exhibit more species and topographic heterogeneity than crop fields.

### ***Lysimeters***

Lysimeters are most commonly in agricultural studies. The first was developed by Edward Lewis Sturtevant in 1875 for the purpose of measuring water percolation in crop fields. Modern lysimeters fall into two categories: weighing and non-weighing, both of which can measure water balance at the plant scale. Non-weighing lysimeters measure loss of water by either maintaining a constant water table or measuring soil water content with sensors. Weighing lysimeters constantly measure mass of the system to calculate the loss of water by weight (Slavik, 1974). The weighing type is more accurate, and for this reason is more frequently used both as an experimental method and as a validation technique for models or emerging methods (Reicosky *et al.*, 1983; Wegehenkel and Gerke, 2013; Liu *et al.*, 2017).

Since the lysimeter method requires plants to be contained within a vessel of constant volume or a container that can be weighed, it cannot be used for observational *in situ* measurements of ET. Rather, lysimeters are often used to measure water use at a plant scale and extrapolate to the ecosystem level using several study plants. This is especially common in agricultural studies, where a crop may be planted in a lysimeter

and installed in a field with other row crops so that environmental conditions are consistent between the sample and the population. This has been done with cotton (Fisher, 2012), alfalfa (Reicosky *et al.*, 1983), grass and silage (Wegehenkel and Gerke, 2013; Anapalli *et al.*, 2016), soybeans (Ünlü, Kanber and Kapur, 2010), coffee (Flumignan *et al.*, 2011), corn (Anapalli *et al.*, 2016), and many other cash crops.

There have been few forest hydrology studies which measure water use using lysimeters. One study in Germany involved the installation of large scale lysimeters under the ground above which experimental stands of Scots pine, European beech, European larch, and Douglas fir were planted. The authors found significant differences in water percolation and ET between overstory stands as well as understory type (Müller and Bolte, 2009). More commonly, lysimeters have been used to analyze the chemistry of leachate from forest soils, such as in studies conducted in Finland (Starr, 1985), France (Ranger *et al.*, 2001), and Sweden (Andreasson *et al.*, 2009).

### ***Sap Flow***

Thermal methods (frequently referred to as sap flow methods) are useful for determining forest transpiration at the tree scale. This method determines the rate of flow through the xylem using heat as a tracer (Granier, 1985). In order to extrapolate to the landscape scale, strategic sampling and appropriate scaling are required.

Sap flow is good method for determining interspecies variability and can be applied to a variety of landscapes. However, it measures only transpiration rather than evapotranspiration. Furthermore, the nature of the design makes it most applicable for mature trees or large understory trees and not for herbs, shrubby understory species, or

saplings, since the probes interrupt water transport in small stems. Most studies which attempt to measure transpiration of the overstory and understory typically account only for saplings in the understory, which they measure by scaling down from canopy trees. Thus, the sap flow method has been shown to underestimate ET from watersheds by as much as 50% compared to estimates made by catchment water budget and eddy covariance (Wilson *et al.*, 2001). Sap flow may be used in conjunction with eddy covariance or watershed budgets, however, in order to partition the water budget into components of a forest stand (Oren *et al.*, 1998).

### ***Eddy Covariance***

Eddy covariance is a method which calculates vertical flux of gas, heat, or water within atmospheric boundary layers based on the assumption of turbulent transport (Burba and Anderson, 2007). A tower which measures gas or vapor concentration, temperature, and wind speed of vertical eddies is needed. One can then calculate vertical flux of a variable of interest with the help of statistical software. Eddy covariance has been shown to produce reliable data when its corresponding assumptions are met; for this reason, it is often used as a method to assess the quality of models (Medlyn *et al.*, 2005; Gharsallah, Facchi and Gandolfi, 2013; Wang *et al.*, 2018).

The eddy covariance technique has several assumptions: vertical transfer is via turbulent flow, terrain is uniform and horizontal, the tower is downwind of the study area, and fluctuations in air density and flow are negligible. Furthermore, one must ensure that the footprint of the tower is big enough to capture the study area, monitoring equipment

is placed in the boundary layer of interest, and that sensors are precise enough to detect small atmospheric changes (Burba and Anderson, 2007).

Because of the complexity of these assumptions, eddy covariance has been primarily applied to agricultural studies. Like lysimeters, eddy covariance has been used to measure ET and crop coefficients for a multitude of cash crops, including potatoes (Parent and Anctil, 2012), soybeans (Anapalli *et al.*, 2018), maize (Li *et al.*, 2008), and cotton (Yang *et al.*, 2016). However, it has also been applied with some success to forested stands. In Japan, an eddy covariance tower was used to measure CO<sub>2</sub> flux from a cool-temperate deciduous forest in order to calculate gross primary production and net ecosystem exchange (Saigusa *et al.*, 2002). Eddy covariance has also been used to measure fluxes of water vapor, CO<sub>2</sub>, and sensible heat from a grassland, aspen forest, and Douglas-fir forest to compare water use efficiency across ecosystems (Ponton *et al.*, 2006). A positive to this method is that it accounts for total forest evapotranspiration rather than just the canopy. However, it is difficult with eddy covariance to partition ET into components of the forest water budget without further instrumentation. Furthermore, assumptions of uniform and horizontal terrain are violated in steep forested watersheds, such as the one in this study. For example, one study measured ET rate using the eddy covariance method and compared to rates calculated from watershed water balances for savanna, grassland, and shrubland ecosystems (Scott, 2010). The two methods produced similar results at the savanna and shrubland site, but not the grassland, which had greater topographic relief than the other sites.

### ***Transpiration Chambers***

The term “transpiration chamber” in this section encompasses any apparatus enclosing one or many plants for the purpose of measuring gas exchange. Chambers have been used for measuring ET as early as the 1960s and can be specialized for either long-term, continuous measurements or short-term, instantaneous measurements.

Permanent or semi-permanent chambers are designed to make continuous measurements of individual plants or plant communities by measuring relative humidity or vapor pressure concentrations within the chamber (Slavik, 1974). Similar chambers may be used to measure CO<sub>2</sub> exchange. The system may be closed, semi-closed, or open (Slavik, 1974). In a closed system, the air stream circulates through an airtight chamber and the rate of increase of absolute humidity is measured. The increase in water vapor is rapid, making ET difficult to quantify. For this reason, closed chambers are rarely used for continuous measurements (Slavik, 1974). Semi-closed systems are frequently used for measuring CO<sub>2</sub> exchange but not as frequently for measuring ET as they would require a perfect air-tight seal (Slavik, 1974). In an open system, the relative humidity of a unidirectional air stream is analyzed as it enters and leaves the chamber. This method is most commonly used owing to its insensitivity to air leakage (Slavik, 1974). However, air flow rate must be accurately measured to obtain an accurate estimate of ET. This design allows for control of the temperature and air humidity entering the chamber. There is some evidence, however, that the internal fans may not provide adequate mixing to capture true gas exchange rates at the outflow (Slavik, 1974). Furthermore, portability of these systems is limited due to their requirement of additional equipment to condition the air entering the chamber so that it corresponds to ambient conditions.



Transpiration chambers, open or closed, have been shown to alter the microclimate within the chamber (Bosian, 1962). These systems may alter the natural wind patterns, light availability, and temperature around the vegetation being measured, all of which influence ET (Greenwood and Beresford, 1979; Leuning and Foster, 1990; Denmead *et al.*, 1993; Sharma, 1985). Wind may increase evaporation from the leaf surface by disrupting the boundary layer and reducing humidity and vapor pressure at the leaf-atmosphere interface (Kramer and Boyer, 1995). ET decreases as relative humidity and vapor pressure increase, as the air around the plant loses its ability to hold any more water (Kramer and Boyer, 1995). Light and temperature influence photosynthesis and stomatal aperture or closure; low light decreases photosynthesis rates, while high light and temperature decreases photosynthetic efficiency and may result in stomatal closure as a protective measure (Kramer and Boyer, 1995).

Short-term chambers (also called instantaneous or rapid chambers) still face the challenge of altering natural climate conditions, but their quick operation time minimizes the interruption in the plant's microclimate (Reicosky and Peters, 1977; Reicosky *et al.*, 1983; Stannard, 1988). Short-term chambers also often have the advantage of being lightweight and portable, making them ideal for use in the field. Furthermore, they can be made using inexpensive materials (Stannard, 1988). Like long-term chambers, these systems may be open or closed, but are frequently closed for increased portability. The method is also similar to long-term chambers in that a relative humidity or vapor pressure sensor is used to measure the increase in water vapor in the chamber over time.

Short-term chambers have most commonly been used to measure crop transpiration (Reicosky and Peters, 1977; Reicosky *et al.*, 1983; Luo *et al.*, 2018),

chaparral vegetation (Grieve and Went, 1962), prairie grasses (Luo *et al.*, 2018), and desert shrubs (Stannard and Wertz, 2006; Garcia *et al.*, 2008). One study comparing ET rates of alfalfa as measured by a weighing lysimeter and portable chamber found that the values were similar and concluded that the portable chamber method was appropriate for use on agricultural plots (Reicosky *et al.*, 1983). Similarly, a 2018 study which measured ET rates in plots of soybeans, corn, and reconstructed prairie found that ET rates measured with a portable chamber were within 5% and 10% of those calculated using eddy covariance and watershed balance, respectively (Luo *et al.*, 2018). The short-term chamber methodology has been applied less frequently to forests. Short-term chambers have been used to estimate ET from the understory of a Jarrah forest in Australia (Greenwood *et al.*, 1985). Similarly, Vincke *et al.* (2005) used a short-term chamber to measure ET from the forest floor in a *Quercus robur* (L.) stand.

Though there is no widely used or accepted method for measuring understory ET rates, chambers remain the most practical and accessible way to make direct measurements *in situ*. Although an instantaneous measurement does not capture long term or seasonal trends in ET, measurements can be repeated across time. A rapid portable chamber was also used by the U.S. Geological Survey (USGS) to make ET measurements of desert shrubs in Nevada (Garcia *et al.*, 2008). In this study, ET measurements were taken hourly for several plant species in order to quantify diurnal variation. They found shrub transpiration rates ranging from about 1 to 20 mm per day. The theory and design of their chamber, described in detail by Stannard (1998), is the inspiration for the chamber used in this study.

## PLANT WATER RELATIONS IN COAST REDWOOD FORESTS

Coast redwood is a high-demand tree timber species due to its great size and attractive, rot-resistant wood. Redwood also demonstrates incredible resiliency and quick regeneration after disturbance, including landslides, flooding, fires, and logging (O'Hara *et al.*, 2017). Redwoods are specialized to survive alongside a natural fire regime. Their thick bark and non-flammable sap make them extremely fire tolerant, even to fires that are severe enough to wipe out cohabiting conifer species. Furthermore, redwoods can sprout rapidly from lignotubers after fires, giving them a competitive advantage over other tree species under moderate fire intensity and frequency (Ramage *et al.*, 2010). It has been suggested that redwoods may even be dependent on fires for seedling development. In the absence of an established fire regime or other disturbance, redwood regeneration is slow (Lorimer *et al.*, 2009; Ramage, O'Hara and Caldwell, 2010; O'Hara *et al.*, 2017). Some ecologists have even predicted that in the absence of fire, upland stands of redwood would gradually be replaced by tanoak and competing conifer species (Stone *et al.*, 1969).

Since European settlement in the 1850s, the natural fire regime of the redwood belt has been suppressed, resulting in smaller and less frequent fires. Because of this interruption in the natural ecology of the region, many agencies and conservation groups have concluded that human management is beneficial for the health and regeneration of coast redwood stands (Hartley, 2012). Thus, California Department of Forestry and Fire Protection (CAL FIRE) now oversees 71,000 acres of forests as Demonstration State Forests for harvesting and watershed protection.

One of the greatest recent concerns in watershed management practices, especially in fire and drought prone regions of the states, is water conservation. A mature coast redwood tree may consume around 600 liters of water per day (Dawson, 1998) and precipitation is sparse in their natural habitat from May through October. Furthermore, the understory may be more resistant to soil drought than overstory species and, therefore, may contribute a higher portion to total stand ET during periods of soil drought, as demonstrated in a Douglas fir forest in Vancouver, British Columbia (Black and Kelliher, 1989). Thus, competition for water between redwoods and other species is important to consider in management practices.

Studies in various climates have shown that the understory and overstory may compete for water in forested ecosystems. A study in northeastern Oregon investigated the abiotic factors that control understory growth by reducing underground biomass (via trenching to sever roots) and aboveground biomass (via commercial thinning) of Ponderosa pine (Riegel *et al.*, 1992). The study demonstrated that commercial thinning significantly increased photosynthetically available radiation but did not increase understory biomass. Reducing underground root competition for soil water, however, significantly increased understory biomass. Soil water, therefore, was the main factor controlling the productivity of understory vegetation. In Switzerland, removal of the understory in a Scots pine forest increased soil water content, annual radial growth of scots pine trees, sap flow, and vitality of shoots as well as reducing decreasing tree water deficit (Giuggiola *et al.*, 2018). Water was clearly the factor limiting Scots pine growth, as removing the understory did not alter light conditions of the canopy. Competition for water between the overstory and understory in the Pacific northwest has also been

demonstrated in an Oregon juniper woodland (Mollnau, Newton and Stringham, 2014), Oregon Ponderosa pine forest (Barrett and Youngberg, 1965), and Ponderosa and Jeffrey pine forest in California (Gordon, 1962).

Literature regarding competition between coast redwood and understory vegetation is somewhat sparse, even though water resources may be particularly stressed in coast redwood stands. *S. sempervirens* is a relatively shallow rooted tree, despite its ability to grow to record-setting heights. Rather than sending roots deep into the soil, redwoods concentrate their biomass aboveground, and interlock their roots with neighboring trees to stay upright (Olson *et al.*, 1990). This means that they must compete for soil water with herbs and other shallow-rooted woody species. One adaptation that *S. sempervirens* has gained in response to water stress is the ability to utilize coastal fog as a water resource. Uptake of fog water by redwood trees may occur either via foliar uptake, in which water is absorbed directly into their foliage, or via fog drip, in which fog water is taken up from the soil after entering the matrix by means of throughfall or stemflow (Dawson, 1998; Burgess and Dawson, 2004). There is also evidence of *S. sempervirens* relying on fog to suppress transpiration during the dry season and periods of drought, thereby alleviating water stress (Burgess and Dawson, 2004).

Although coast redwoods' height gives them an advantage over other species in the use of fog water, it is not the only species in the coast redwood ecosystem that exhibits foliar water uptake. For instance, eight dominant redwood forest species: western sword fern, California polypody, evergreen huckleberry, salal, tanoak, madrone, Douglas fir and coast redwood, have been shown to absorb water directly into their foliage (Limm

*et al.*, 2009). California bay and redwood sorrel, which were also included in the study, showed no evidence of foliar water uptake.

In addition to interspecies variability in foliar water uptake, there may be intraspecies variability within an ecosystem. Limm and Dawson (2010) observed variation in foliar uptake of water by western sword fern across seven sites distributed throughout the coast redwood system. They attributed this to intraspecies variation in leaf surface roughness, which may be caused by geographical variation in wind and moisture patterns. Additionally, the authors noted that ferns in central region redwood stands may benefit the most from fog inputs, as they receive less precipitation than the northern region but form a larger fern canopy than in the southern region. Since foliar uptake induces reverse sap flow in woody species, dense fern cover may redistribute or even increase fog drip input to the soil. As the frequency of both fog and precipitation events are expected to change in coming decades, it is important to understand the role each plays in the coast redwood system. Limm and Dawson (2010) note that variation in fog drip inputs and foliar water uptake may lead to local extinction of species or entire stands. Furthermore, disturbance may impact the relationships observed between the canopy, the subcanopy, and the hydrologic regime of a forest.

## **HYDROLOGICAL AND ECOLOGICAL IMPACTS OF DISTURBANCE**

The impacts of logging on the hydrology of a forested watershed have been well documented. Since the early 1900s, paired watershed studies have been conducted for the purpose of studying harvesting effects on streamflow, sediment yield, soil moisture, and stream hydrographs. Generally, one watershed is left unmanipulated as a control while

one of a similar size and location is manipulated (Stednick, 1996). As is the case with Caspar Creek, these watersheds are often complimentary forks of a higher order stream. This design allows for year-to-year variability in precipitation. The first of these studies in the U.S. was at Wagon Wheel Gap, Colorado, beginning in 1909. The study demonstrated an increase in annual water yield associated with overstory tree removal (Bates and Henry, 1928). By 1950, around 150 paired watershed studies with mostly similar results had been performed (Stednick, 1996). Many of these experiments involved clear-cutting and the majority of them reduced overstory basal area by at least 50% (Stednick, 1996). The resulting increase in streamflow can be attributed primarily to a loss of evapotranspiration and interception by trees, but is compounded by the decrease in infiltration due to heavy equipment and the construction of access roads (Grant and Jones, 1996). These impacts may be more severe during periods of low flow (Smakhtin, 2001; Price *et al.*, 2011; Surfleet and Skaugset, 2013). The negative impact of harvesting on low flow was demonstrated in a 20 year paired watershed study at Caspar Creek by Keppeler and Ziemer (1990). The study also saw an increase in annual flow as a result of selective logging, the highest of which was in the first year after harvesting.

The effects of partial cutting on streamflow are conflicting. Some studies which have investigated the effect of partial cutting (less than 30% reduction in basal area) did not observe a significant increase in streamflow (Harr, Fredriksen and Rothacher, 1979). In a 1967 review of 39 forest harvesting experiments, Hibbert observed no clear relationship between percent harvest and streamflow changes when 30 of these watersheds were plotted collectively. However, a few watersheds demonstrated a mostly linear positive relationship between reduction in forest cover and first year increase in

stream flow (Hibbert, 1967). The seemingly weaker effect of partial cutting on streamflow may likely be attributed to the remaining canopy trees and understory vegetation which may capitalize on the reduced competition for light and water. Thus, the anticipated water surplus is depleted by vegetation photosynthesizing at an accelerated rate (Kittredge, 1948).

Despite evidence that the forest understory may be an important water flux in disturbed ecosystems, ET from subcanopy vegetation is rarely quantified. However, several studies indicate that the understory contributes substantially to total forest ET in both disturbed and undisturbed forests. For instance, one study used a combination of eddy covariance, local watershed balance, and sap flow sensors to determine canopy and subcanopy ET rates in an undisturbed forest. They found that subcanopy transpiration constituted about a third of total stand ET on average (Oren *et al.*, 1998). A paired watershed study from the Coweeta Hydrologic Laboratory in the Southern Appalachians of North Carolina removed the understory of a forested headwater stream watershed but left the overstory intact (Johnson and Kovner, 1956). The dense understory consisted of mountain laurel and rosebay rhododendron, considered unimportant and troublesome competitors to valuable timber species. As a result of the experiment, water yield in the harvested watershed increased by an average of 51 mm (4%) for the first 6 years after treatment. The increase in streamflow above baseline gradually declined each year after the treatment as understory vegetation was allowed to regrow. Similarly, overstory ET rates in a Douglas fir forest increased following plot-scale removal of the salal dominated understory (Kelliher *et al.*, 1986). This increase was greatest in plots where the salal had been most dense prior to removal.



Few, if any, studies have attempted to quantify understory ET after harvest of the overstory or along a range of thinning treatments. In 1985, Greenwood *et al.* measured understory water use in an undisturbed Jarrah forest in southwestern Australia and speculated that increased ET from the understory may counteract decreased ET from the overstory as a result of timber harvesting. However, a thorough search of the available literature revealed that a study such as the one mentioned by Greenwood *et al.* has not yet been conducted.

More commonly, studies have investigated the effects of harvesting or other disturbances which cause canopy gaps on understory density or biomass, likely because it is a more easily measured metric of understory productivity. For instance, an increase in shrub cover was observed in an Oregon juniper woodland following the removal of juniper trees (Mollnau *et al.*, 2014). An analysis of pre-harvest juniper sap flow measurements and soil water data revealed that shrubs likely consumed a significant amount of the surplus soil water that resulted from the loss of ET by juniper. An increase in understory cover following thinning of cove hardwood stands was observed in western North Carolina and northern Georgia (Beck, 1983). Yanai *et al.* (1998) also measured the density of woody understory species before and after thinning of the canopy. They observed an increase in 30-90 cm stems for 3-5 years after thinning treatments. Furthermore, the number of understory stems was highest in plots with low residual density (Yanai *et al.*, 1998). Similarly, understory cover has been demonstrated in harvested stands following variable retention harvesting in a boreal mixed-wood forest in Alberta, Canada (Craig and Macdonald, 2009) and in mixed oak-hickory forests of the Missouri Ozark Highlands (Zenner *et al.*, 2006). Changes in understory cover post-

harvesting are frequently researched from the angle of competition with regenerating timber species, as the canopy is often thinned in silvicultural practices to encourage sprout growth (Graney, 1988; Mallik, 2003; Dech, Robinson and Nosko, 2008).

An increase in understory density has also been demonstrated in forest stands in which beetle-kill has reduced the density of canopy trees. A study in northern Utah observed understory growth proportional to lodgepole pine mortality following a mountain pine beetle epidemic (Stone and Wolfe, 1996). Increased cover of understory herbs has also been observed in loblolly pine stands following an epidemic of southern pine beetle (Maine and Leuschner, 1980) and in spruce-fir stands following spruce beetle infestation (Yeager and Riordan, 1953).

Disturbance of a forest ecosystem changes community structure. In the subcanopy, disturbance may increase both the density and diversity of species. The “intermediate disturbance” hypothesis, proposed by Connell (1978), states that species richness is maintained and enhanced by nonequilibria. Thus, moderate disturbance of the canopy which interrupts competitive equilibrium but allows for species to recover is most successful at increasing species diversity in the understory (Huston, 1979). Increased understory diversity has been observed in early successional forests which have lost biomass via beetle-kill (Yeager and Riordan, 1953; Stone and Wolfe, 1996), forest fires (Grandpré *et al.*, 1993; Hart and Chen, 2008), and logging (Atauri *et al.*, 2004; Hart and Chen, 2008). However, the effects of logging on understory diversity are inconsistent. A recent review found no significant trends in subcanopy richness following canopy reduction, regardless of the intensity (Duguid and Ashton, 2013).

As is the practice with many forests, coast redwood stands are thinned to promote regeneration and productivity. Studies have shown an increase in average tree size as a result of stand density reduction (Lindquist, 2007; Hara, Narayan and Cahill, 2015). Additionally, higher densities of redwood sprouts and seedlings have been observed in thinned forests (Allgood, 1996). As an adaptive strategy to the natural fire regime, coast redwood has the competitive advantage of sprouting vegetatively from lignotubers and dormant buds. Thus, redwoods may sprout from cut stumps, logs, snags, roots, and dead or live standing trees. However, cohabiting woody species in the redwood ecosystem have also evolved with this ability. Evergreen huckleberry in particular is commonly seen growing on redwood snags and stumps (Figure 1).



**Figure 1: Images of Stump-Sprouting Vegetation**

Left: Evergreen huckleberry sprouting from stump and recently cut log with redwood sprouts in Ziemer watershed of South Fork Caspar Creek. Right: Evergreen huckleberry and some herbaceous vegetation sprouting from spanner log in North Fork Caspar Creek.

While more research is needed to for the effects of harvesting on species diversity to be conclusive, it is clear that disturbance of an ecosystem influences community structure. Growth of nonnative vegetation (Bailey *et al.*, 1998; Nelson *et al.*, 2008; Sutherland and Nelson, 2010), dominance of certain species which may impact competition for resources (Allgood, 1996; Atauri *et al.*, 2004), and decline or change in understory fauna (Bury, 1983; Politi *et al.*, 2012; Arcilla *et al.*, 2015) are of concern. The importance of studying and implementing ecologically sound forest management practices is increasing as the changing climate catalyzes forest dieback and shifts in species distribution (Allen *et al.*, 2010; Reichstein *et al.*, 2013).

## **CALIFORNIA FOREST PRACTICE ACT AND RIPARIAN ZONE PROTECTION**

In 1973, California enacted the modern Forest Practice Act (FPA), which expanded forestry regulations and sustainability efforts in logging, especially those pointed at lessening the impacts of logging on water quality and fish and wildlife habitat (Cubbage & Ellefson, 1980). Since 1973, the modern FPA, has been updated and modified based on monitoring and assessment of their effectiveness. The most recent harvesting activities in South Fork Caspar Creek Watershed, around which this study has been designed, was conducted in accordance with the updated FPA.

A significant update to the FPA includes regulation of activities that may cause harm to the beneficial functions of the riparian zone in watersheds with listed anadromous salmonids. This includes watercourses with confined channels, both inside and outside the coastal anadromy zone, and watercourses with flood prone areas or

channel migration zones that house anadromous salmonids. The coastal anadromy zone includes “any planning watershed(s) in the Central California Coast coho salmon Evolutionary Significant Units (ESUs), South Central Steelhead Distinct Population Segment (DPS), Central California Coast steelhead DPS, Northern California steelhead DPS, California Coastal Chinook salmon ESU, and Southern Oregon/Northern California Coast coho salmon ESU as defined in 70 Federal Register 37160, dated June 28, 2005, where salmonids listed as threatened, endangered, or candidate under the State or Federal Endangered Species Acts (ESA) are currently present or can be restored (“California Forest Practice Rules,” 2020).” West coast salmonids that have been listed under the ESA include Chinook salmon, Chum salmon, Coho salmon, Pink salmon, Sockeye salmon, and steelhead. Thirty-two percent of California’s land area is covered by ESUs.

The current FPRs were written with the overarching goals of providing protection for water temperature control, streambed and flow modification by large woody debris, filtration of organic and inorganic material, upslope stability, bank and channel stability, salmonid habitat, and vegetation structure diversity for aquatic and terrestrial habitat. These are referred to in the FPRs as the “beneficial functions of the riparian zone.”

The FPRs protect the beneficial functions of the riparian zone by establishing buffers known as Watercourse and Lake Protection Zones (WLPZ). These are defined as “strip(s) of land, along both sides of a Watercourse or around the circumference of a lake or spring, where additional practices may be required for protection of the quality and beneficial uses of water, fish and Riparian wildlife habitat, other forest resources and for controlling erosion (“California Forest Practice Rules”, 2015).” The width of the WLPZ varies depending on: 1) the slope of the stream valley, determined by taking the weighted

average of the sideslope between the watercourse and a point 100 feet upslope; 2) method of harvesting; and 3) class of the stream, which is generally defined by presence or absence of salmonids or aquatic life that provide beneficial functions in the riparian zone. A Class I stream, for example, houses fish seasonally or year-round and/or includes habitat to sustain fish migration and spawning. The width of the WLPZ is never less than 50 feet for Class I and II streams.

Within the WLPZ, 75% of surface cover must be retained and undisturbed by harvesting operations. This is to dissipate raindrop energy in order to prevent erosion, as well as to provide wildlife habitat. The FPA specifies not only the proportion of vegetation that must be left intact within the WLPZ, but also the type of vegetation. The multi-story dynamic of the forest as well as the diversity of vegetation is required to be maintained within the WLPZ. At least 50% of the understory must remain intact with a similar diversity to that of pre-harvest, in order to buffer water temperature, prevent erosion, and protect wildlife habitat. Additionally, 50% of the overstory must be left intact, and contain at least 25% of pre-harvest conifer species.

In watersheds with anadromous salmonids that have been listed under the Endangered Species Act, there are additional requirements implemented to protect watercourses. These regulations also extend to watersheds immediately upstream, and contiguous to, watersheds with salmon, in an attempt to mitigate cumulative impacts of fine sediment input and transport. Regulations require landowners to comply with the terms of a Total Maximum Daily Load (TMDL) and prevent significant sediment load increase to the watercourse, instability of a channel or bank, blockage of any aquatic migratory routes for any life stage of anadromous salmonids or listed species, adverse

effects to streamflow, and increases in peak flows or large flood frequency. Additionally, protecting and restoring vegetation, including snags and downed large woody debris, is a priority. Live vegetation provides nutrient input to streams as well as shade, which buffers temperature changes in streams to keep them within the ideal temperature range for anadromous salmonids. Dead trees may eventually make their way towards the waterway, which provides channel complexity and habitat for salmonids.

Within the WLPZ of waterways with listed salmonids, there are more stringent rules governing harvesting practices. The FPA defines three “zones” of the WLPZ for waterways within the coastal anadromous zone: the core zone, the inner zone, and the outer zone. The core zone is the section of land adjacent to either side of the watercourse. In order to promote bank stability, wood recruitment by bank erosion, and canopy retention, harvesting is generally prohibited within the core zone of waterways within the coastal anadromous zone.

The inner zone is upslope of the core zone. The primary goal of the inner zone is to maintain canopy diversity and high basal area. Large trees are favored in this zone for shading and large wood recruitment. Maintaining species diversity is also important for providing nutrient input to streams and influencing structural diversity of the stand. The inner zone may also overlap with the channel migration zone and flood prone areas. Therefore, it’s important to maintain vegetation which may provide salmonid habitat in the case of inundation. As a result, harvesting in this zone is also limited.

The main purpose of the outer zone is to provide a buffer for the WLPZ. This zone is at least 50 feet in width extending upslope from the inner zone. It provides wind resistance to minimize windthrow, additional wood recruitment, microclimate control,

terrestrial wildlife habitat, and erosion control on steep slopes. Selective harvesting is allowed in this zone so long as 50% of pre-harvest basal area is maintained, including 25% of original conifer canopy and a mix of deciduous and coniferous trees. Priority is given to wind-firm individuals when deciding which trees to maintain in order to meet basal area requirements.

As Caspar Creek is located within the coastal anadromous zone, special harvesting regulations are in effect to ensure conservation and protection of habitat for salmonid species listed under the ESA. Thus, targeted basal area reductions for each watershed could not be met in the WLPZ, which encompassed the riparian and toeslope plots.

## **SITE DESCRIPTION**

The Caspar Creek Experimental Watersheds, which include North Fork Caspar Creek Watershed and South Fork Caspar Creek watershed, drain an area of 2167 ha of Mendocino County in Northwestern California into the Pacific Ocean (Figure 2). 90% of Caspar Creek watershed is contained within the Jackson Demonstration State Forest (39°21' N, 123°44' W), which is managed by CAL FIRE. Caspar Creek has a Mediterranean climate, characterized by wet, mild winters and dry summers which bring coastal fog. 30-year mean annual precipitation from 1989 to 2018 was 1,168 mm. 93% of the yearly precipitation falls between October and April, the majority of which is rain—snowfall is rare. The mean monthly temperature from 1989 to 2018 as measured near the South Fork weir averaged 6.1 °C in December and 13.7 °C in August.



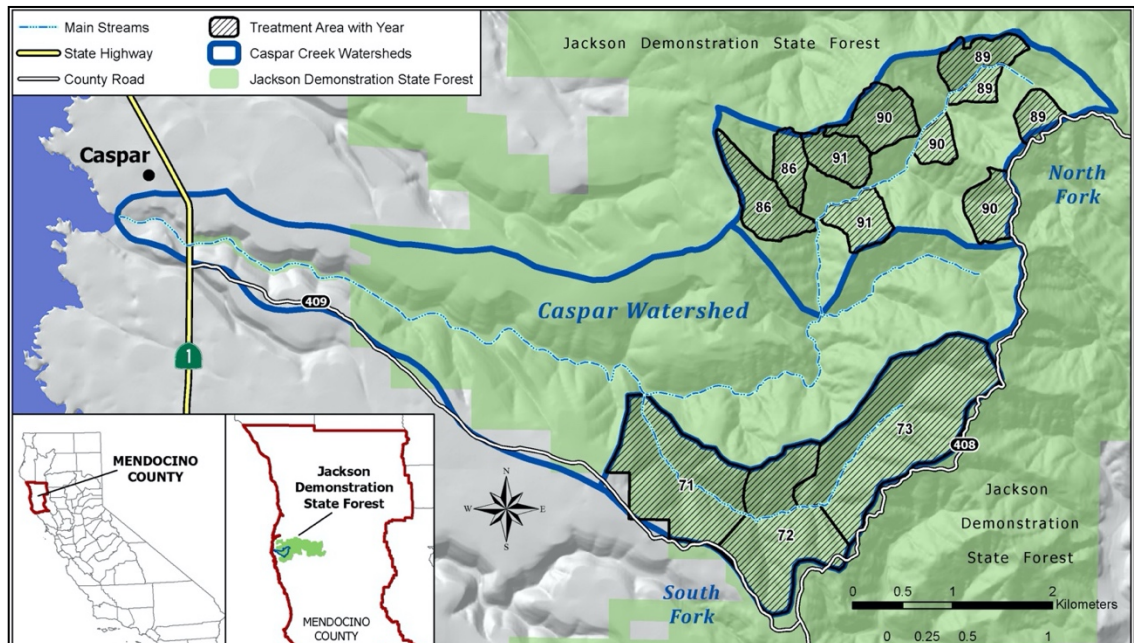


**Figure 2: Caspar Creek Experimental Watersheds Map (Cafferata and Reid, 2013)**

Canopy vegetation across the watershed is predominantly second and third growth *Sequoia sempervirens* (D. Don) Endl. (coast redwood), as well as *Pseudotsuga menziesii* (Mirbel) Franco (Douglas fir), *Abies grandis* (Dougl. ex D. Don) Lindl. (grand fir), and *Tsuga heterophylla* (Raf.) Sarg. (western hemlock) (Henry, 1998). The mid-canopy consists mainly of *Rhododendron macrophyllum* Don ex G. Don (Pacific rhododendron), *Notholithocarpus densiflorus* (Hook. & Arn.) Manos, Cannon & S. Oh (tanoak; formerly *Lithocarpus densiflorus*) and *Vaccinium ovatum* Pursh (evergreen huckleberry). The understory is dominated by ferns and other low-lying herbs. *Polystichum munitum* (Kaulf.) C. Presl (sword fern), *Struthiopteris spicant* (L.) F.W. Weiss (deer fern), *Trillium ovatum* Pursh (Pacific trillium), and *Gaultheria shallon* Pursh (salal) are common along with redwood, tanoak, and evergreen huckleberry sprouts. Ground cover is sparse in disturbed areas, which are heavy with duff, but is predominately *Oxalis oregana* Nutt.

(redwood sorrel) and *Viola sempervirens* Greene (redwood violet). Soils consist of mainly well-drained clay loam Ultisols and Alfisols with underlying Franciscan sedimentary bedrock. Slopes in Caspar Creek Watershed can reach above 50% and elevation ranges from 46 m to 323 m (Henry, 1998). The South Fork and North Fork drain an area of 424 ha and 473 ha, respectively.

Several large-scale harvesting experiments have been conducted in the Caspar Creek Experimental Watersheds since their establishment in 1961 by the USFS Pacific Southwest Research Station (PSW) and CAL FIRE. The first experiment, which took place from 1962 to 1985, involved selection cutting and tractor yarding 60-70% of stand volume in the South Fork, while the North Fork served as a control (Rice, Tilley and Datzman, 1979). The second experiment, which began in 1985, investigated the effects of clear-cutting in the North Fork on downstream streamflow and suspended sediment (Lewis *et al.*, 2001). In 2018, South Fork Caspar Creek watershed was harvested in accordance with the updated California Forest Practice Rules (FPRs) for a third experiment (Dymond, 2016). Several sub-catchments were harvested to varying degrees of intensity with the goal of monitoring hydrological and ecological response to stand density reduction.

As part of the third experiment, plots were established in four of these sub-catchments (henceforth simply referred to as “watersheds”): Williams (WIL), Treat (TRE), Uqlidisi (UQL), and Ziemer (ZIE), which were logged in 2018 to a targeted basal area reduction of 0%, 35%, 55%, and 75% of initial stand volume, respectively (Table 1; Figure 3). Additional “submerch” tree felling was conducted in some plots in May of

2019 to reach targeted basal area reduction. Harvesting operations were conducted in accordance with the modern California FPR guidelines.

The five study plots spanned a topographic gradient from the riparian zone to the summit (Figures 3 & 4). The 1/20<sup>th</sup> ha circular plots were surveyed for slope, aspect, and elevation when they were established in 2016 (Table 1).

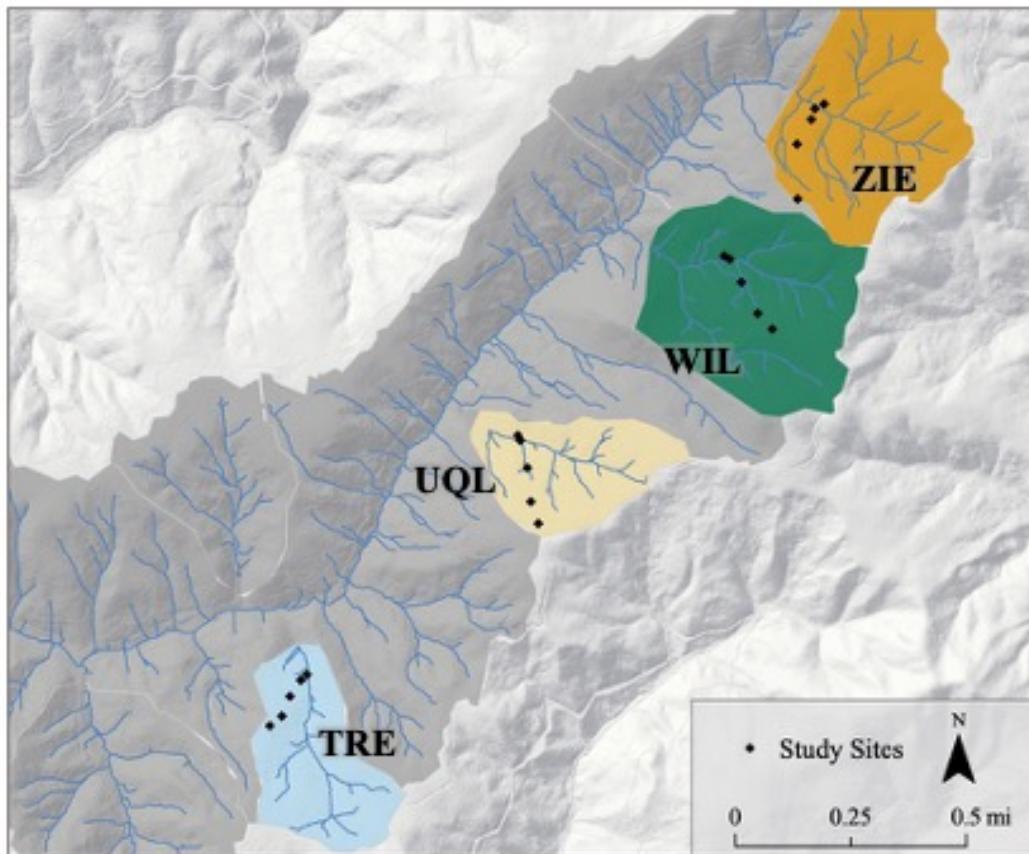


**Figure 3: Map of Watersheds and Study Sites**

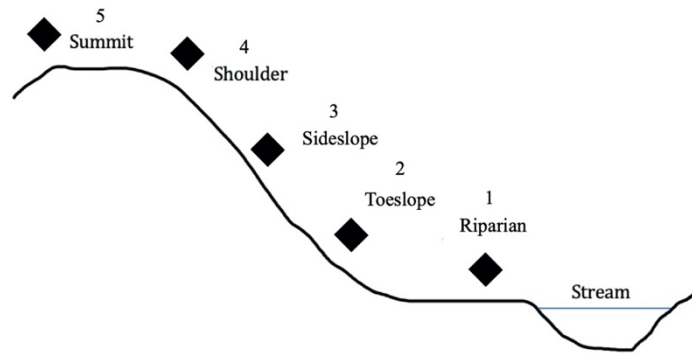


**Figure 4: Schematic Showing Topographic Positioning of Study Plots**

**Table 1: Watershed and Study Plot Characteristics**

There are a total of 20 study plots.

Watershed Name / ID	Targeted Basal Area Reduction	Area (ha)	Topographic Position	Slope (%)	Aspect (°)	Elevation (m)
Treat (TRE)	35%	14	1-Riparian	60	86	89.0
			2-Toeslope	55	77	101.2
			3-Sideslope	45	38	130.2
			4-Shoulder	70	105	148.7
			5-Ridge	36	91	165.1
Uqlidisi (UQL)	55%	13	1- Riparian	19	305	135.4
			2-Toeslope	53	355	142.2
			3-Sideslope	57	357	179.8
			4-Shoulder	32	21	217.1
			5-Ridge	8	3	233.0
Williams (WIL)	0%	26	1- Riparian	46	300	166.4
			2-Toeslope	50	320	173.1
			3-Sideslope	80	350	203.9
			4-Shoulder	55	357	251.5
			5-Ridge	25	288	274.0
Ziemer (ZIE)	75%	25	1- Riparian	15	10	196.2
			2-Toeslope	55	0	201.9
			3-Sideslope	85	18	224.1
			4-Shoulder	28	351	248.0
			5-Ridge	19	294	270.4

## **METHODS**

### **FIELD PROCEDURES**

#### *Sampling Scheme*

Data were collected within each of the twenty plots pre-established by USFS in the recently harvested South Fork Caspar Creek watershed. Pre-harvest, overstory tree characteristics and vegetation density were quantified and recorded in each plot.

Overstory tree characteristics included the number of trees by species, diameter at breast height (DBH), distance and azimuth from plot center, tree height, and live crown height.

Plot trees were also remeasured and inventoried post-harvest.

In summer 2019, post-harvest sub-canopy vegetation of each circular study plot was surveyed within six 1x1 meter square subplots (Figure 5). The subplot centers were positioned at a horizontal distance of four meters from the plot center at azimuths of 0, 60, 120, 180, 240, and 300 degrees. Within each subplot, the number of stems and sprouts by species and the percent cover of low-lying herbaceous vegetation were recorded. As it was difficult to determine the number of individual ferns without digging up the root wad and thus destroying the plant, the number of fronds were counted rather than the number of individuals. Similarly, since several woody species possess the capability to sprout from lignotubers and were difficult to determine as distinct individuals, individual stems were counted for all species.

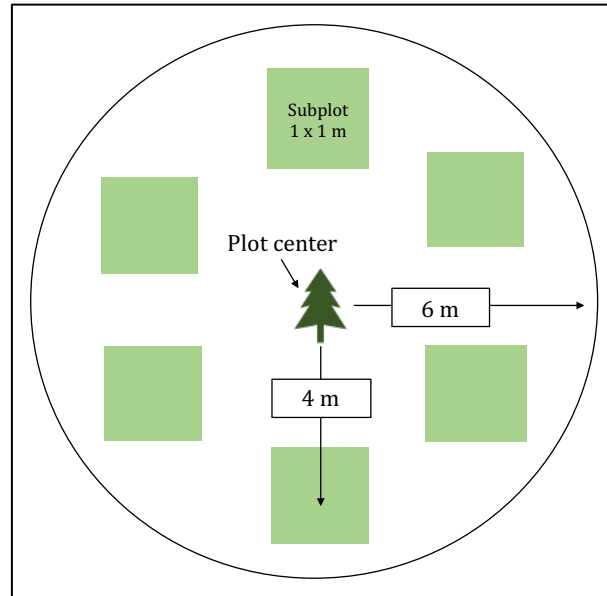


**Figure 5: Layout of Study Plots**

Understory vegetation density sampling was done within square subplots.

### *Evapotranspiration Measurements*

Seasonal measurements of post-harvest understory evapotranspiration were conducted using a portable rapid evapotranspiration chamber, which operates similarly to a closed gas exchange system (Stannard, 1988). The chamber consisted of a PVC frame in the shape of a rectangular frustum surrounded by a sheet of 4 mm thick, clear polyethylene plastic (Figure 6). This plastic was removed and replaced with new plastic after the first set of measurements in June. The chamber measured  $0.11 \text{ m}^2$  at the top and  $0.66 \text{ m}^2$  at the bottom, for a total volume of  $0.32 \text{ m}^3$ .

Two 4x4 inch brushless fans powered by 9 volt batteries were used to facilitate mixing within the chamber. These fans were attached to stakes at heights of 48 and 28 cm and placed in opposite corners, facing the center of the chamber. A HOBO Pro v2 Temperature/Relative Humidity data logger (Onset Computer Corporation, Bourne, MA,

USA) was suspended in approximately the middle of the chamber and set to record temperature and relative humidity (RH) every 10 seconds. Additionally, a HOBO Pendant Temperature/Light sensor was suspended from the top of the frame to record light intensity (in lux) within the chamber every 30 seconds (Onset Computer Corporation, Bourne, MA, USA). Ideally, the chamber should be centered around the targeted plant with one fan pointing at the base and one pointing at the crown. However, it was sometimes necessary for the plant to be positioned closer to one edge of the chamber, as was the case for plants on the edge of an eroding bank or at the base of a tree.

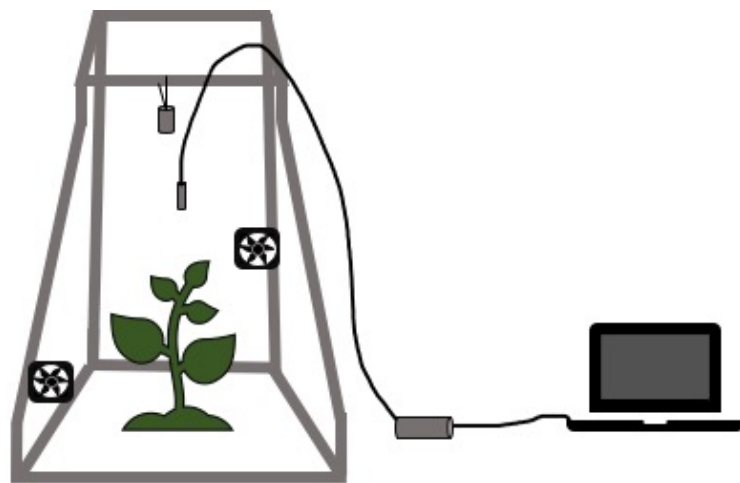


**Figure 6: Schematic of Chamber Setup with Sensors and Fans**

Measurements were conducted by first placing the frame of the ET chamber over the study plant with the plastic folded up so that the sides were open and the plant was exposed to ambient air. After the fans and sensors were positioned and turned on, the chamber was sealed by unfolding the plastic and tucking it under the bottom of the chamber to create a tight seal. The chamber was closed as quickly as possible, as lush



vegetation can saturate the volume within the chamber with water in as little as 15 seconds (Stannard, 1988). Often the chamber did not sit flush with the ground due to steep slopes, rocks, stumps, or otherwise uneven terrain. If needed, rocks, dirt, or hands were used to hold the plastic down for the duration of the measurement.

Once the chamber was sealed, the increase in vapor concentration within the chamber was measured. The constant rate of vapor pressure increase is proportional to the plant's ET rate (Figure 7). Measurements continued until ET rates slowed due to high vapor concentration within the chamber. This was determined by looking at the real-time plot of RH over time and ceasing data collection when RH stabilized. Periods of measurement ranged from 30 seconds to 10 minutes, but actual humidity usually stabilized around 2 minutes after the start of the measurement.

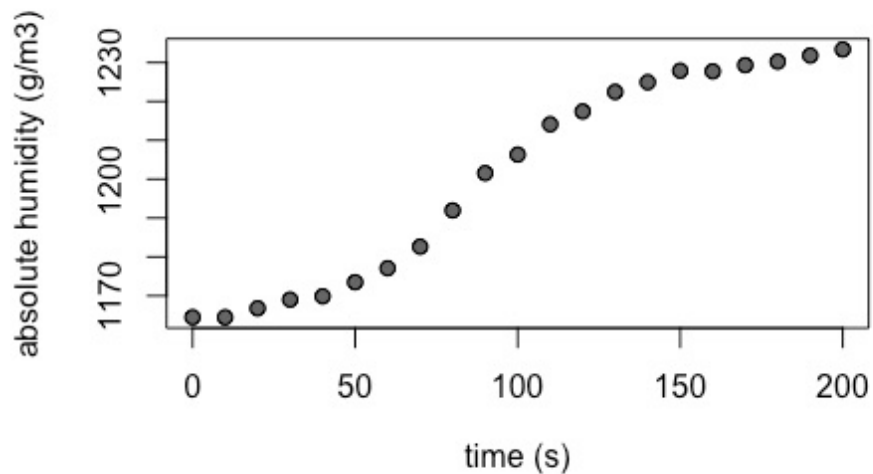


**Figure 7: Example Time Series Produced by ET Chamber Measurement**

This figure shows a typical curve created by the rise in water volume in the air of the chamber during ET measurements.

Within each plot, two plants of each target species were selected for ET measurements. Target species were chosen for their frequency across sites, but not every species was present in every plot. The plant species selected for ET measurements were *V. ovatum* (evergreen huckleberry), *S. sempervirens* (coast redwood), *L. densiflorus* (tanoak), *S. spicant* (deer fern), and *P. munitum* (western sword fern). For each plant, azimuth and horizontal distance from plot center were recorded. Height at the time of each measurement and plant vitality on a scale of 1-5, where 1 represented poor health and 5 represented great health, were also recorded.

ET measurements were conducted during active daylight hours (typically 7:30 am – 4:30 pm PST) with similar insolation and weather conditions in order to reduce environmental variability across the measurements. Each watershed was measured on approximately the same schedule so that each topographic position was measured at about the same time of day. Measurements were conducted twice during the dry season (June and July).

Volumetric water content (VWC) in the upper 20 cm of soil was measured using Campbell Scientific HydroSense soil moisture probe (Campbell Scientific, Inc., Logan, UT, USA). At the time of ET measurements VWC was measured upslope, sideslope, and downslope within 6 inches of each plant, when possible. For stump sprouts, VWC was measured upslope, sideslope, and downslope of the stump. VWC for plants growing from trunks which were no longer rooted was not measured.

### *Effect of Chamber on Light Intensity*

Since the polyethylene plastic used to enclose the chamber was not perfectly translucent or wrinkle-free, an analysis was conducted to test whether the chamber significantly altered light intensity (LI) over the plant. Data were collected every 10 seconds for 5 minutes ( $n = 30$ ) with the LI sensor A) exposed to ambient light, B) covered by a piece of new polyethylene plastic, and C) covered by a piece of plastic that had been wrinkled by use. The test for each treatment was conducted in the same location with consistent lighting.

A t-test was conducted to assess the null hypothesis that mean LI outside the chamber was not significantly different from mean LI inside the chamber ( $H_0: \mu_{in} - \mu_{out} = 0$ ) for each type of plastic. The presence of plastic influenced light penetration ( $F = 13.25$ ,  $p = 9.5e-06$ ). The control, in which the sensor was exposed to ambient light ( $\mu = 498.74$  lux), was significantly different from the new plastic ( $p = 5.4e-06$ ) and the old plastic ( $p = 9.2e-03$ ). However, the old and new plastic were not significantly different from each other ( $p = 9.6e-02$ ). The new plastic ( $\mu = 367.41$  lux) actually allowed for less light penetration than the old plastic ( $\mu = 421.23$  lux). Thus, the data from the two plastic treatments were combined into one, since the plastic was at some state between these two endpoints for most measurements. This suggests that the polyethylene plastic used to construct the chamber may alter light penetration by 15 – 26%. LI for this treatment group was also significantly different from the control ( $p = 3.2e-05$ ).

### ***Isotope Sample Collection***

Bulk plant and soil samples were collected for stable isotope analysis in order to determine where understory plants are accessing water. Vegetation samples were taken from non-photosynthetic tissue. For woody species, a suberized stem was collected. For herbaceous species, the rhizome was collected. One vegetation sample was taken for each species in every plot, for a total of 3-5 vegetation samples per plot. The targeted species for isotope collection were Evergreen Huckleberry (*Vaccinium ovatum*), Western Sword Fern (*Polystichum munitum*), Pacific Trillium (*Trillium ovatum*), Tanoak (*Lithocarpus densiflorus*), Coast Redwood (*Sequoia sempervirens*), and Pacific Rhododendron (*Rhododendron macrophyllum*). Soil samples were taken from 10 and 30 cm depths near each plant sampled. The azimuth and horizontal distance from the plot center were recorded for each plant sampled. Additionally, groundwater, stream, and fog water samples were collected by the USFS Fort Bragg field crew. All samples were stored in glass vials sealed with parafilm to prevent loss by evaporation and stored in a cool, dark cooler until the time of analysis. Water, soil, and vegetation samples were analyzed at the University of Minnesota Duluth using a Picarro cavity ring-down spectrometer (CRDS). However, due to shutdowns during the COVID-19 pandemic, isotope analysis could not be completed.

### **DATA ANALYSIS**

#### ***Diversity, Richness, and Evenness***

Species richness and density were calculated for each watershed using R statistical software version 1.1.456 (R Core Team, 2017). Shannon's Diversity Index (H)

was also calculated for each watershed in order to characterize species diversity (Shannon and Weaver, 1949):

$$H = - \sum_{i=1} p_i \ln p_i \quad (\text{Eqn. 1})$$

Where  $p_i$  is the proportion of the abundance of a species relative to the total number of individuals. Since this index account for both abundance and evenness of a species, it is often considered a more informative indicator of species diversity than richness alone.

Shannon's equability, a measure of the homogeneity of species proportions, was also calculated (Shannon and Weaver, 1949). An equability of 1 indicates a lack of species dominance within a community, i.e., all species are present in equal proportions. An equability closer to 0 means that one or several species are more dominant than others. Equability is calculated by dividing the diversity index by the natural log of the number of species.

### ***Evapotranspiration Calculations***

ET was calculated by adapting methods which were first described by Stannard et al. (1998). Temperature ( $^{\circ}\text{C}$ ) and RH (%) data were collected every 10 seconds during measurements. Saturation vapor pressure ( $e^*$ ) was calculated from temperature at each time step:

$$e^* = 611 * \exp\left(\frac{17.27*T}{T+237.3}\right) \quad \text{Eqn. 2}$$

where T is temperature in  $^{\circ}\text{C}$  and  $e^*$  is in Pa.

Saturation vapor pressure and relative humidity were used to calculate absolute humidity ( $P_v$ ):

$$P_v = \frac{1000*RH*e^*}{(T+273.15) * R_v} \quad \text{Eqn. 3}$$

where  $T$  is the temperature in  $^{\circ}\text{C}$ ,  $R_v = 461.5 \text{ J/kgK}$  is the gas constant for water vapor, and  $P_v$  is in  $\text{g/m}^3$ . A typical series of absolute humidity over time for a measurement is shown in Figure 7.

The maximum slope between two points, or over a 10 second interval, was calculated using a least squares linear regression. The slope of this line,  $M$ , is related to the ET rate:

$$ET = 86.4 * \left( \frac{MVC}{A} \right) \quad \text{Eqn. 4}$$

where  $ET$  is the evapotranspiration rate in  $\text{mm/day}$ ,  $M$  is the slope in  $\text{g/m}^3\text{s}$ ,  $V$  is the volume of the chamber in  $\text{m}^3$ ,  $C$  is the chamber calibration factor,  $A$  is the area of the chamber on the ground in  $\text{m}^2$ , and 86.4 is a conversion factor.

ET calculations are on an individual plant basis, and do not represent understory transpiration at the landscape scale. All measurements include bare soil evaporation from the area of the ground within the chamber. For the purposes of comparison, the chamber was assumed to be completely hydrophobic for ET calculations ( $C = 1$ ).

### ***Measuring Plant Leaf Area and Biomass***

To estimate the leaf area of coast redwood sprout samples, 10 stems were collected from redwood sprouts and scanned to a computer for analysis. LA of the scanned sprouts was measured using the “Analyze Particles” tool in Fiji (Schindelin, Arganda-Carreras, & Frise, et al. 2012). Stems were erased from the image before measurement so as to not be included in the total leaf area. Stem length was also measured in Fiji and verified using a ruler to ensure that the image scale was accurate. A

linear regression of leaf area as a function of stem length was then conducted using R statistical software version 1.1.456 (R Core Team, 2017). The leaf area of each ET study plant was calculated from the regression equation using the number of stems in the plant as recorded in the field.

For evergreen huckleberry and tanoak, an average leaf size was found using “Analyze Particles” in Fiji on scans of leaves from 5 individual stems. The number of leaves per stem was then counted and divided by the length of the stem to find leaf density. This density was multiplied by the average leaf size to determine average leaf area per unit length of stem for the two species. This average leaf area per unit length of stem was then multiplied by each sample plant’s stem length and number of stems to calculate a total leaf area per sample plant.

For all ferns, biomass, rather than leaf area, was estimated using equations created by Gholz et al. (1979). These equations estimate biomass of ferns from average frond length and number of fronds. The equations were developed using a regression approach based on data collected from ferns at low elevations in the H.J. Andrews Experimental Ecological Reserve, Blue River, Oregon. (Table 2). Like the Jackson Demonstration State Forest, the H.J. Andrews Experimental Ecological Reserve is a mature coniferous forest in a Mediterranean climate.

**Table 2: Regression Equations for Calculating Fern Biomass by Species**

Column x is the input, where NFR is the number of fronds and LAF is the average frond length. All lengths are in cm and biomass is in grams. Regression statistics are presented in the right four columns as reported by Gholz et al. (1979).

Species	x	Equation	Range (# fronds; cm)	$S^2_{y,x}$	n	$R^2$
<i>Polystichum munitum</i>	NFRxLAF	$Y = -2.5695 + 0.0643X$	4-70; 34.0-130.0	1162.6	41	0.9
<i>Struthiopteris spicant</i>	NFRxLAF	$Y = -0.4345 + 0.0116X$	2-39; 35.0-100.0	55.193	21	0.8

### ***Evapotranspiration Rate Statistics***

All variables were assessed for normality and equal variance using boxplots and Q-Q plots. If either assumption was violated, the offending variable was transformed using a log<sub>10</sub> transformation. Residuals were plotted for all models to assess assumptions of normality and equal variance before analysis of variance testing. All calculations and statistical analyses were conducted using R version 1.1.456 (R Core Team, 2017). The “tapply” function was used to calculate all means and standard deviations for groups and variables of interest and Tukey HSD tests (Tukey, 1949) were conducted to determine significant pairwise differences between ET rates for the different groups. The significance threshold was set at  $\alpha = 0.05$  for all analyses. “ET rate” refers to the mean group rate, culminated across sampling periods and species, unless otherwise specified.

One-way ANOVA testing was used to test the null hypothesis that ET rates did not vary significantly across watersheds ( $\mu_{WIL} = \mu_{TRE} = \mu_{UQL} = \mu_{ZIE}$ ). Additionally, a two-way t-test was conducted between the control watershed and the heavily harvested watershed. Because the targeted reduction in basal area was not precisely achieved in



every plot, ET rate was also compared to actual percent harvest. Percent harvest was binned into four harvesting intensity categories using the “cut” command in R: low harvest (0-19.2% reduction), moderate harvest (19.2-38.5% reduction), moderate-high harvest (38.5-57.8% reduction), and high harvest (57.8-77.1% reduction). One-way ANOVA testing was used to test the null hypothesis that ET rates did not vary significantly across harvesting intensity ( $\mu_{\text{Light}} = \mu_{\text{Moderate}} = \mu_{\text{Moderate-High}} = \mu_{\text{High}}$ ). Since plots were not harvested proportionally to pre-harvest basal area, and natural variations in pre-harvest basal area were expected, understory ET rates were also compared to residual overstory basal area using linear regression.

Lastly, differences in ET rate by topographic position were also analyzed. A one-way ANOVA was conducted comparing ET rate to topographic position as a factor to test the null hypothesis that ET rate does not vary significantly across topographic position ( $\mu_{\text{riparian}} = \mu_{\text{toeslope}} = \mu_{\text{sideslope}} = \mu_{\text{shoulder}} = \mu_{\text{summit}}$ ). ANOVAs of ET rate by topographic position were also conducted within each individual watershed.

### ***Multiple Regression Models***

To investigate the relationship between transpiration and environmental influences in the study watersheds, ET rate was related to several climactic and physiological variables using the linear model function in R (R Core Team, 2017). This was done for sprouts and ferns individually for two reasons: 1) ferns have a different physiology than other plants and thus may react differently to environmental variables, and 2) the variables available for measuring plant size were not consistent between ferns and sprouts.

Correlation matrices were visually analyzed to assess multicollinearity of variables. Additionally, variance inflation factors (VIFs) were calculated for each predictor variable. The VIF of a term is defined as the ratio of the full model's variance to the variance of the model that includes that term alone. A VIF of 1 indicates complete independence, while a high VIF indicates collinearity with other variables. Any variables that were correlated to another variable were removed from the model. Residuals plots and Added-Variable plots were used to assess residual normality and linearity of each model, respectively.

A full model was developed for both ferns and sprouts, correlating ET rate to all possible predictor variables (Table 3) across watersheds, as well as for each watershed individually. Second order interactions between VWC, light intensity, and temperature were considered in the model selection process. The predictor variables were scaled to the same range so the different models could be directly compared. Sums of squares-based effect size indices were calculated for each variable using "modelEffectSizes" from the lmSupport package in R (Curtin, 2018).

"StepAIC" from the "MASS" package (Venables & Ripley, 2002) was used to select models that were most effective at predicting ET rate within watersheds and species groups. StepAIC adds and subtracts variables to the model until it finds the best fit, defined as the model with the lowest Akaike information criterion (AIC) (Akaike, 1974). The AIC is an estimation of model quality in comparison to other models for a given set of data. A model is penalized for both underfitting and overfitting; i.e., it selects the simplest model that accounts for the most variation.

**Table 3: Variables Considered in Full Model**

Variable	Symbol	Units
ET Rate (response variable)	ET	mm/day
Light Intensity	LI	lux
Temperature	T	°C
Volumetric Water Content	VWC	%
Elevation	EL	meters
Basal area	BA	ft <sup>2</sup>
Percent harvest	PH	%
Estimated Leaf Area (sprouts)	LA	cm <sup>2</sup>
Biomass (ferns)	BM	g
Species	SP	<i>V. ovatum</i> (VAOV) <i>S. sempervirens</i> (SESE) <i>L. densiflorus</i> (LIDE) <i>S. spicant</i> (STSP) <i>P. munitum</i> (POMU)

For both the sprout and fern groups, the stepwise AIC method was used on the full model to select the best fit model for predicting ET rate across watersheds. The best fit model that was found for all sprout samples was also applied to watersheds individually. Thus, the effects of the most influential variables could be directly compared at the watershed scale by analyzing effect size indices. Finally, stepAIC was used to find best-approximating models within each watershed for both sprouts and ferns.

Marginal mean predictions were generated for the response variable from each model term using the function “ggpredict” from the ggeffects package (Lüdtke, 2018). This function holds all other variables at a constant value while varying a term of interest. Thus, the effect of a variable on ET rate can be investigated independently from other

variables. For sprouts, predictions were made from the variables included in the overall best fit model, but subset for each watershed. For the ferns, predictions were made using the full fern model. These predictions were plotted alongside raw data using `ggplot2` (Wickham, 2009).

## RESULTS

### *Watershed Vegetation*

Species richness and Shannon's diversity index were highest in the moderately harvested UQL watershed (Figure 8; Table 4), followed by the low harvest TRE watershed. Stem density at UQL was only slightly lower than the highly harvested watershed, ZIE. While ZIE had high species density, it had low diversity and richness (Table 4). The lowest richness, diversity, and density of understory vegetation was at the unharvested control watershed, WIL (Figure 8). However, while other watersheds lacked much vertical heterogeneity, WIL had a more developed mid-story of mature *Vaccinium ovatum*, *Lithocarpus densiflorus*, and *Rhododendron macrophyllum*. There were no significant differences in density of understory vegetation between watersheds. However, richness at UQL was significantly different than that of ZIE ( $p = 4.6e-02$ ) and WIL ( $4.9e-03$ ; Table A1). Diversity at UQL was also significantly higher than that of WIL ( $p = 1.2e-02$ ; Table 4).

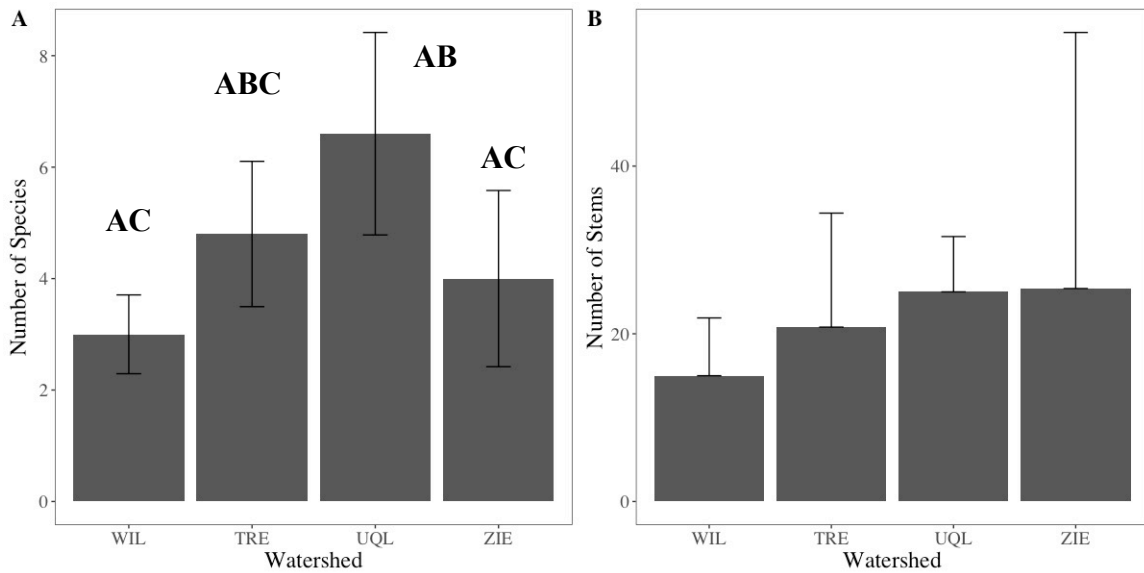


**Figure 8: Species Richness and Stem Density of Understory Vegetation by Watershed**

A) Mean number of species (richness) within study plots for each watershed. B) Mean number of stems (density) within study plots for each watershed. Error bars represent 95% confidence intervals. Groups that were not significantly different are labeled with the same letter.

**Table 4: Diversity of Understory Vegetation by Watershed**

Mean density, richness, diversity, and evenness of plots by watershed. Standard deviations are shown in parentheses.

Watershed	Percent Harvest	Number of Species	Number of Individuals	Shannon's Diversity Index	Shannon's Evenness
WIL	0	3.0 (0.7)	15.0 (6.9)	0.87 (0.30)	0.80 (0.12)
TRE	35	4.8 (1.3)	20.8 (13.6)	1.36 (0.19)	0.88 (0.049)
UQL	55	6.6 (1.8)	25.0 (6.5)	1.57 (0.26)	0.85 (0.061)
ZIE	75	4.0 (1.6)	25.4 (30.5)	1.16 (0.42)	0.87 (0.045)

*Sequoia sempervirens*, *Vaccinium ovatum*, *Lithocarpus densiflorus*, and *Polystichum munitum* were the most common understory plant species and were present in every watershed (Figure 9). *Struthiopteris spicant* was present at UQL and TRE, but not WIL and ZIE. *Gaultheria shallon* and *Trillium ovatum* were also well represented across watersheds (Figure 9). A full list of plants recorded at each plot can be found in Appendix A.

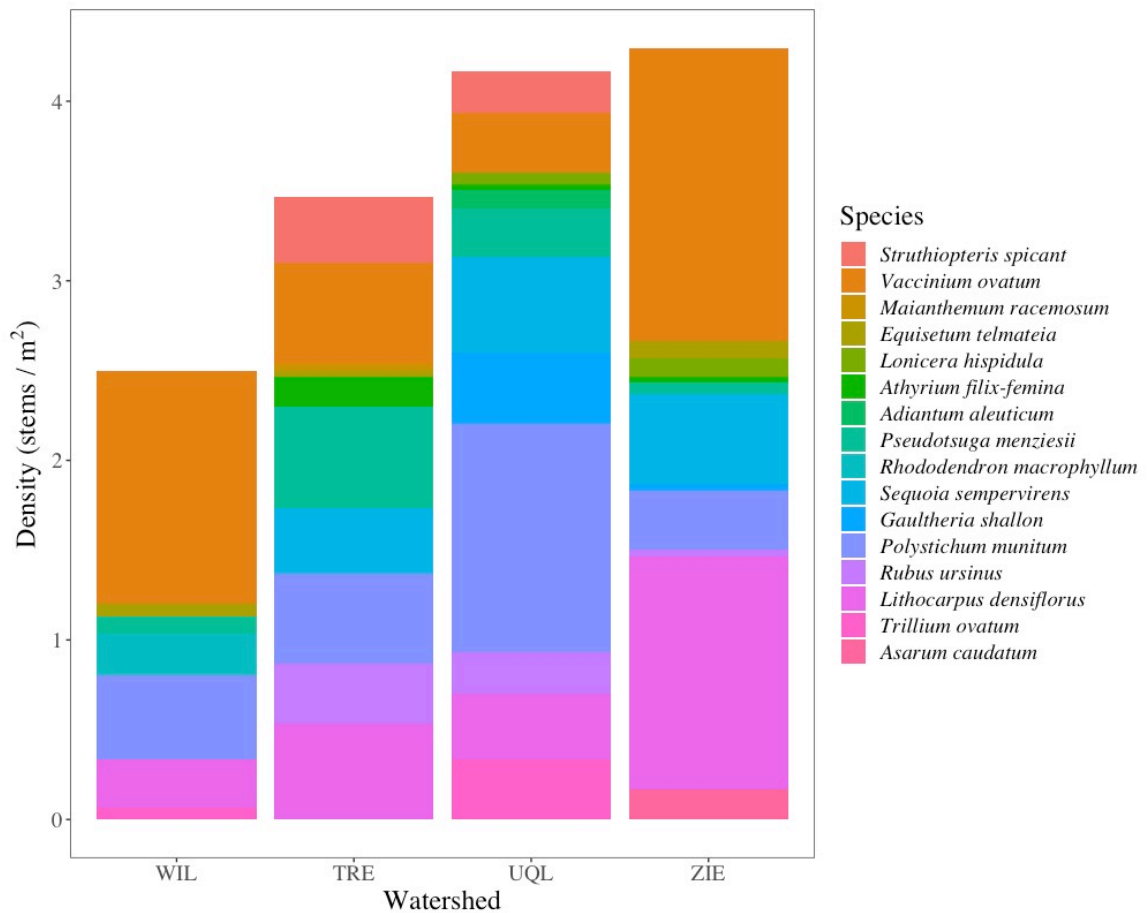


**Figure 9: Density of Each Understory Species by Watershed**

Mean density of species observed as averaged across all subplots and plots. Grasses and herbaceous groundcover less than three inches in height are not included in these counts.

### ***Basal Area Reduction by Plot***

With the exception of the riparian plots, which were located within the WLPZ and thus could not be harvested in accordance with the FPR, most plots were harvested within a few percent of the targeted basal area reductions (Table 5). Due to the increased occurrence of large, old-growth trees and limitations on harvesting in the WLPZ, residual basal area in the riparian zone plots was much higher than the other four plots across watersheds (Figure 10).

**Table 5: Basal Area of Plots Before and After Harvesting**

<b>Watershed</b>	<b>Plot</b>	<b>Initial Basal Area (m<sup>2</sup>)</b>	<b>Targeted Basal Area Reduction (%)</b>	<b>Actual Basal Area Reduction (%)</b>	<b>Residual Basal Area (m<sup>2</sup>)</b>
TRE	1- Riparian	1.5		3	1.5
	2-Toeslope	1.4		32	0.9
	3-Sideslope	0.5	35	35	0.3
	4-Shoulder	0.5		27	0.3
	5-Ridge	1.3		70	0.4
UQL	1- Riparian	2.2		10	2.0
	2-Toeslope	0.1		56	0.04
	3-Sideslope	0.5	55	54	0.2
	4-Shoulder	0.8		55	0.4
	5-Ridge	1.2		57	0.5
WIL	1- Riparian	2.8		0	2.8
	2-Toeslope	0.7		0	0.7
	3-Sideslope	0.8	0	0	0.8
	4-Shoulder	1.6		0	1.6
	5-Ridge	1.0		0	1.0
ZIE	1- Riparian	4.8		3	4.6
	2-Toeslope	0.1		57	0.1
	3-Sideslope	1.5	75	70	0.4
	4-Shoulder	0.5		77	0.1
	5-Ridge	1.1		74	0.3



The toeslope of ZIE and TRE were also slightly under-harvested, as merchantable trees within the plot could not be harvested in accordance with the FPR. Basal area reduction across plots 2-4 averaged 69.3% at ZIE and 40.8% at TRE. TRE 5 was heavily over-harvested due to a misunderstanding over tree markings, but its residual basal area was similar to that of plots 3 and 4. UQL came closest to its targeted 55% reduction rate, with a mean reduction rate of 55.4% across plots 2-4 (Table 5). In other plots, exact basal area reductions simply could not be met due to the variability in size and position of residual trees (Table 5).

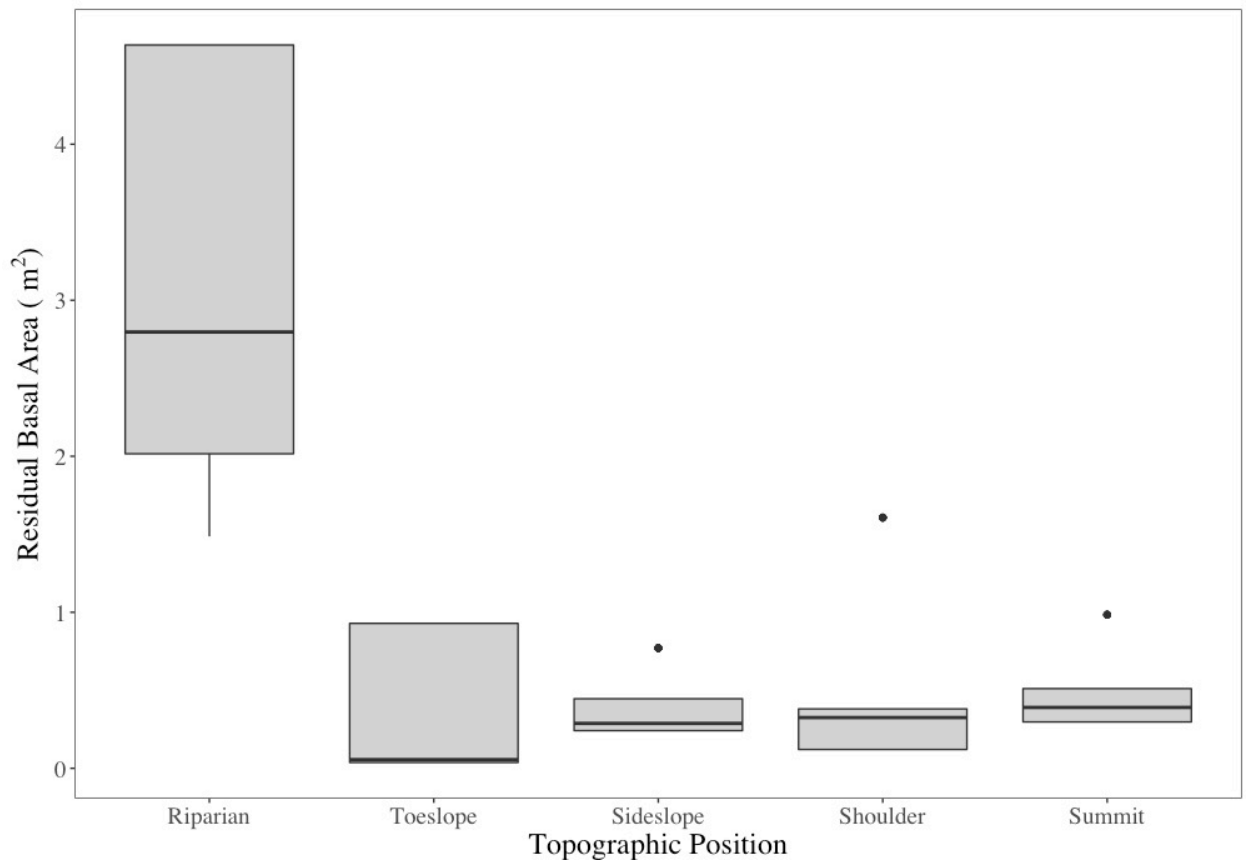


**Figure 10: Mean Residual Basal Area by Topographic Position Across all Four Watersheds**

### ***Evapotranspiration Rate by Watershed***

When averaged across species and sampling period, there were significant differences in  $\log_{10}$ ET rate by watershed ( $F = 30.83$ ;  $p < 2e-16$ ). The highly harvested ZIE watershed had the highest average ET rate (Figure 11A; Table 6), which was significantly higher than ET rates in the other watersheds (Table A2). The lowest ET rate was at the control watershed, WIL ( $\mu = 31 \pm 19$  mm/day). Differences between WIL, TRE, and UQL were not statistically significant (Table A2). While not significant, the mean ET rate for each watershed was still directly proportional to the mean reduction in basal area (Table 6; Figure 11A).

ET rates decreased from June to July across all watersheds (Figure 11B). Collectively, the mean understory ET rate decreased from 53 mm/day in June to 41 mm/day in July ( $p = 2.5e-04$ ). The biggest difference in mean ET rate from June to July was observed in WIL, which decreased from 38.04 mm/day in June to 21.81 mm/day in July ( $p = 1.6e-03$ ).

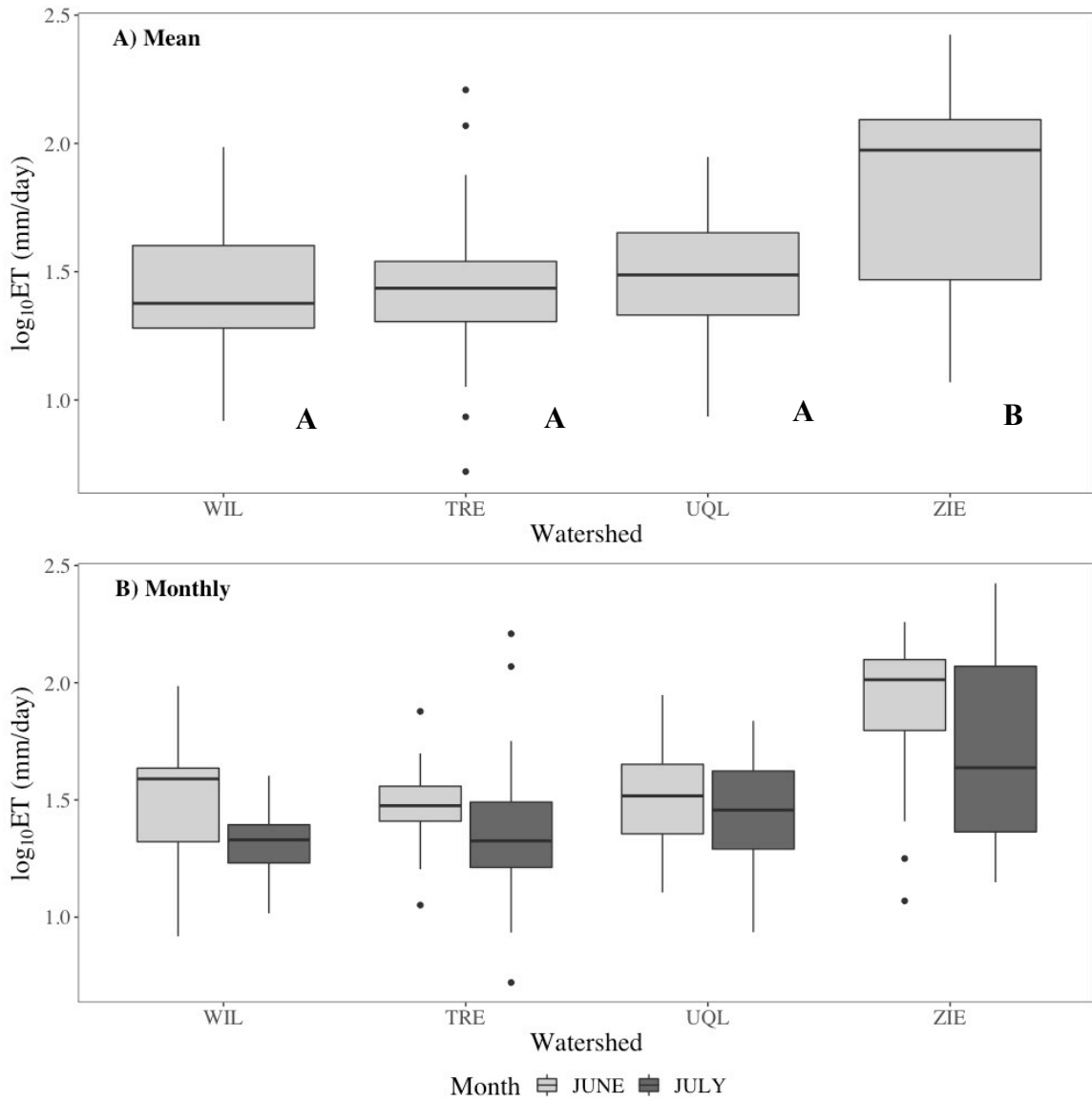


**Figure 11: Boxplot of Understory Plant ET Rates by (A) Watershed and (B) Sampling Period**

Groups that were not significantly different are labeled with the same letter.

**Table 6: Mean ET Rate of Understory Vegetation by Watershed**

<b>Watershed</b>	<b>TRE</b>	<b>UQL</b>	<b>WIL</b>	<b>ZIE</b>
<b>Mean ET Rate (mm/day)</b>	32	35	31	87
<b>Standard Deviation</b>	24	18	19	56

***Evapotranspiration Rate as a Function of Basal Area***

Because the targeted percent harvest was not achieved in every plot, the mean ET rate across species and sample dates from each plot was compared to the plots' actual basal area reduction. When binned into four harvest intensity classes, there was a significant relationship between ET rate and percent harvest across all plots and watersheds ( $F = 34.66$ ,  $p < 2e-16$ ). Generally, understory ET rates increased with increasing harvest intensity (Figure 12). There were significant differences between most groups (Table A3). However, ET rates within the "moderate harvest" bin were not significantly different from those in the "low harvest" or "moderate-high harvest" bins.

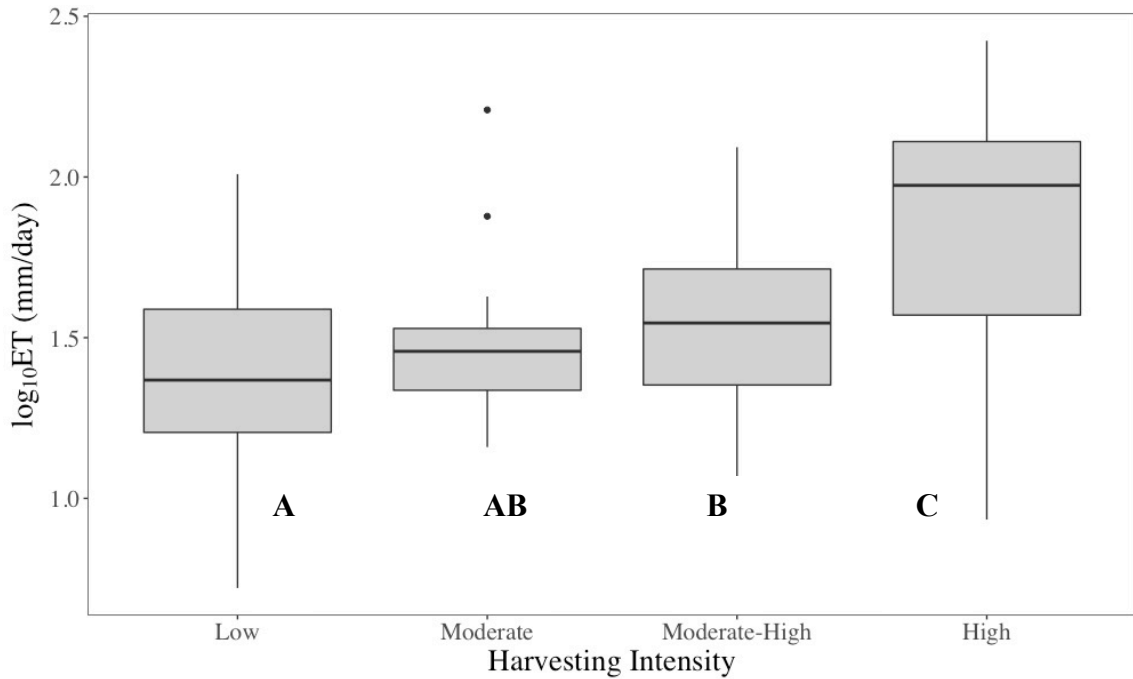


**Figure 12: ET Rate vs. Basal Area Reduction**

ET rate vs. plot basal area reduction. Harvesting intensity was categorized into four levels for ANOVA testing. Groups that were not significantly different are labelled with the same letter.

Within the watersheds, final plot basal area varied greatly due to variation in both actual percent harvest and pre-harvest basal area. Thus, ET rate was also compared to post-harvest basal area using a linear regression model (Figure 13). Log10 transformed understory ET rates and log10 transformed overstory basal area were significantly correlated according to the Pearson's correlation test ( $t = -4.66$ ,  $p = 5.3e-06$ ) and displayed an inverse relationship (Figure 13).

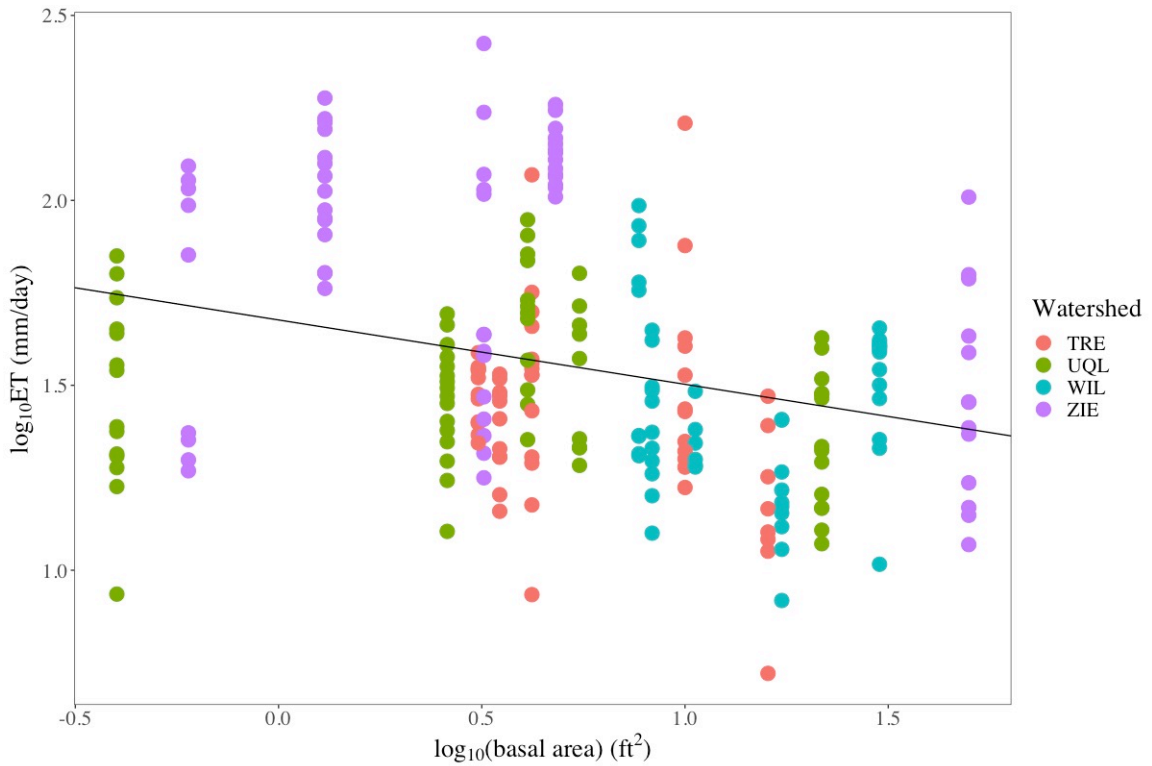


**Figure 13: ET Rate vs. Residual Basal Area with Regression Line**

***Variation in Evapotranspiration Rate along the Hillslope***

Ignoring the treatments and differences in residual basal area, only the riparian sites displayed significant differences in mean  $\log_{10}$  ET than the topographic position ( $F = 4.435$ ,  $p = 1.8e-03$ ). Mean ET rate in the riparian zone was significantly lower than all other plots (Table A1). ET rates were highest at the shoulder plots ( $\mu = 62 \pm 46$  mm/day), although this was not significantly higher than the other hillslope positions (Table 7; Figure 14).

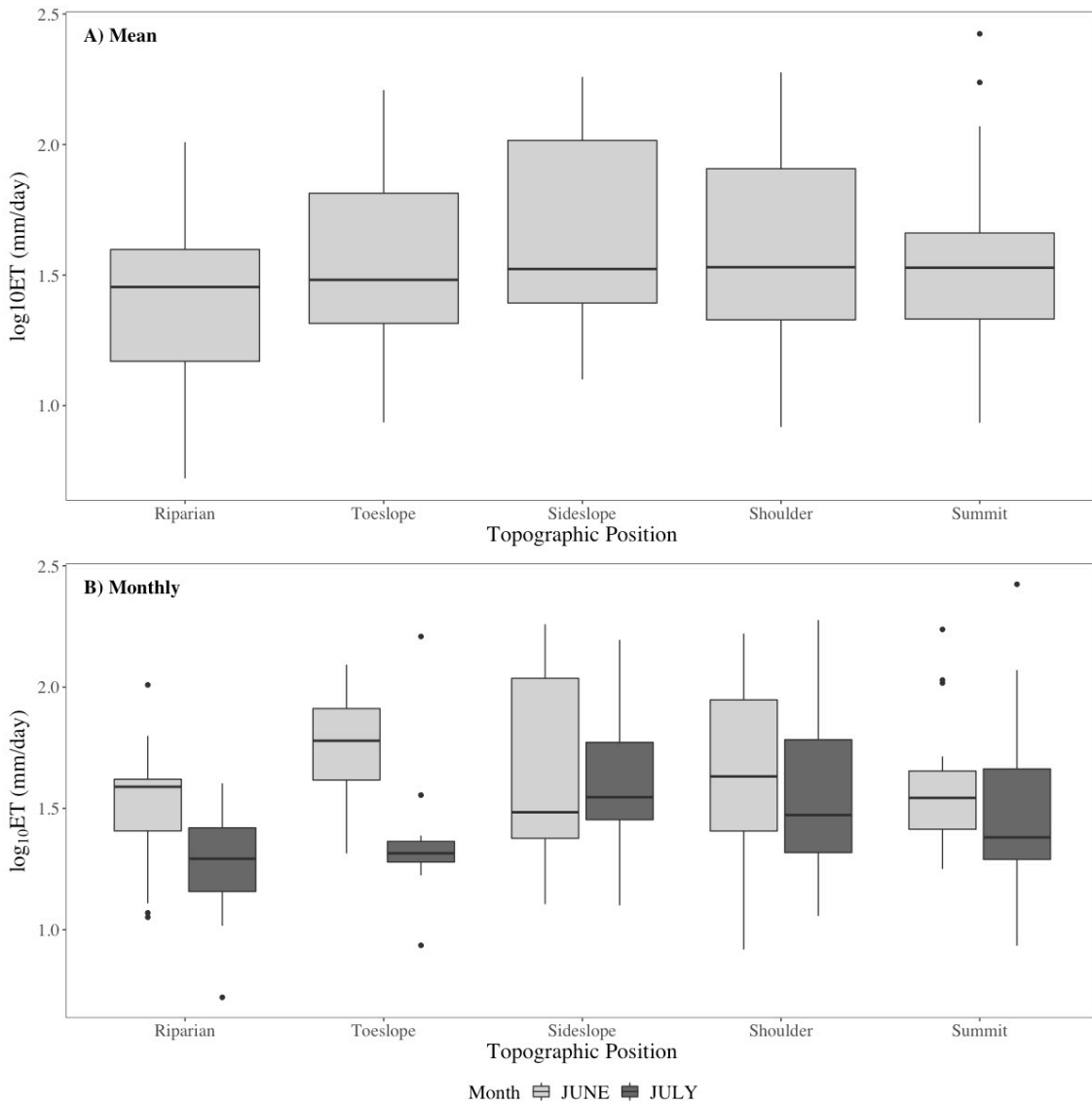


**Figure 14: Boxplot of ET Rate by Topographic Position**

A) ET rate at each topographic position as averaged across sampling periods and watersheds. B) ET rate by sampling period at each topographic position as averaged across watersheds.

**Table 7: Mean and Standard Deviation of ET Rate by Topographic Position**

ET rate is in mm/day.

<b>Topo</b>	<b>Riparian</b>	<b>Toeslope</b>	<b>Sideslope</b>	<b>Shoulder</b>	<b>Summit</b>
<b>Mean</b>	29	47	57	57	48
<b>SD</b>	17	35	49	47	48

The aforementioned differences across hillslopes do not hold true when looking at hillslopes across each of the watersheds (Figure 15). In the heavily harvested ZIE watershed, Log10ET rates of understory plants were significantly correlated to topographic position ( $F = 13.21$ ,  $p = 8.9e-08$ ). Significant differences were also observed between several topographic positions (Table A5). The mean ET rate in the ZIE watershed was highest for the sideslope plot ( $\mu = 134 \pm 24$  mm/day) and lowest for the riparian plot ( $\mu = 36 \pm 26$  mm/day). It is interesting to note, however, that the riparian plot was not significantly different from other plots at ZIE, as it was for the data averaged across watersheds (Table A5).

Topographic position was also a significant factor in predicting log10 transformed ET rates in the control plots ( $F = 7.742$ ,  $p = 7.8e-05$ ). Mean ET rate in this WIL watershed was highest at the toeslope plot ( $\mu = 52 \pm 31$  mm/day) and lowest at the shoulder plot ( $\mu = 16 \pm 6$  mm/day). The toeslope was significantly higher than all other plots aside from the riparian (Table A6). Unlike the other watersheds, mean ET rate was quite high in the riparian plot of WIL in comparison to other positions along the hillslope ( $\mu = 34 \pm 10$  mm/day; Figure 15C).



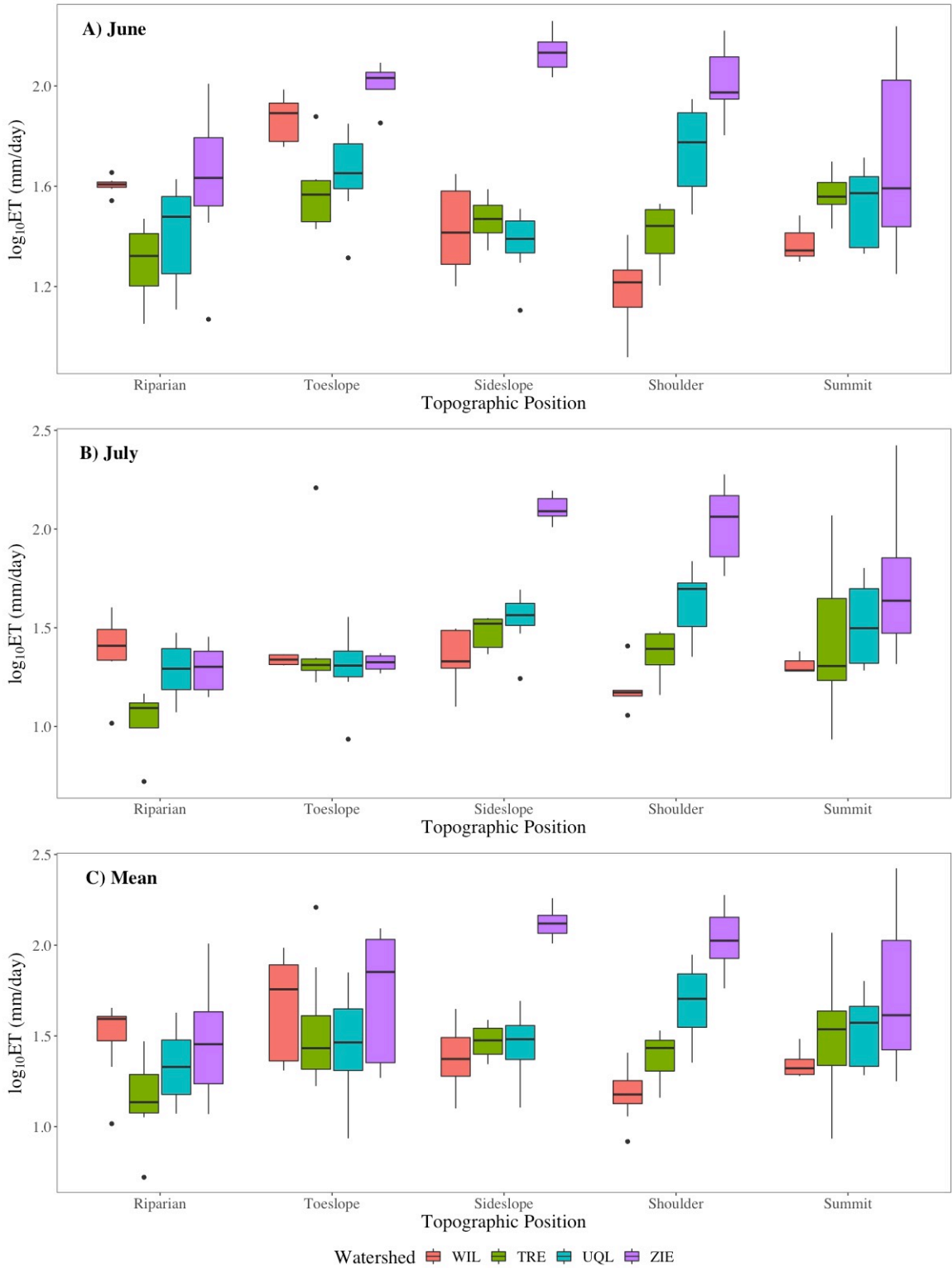


**Figure 15: ET Rate of Understory Vegetation by Plot for June, July, and for all Data**

In the lightly-harvested TRE watershed, ET rate was highest at the toeslope plot ( $\mu = 42 \pm 41$  mm/day) and lowest at the riparian plot ( $\mu = 16 \pm 8$  mm/day). While still statistically significant ( $F = 4.229$ ,  $p = 4.9e-03$ ), the influence of topographic position on ET rates was weaker in TRE than in ZIE and WIL – significant differences were observed only between riparian zone plots and the toeslope, sideslope, and summit plots (Table A7). Like ZIE and TRE, mean ET rate in the moderately-harvested UQL watershed was lowest at the riparian plot ( $\mu = 24 \pm 10$  mm/day). The highest mean ET rate, however, was at the shoulder plot ( $\mu = 53 \pm 21$  mm/day). As with all other watersheds, topographic position was significant in influencing variation in ET rates in UQL ( $F = 4.957$ ,  $p = 1.6e-03$ ), but only a couple of plots were significantly different from one another (Table A8).

From June to July, the mean ET rate of the sample population decreased in 60% of the plots. The decrease in ET rate was greatest in the riparian and toeslope plots (Table 8). The intensely harvested watershed (ZIE) and the control watershed (WIL) displayed the most significant differences in plant ET rates between June and July ( $t = -7.3144$ ,  $p = 4.355e-11$ ). This difference was statistically significant for both measurement periods, but was more significant in June ( $t = -5.68$ ,  $p = 4.2e-07$ ) than in July ( $t = -5.04$ ,  $p = 1.2e-05$ ). ET rates at the riparian ( $p = 0.791$ ) and toeslope ( $p = 0.432$ ) of ZIE were not significantly different from the riparian and toeslope of WIL. However, the sideslope ( $p = 1.0e-11$ ), shoulder ( $p = 2.5e-07$ ), and summit plots ( $p = 0.0178$ ) at ZIE had significantly higher ET rates than those of WIL. The biggest difference was between the sideslope plots (Figure 15).

**Table 8: Mean ET Rate at Each Plot by Sampling Period**

ET rate is in mm/day.

<b>Watershed</b>	<b>Riparian</b>	<b>Toeslope</b>	<b>Sideslope</b>	<b>Shoulder</b>	<b>Summit</b>	<b>Mean</b>
Early June						
WIL	40	75	29	16	24	38
TRE	21	41	30	26	38	32
UQL	28	48	24	60	35	38
ZIE	50	103	139	110	71	96
<b>All</b>	36	64	59	61	46	53
Late July						
WIL	26	22	23	16	21	22
TRE	11	43	30	24	39	31
UQL	20	21	36	45	38	31
ZIE	20	21	128	116	79	77
<b>All</b>	20	28	55	52	49	41

### *Environmental Controls on Evapotranspiration*

#### *1) Light Intensity*

Light intensity (LI) was an order of magnitude higher in ZIE ( $\mu = 16555.63$  lux) than in all other watersheds. LI was lowest in WIL ( $\mu = 1609.33$  lux), 2<sup>nd</sup> lowest in TRE ( $\mu = 6999.65$  lux), and 2<sup>nd</sup> highest at UQL ( $\mu = 8522.76$  lux). This same pattern of LI by watershed, which displays an inverse correlation to harvesting intensity, was observed both for June and July measurements (Table 9).

**Table 9: Mean Light Intensity by Month and Watershed**

Light intensity is in lux. Standard deviations are shown in parentheses.

<b>Watershed</b>	<b>June</b>	<b>July</b>	<b>Mean</b>
WIL	1432.84 (723.60)	1819.98 (687.72)	1609.33 (741.06)
TRE	5066.46 (6294.81)	8995.21 (20929.80)	6999.65 (15354.67)
UQL	7007.69 (5935.10)	10143.53 (14777.86)	8522.76 (11299.94)
ZIE	9323.49 (8514.06)	25595.80 (20502.07)	16555.63 (16313.68)

Topographically, LI decreased linearly from the shoulder to the riparian zone (Table 10). Summit plots, however, had lower light intensity on average than the shoulder plots. This same pattern was demonstrated in June and July (Table 10). In general, the ET rate was positively correlated to plot LI across watersheds (Figure 16). This relationship was best described by a second-order polynomial function (Adjusted  $R^2 = 0.4449$ , p-value:  $< 2.2e-16$ ).

**Table 10: Mean Light Intensity of Plots by Month**

Light intensity is in lux.

<b>Watershed</b>	<b>Riparian</b>	<b>Toeslope</b>	<b>Sideslope</b>	<b>Shoulder</b>	<b>Summit</b>
Early June					
Williams	715.13	2019.94	1725.83	822.36	1357.60
Treat	857.53	2432.65	2392.68	5625.96	13125.88
Uqlidisi	2501.42	4688.78	2578.57	16275.11	11007.95
Ziemer	2318.87	7721.33	24068.22	8292.13	4836.13
<b>All</b>	1653.70	3940.33	7516.19	8116.39	8417.22
Late July					
Williams	2296.32	2647.94	1137.62	960.14	1889.08
Treat	1077.28	19994.97	2525.95	5597.26	14811.23
Uqlidisi	9182.27	3793.70	5673.79	31229.84	8094.49
Ziemer	2913.45	3885.78	45122.52	42504.71	20972.98
<b>All</b>	4457.88	6954.48	11932.96	24104.09	12697.89

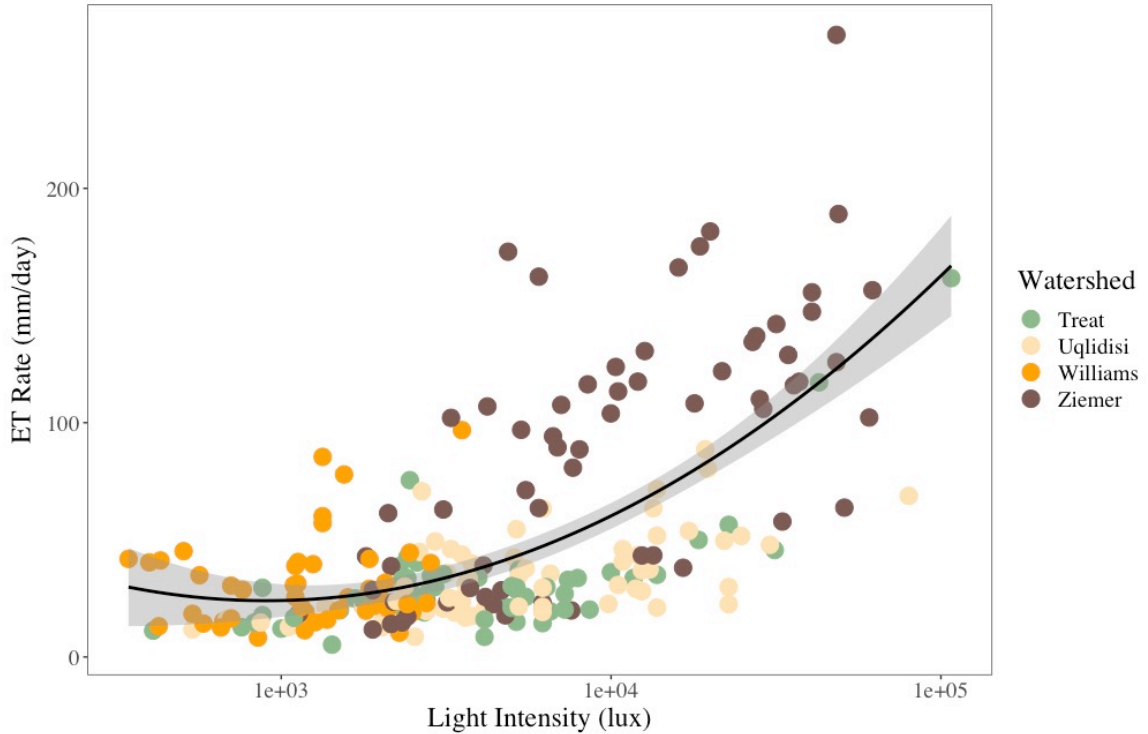


**Figure 16: ET Rate vs. Light Intensity by Watershed**

Trend line represents a second-order polynomial function. Shading represents the 95% confidence interval.

## 2) Soil Volumetric Water Content

At the time of the early June measurements, soil volumetric water content (VWC) was highest at ZIE ( $\mu = 24.1\%$ ) and lowest at WIL ( $\mu = 19.3\%$ ). In July, however, VWC was highest at TRE ( $\mu = 19.2\%$ ), followed by ZIE ( $\mu = 17.1\%$ ). The control WIL watershed remained the watershed with the lowest VWC ( $\mu = 12.1\%$ ). Mean VWC was lower in late July than in early June for all watersheds (Table 11).

Mean soil VWC was highest at the summit plots ( $\mu_{\text{June}} = 25.83$ ,  $\mu_{\text{July}} = 20.29$ ) and lowest at the riparian plots ( $\mu_{\text{June}} = 19.74$ ,  $\mu_{\text{July}} = 13.50$ ) for both June and July

measurements. The toeslope ( $\mu_{\text{June}} = 20.98$ ,  $\mu_{\text{July}} = 15.98$ ), sideslope ( $\mu_{\text{June}} = 22.07$ ,  $\mu_{\text{July}} = 15.43$ ), and shoulder ( $\mu_{\text{June}} = 21.14$ ,  $\mu_{\text{July}} = 13.56$ ) plots did not display a consistent temporal pattern (Table 11).

**Table 11: Mean Soil VWC (%) by Plot**

<b>Watershed</b>	<b>Riparian</b>	<b>Toeslope</b>	<b>Sideslope</b>	<b>Shoulder</b>	<b>Summit</b>
Early June					
Williams	17.90	21.66	18.37	16.94	20.43
Treat	23.10	23.25	20.93	21.82	29.34
Uqlidisi	16.70	20.15	18.51	20.88	26.51
Ziemer	23.07	18.82	30.80	22.46	24.73
<b>All</b>	19.74	20.98	22.07	21.14	25.83
Late July					
Williams	10.00	14.99	12.00	9.70	12.45
Treat	17.47	20.98	15.03	16.12	25.47
Uqlidisi	12.08	13.49	13.96	12.17	21.99
Ziemer	15.15	16.06	22.35	14.79	17.87
<b>All</b>	13.50	15.98	15.43	13.56	20.29

ET rate did not exhibit a consistent trend with VWC, either within or across watersheds (Figure 17).

Between June and July, VWC decreased across all watersheds, while LI increased across most watersheds (Table 12). The largest change in VWC was in WIL, which also experienced the largest decrease in ET rate. ZIE had the largest increase in LI, while LI at UQL actually decreased from June to July. TRE experienced the smallest change in both VWC and LI, which corresponded to only a 2.7% decrease in ET rate.

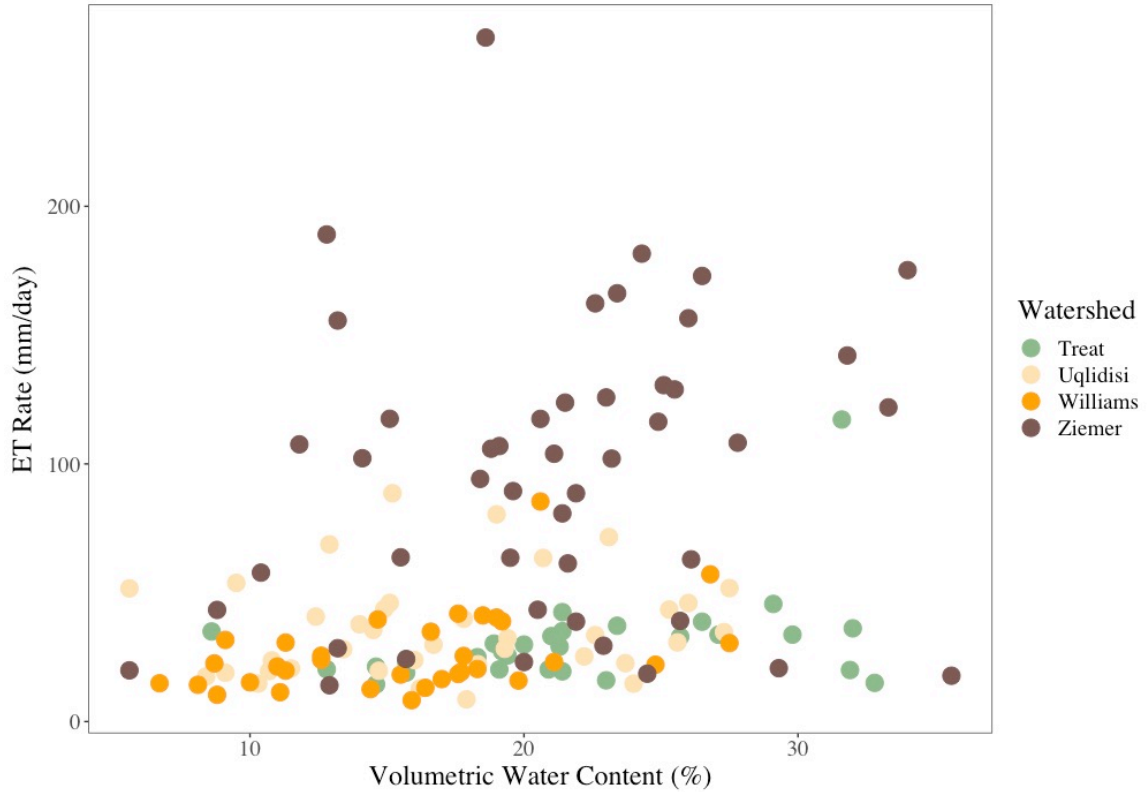


**Figure 17: ET rate vs VWC by Watershed**

**Table 12: Percent Change in ET Rate, VWC, and LI from June to July**

<b>Watershed</b>	<b>ET rate</b>	<b>VWC</b>	<b>LI</b>
WIL	-42.7%	-39.1%	+39.15%
TRE	-2.7%	-13.2%	+12.84%
UQL	-17.6%	-17.1%	-26.47%
ZIE	-20.2%	-27.7%	+333.67%
ALL	-23.0%	-21.4%	+50.86%

## ***Multiple Regression Models***

### **Sprouts**

Multiple regression modeling suggests that temperature, leaf area, and light intensity had the largest effect on sprout ET rate across watersheds (Table A9). Species and VWC were of lesser importance, but were still significant terms in the full model. Percent harvest was slightly correlated with both basal area and elevation, so it was removed from the full model. All interaction terms had high VIFs, meaning they increased multicollinearity in the model, so they were removed as well. The best model for predicting ET rate across all watersheds, as selected by AIC using the “stepAIC” command, was:

$$y_{ij} = 0.000924*LI + 3.98*T + 0.851*VWC + 0.00692*LA + Intercept_j + \varepsilon_{ij} \quad \text{Eqn. 5,}$$

where LI is light intensity (lux), T is temperature (°C), VWC is volumetric water content (%), LA is leaf area (cm<sup>2</sup>),  $y_{ij}$  is evapotranspiration rate for plant i of species j,  $Intercept_j$  is the intercept for species j (Table 13), and  $\varepsilon_{ij}$  is the random error.

All of these terms were statistically significant aside from species (Table 14; Table A10). Temperature had the highest influence on sprout ET rate. Despite the fact that this model was not watershed-specific, the fit was quite high ( $R^2 = 0.7545$ ). Because of its high predictive power, this model was also used on data subset for each watershed. This was done for the purpose of directly comparing the effects of the most influential variables (VWC, LI, LA, and T) on sprout ET rate within each watershed (Figure 18; Appendix).



**Table 13: Best-Approximating Model Intercepts for each Sprout Species**

<b>Species</b>	<b>Intercept</b>
VAOV	-71.3
SESE	-7.07
LIDE	-8.01

**Table 14: Variables that were Significantly Correlated with Sprout Evapotranspiration Rate within each Watershed**

Bolded variables indicate a positive relationship, while standard-type indicates a negative relationship. Significance threshold was set at  $\alpha = 0.05$ . VWC, volumetric water content (%); T, temperature ( $^{\circ}\text{C}$ ); BA, basal area ( $\text{ft}^2$ ); LI, light intensity (lux); EL, elevation (m); LA, leaf area ( $\text{cm}^2$ ).

<b>Watershed</b>	<b>Significant variables</b>
All	<b>T, LI, LA, VWC</b>
WIL	BA, T
TRE	<b>LI, EL</b>
UQL	<b>Log<sub>10</sub>(LI)</b>
ZIE	<b>T, LI, LA</b>

Marginal effect predictions suggest that ET rate responds to environmental variables differently across watersheds. While VWC had little effect on ET rate in the intensely harvested watershed ZIE and the lightly harvested watershed TRE, it greatly influenced ET rate in the control watershed WIL and the moderately harvested watershed UQL (Figure 18). Species, LI, and LA had little effect on ET rate in WIL compared to temperature and VWC (Table A11). However, LI had a large effect on ET rate in TRE (Table A12) and UQL (Table A13) and LA was important in ZIE (Table A14).

Temperature, which was the most important variable in predicting ET rate across watersheds (Table A10) had a strong effect on ET rate in WIL and ZIE (Figure 18).

However, ET and temperature display a slightly negative trend at TRE. Light intensity displayed the most consistent positive correlation with sprout ET rate.

The full model was also applied to each watershed individually and used to find watershed-specific best-approximating models. At the control watershed WIL, variation in ET rate was best described by temperature, followed by basal area. Effect size indices for all other variables were rather low (Table A15). BA and temperature explained 70% of the variation in ET rate at WIL (Table 14; Table 15) and both terms were statistically significant (Table A16).

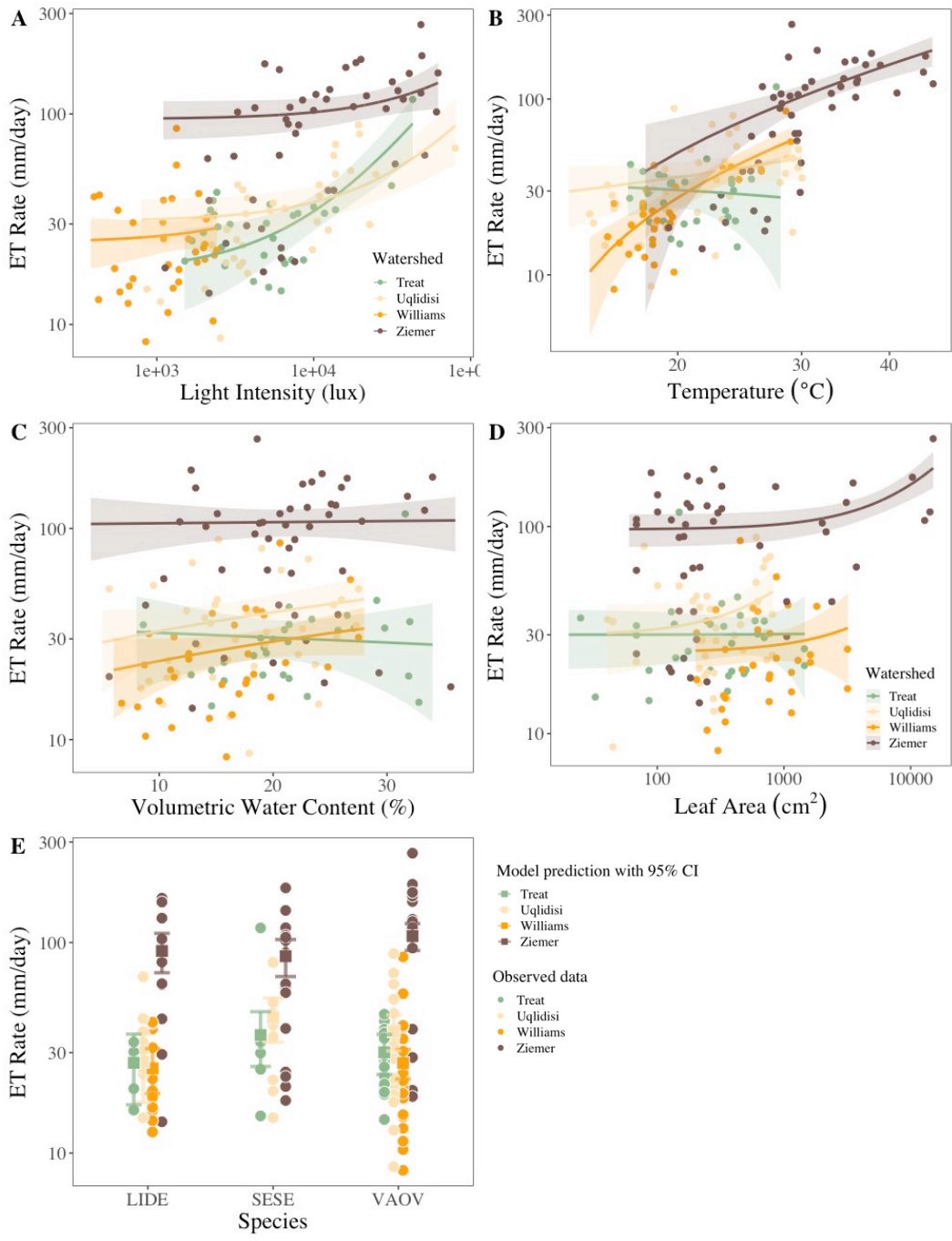


**Figure 18: Marginal Effects of Several Predictor Variables on Sprout ET Rate**

Predictions were made using ggeffects via the overall best fit sprout model using data subset for each watershed. Marginal effects of each variable were made by holding other variables at their mean value. The species intercept for VAOV was used as the baseline intercept for plots A-. Lines denote model predictions with a 95% confidence interval while points denote observed data.

**Table 15: Best-Approximating Models for Sprout Evapotranspiration Rate by Watershed**

The best-approximating models were those with the lowest AIC values. See Appendix B. VWC, volumetric water content (%); T, temperature (°C); BA, basal area (ft<sup>2</sup>); LI, light intensity (lux); EL, elevation (m); LA, leaf area (cm<sup>2</sup>);  $y_i$ , evapotranspiration rate for plant  $i$  (mm/day);  $\varepsilon$ , random error.

<b>Watershed</b>	<b>Best-approximating model</b>	<b>Adj. R<sup>2</sup></b>	<b>p-value</b>
All	$y_{ij} = 0.000924*LI + 3.98*T + 0.851*VWC + 0.00692*LA + Intercept_j + \varepsilon_{ij}$	0.7545	< 2.2e-16
WIL	$y_i = 3.90*T - 0.447*BA - 43.4 + \varepsilon_i$	0.7017	5.013e-09
TRE	$y_i = 0.00210*LI - 1.65*BA - 0.0392*EL + 79.0 + \varepsilon_i$	0.6832	4.93e-07
UQL	$y_i = 26.8*\log_{10}(LI) + 0.121*EL - 86.6 + \varepsilon_i$	0.5559	3.848e-07
ZIE	$y_i = 0.000743*LI + 5.56*T + 0.00716*LA - 99.9 + \varepsilon_i$	0.6507	1.561e-10

At the lightly harvested watershed TRE, LI had the largest effect on ET rate. Elevation, temperature, species, and VWC also had high effect sizes. (Table A17). The best model at TRE was based on LI, elevation, and BA (Table 14) and described 68% of the variation in ET rate. BA, however, was not statistically significant (Table A18).

LI also had the largest effect on ET rate in the moderately harvested watershed UQL. Variation was relatively evenly distributed among the other variables, but basal area was the least important (Table A19). The top model at UQL was based on LI and elevation, but the adjusted R-squared was very low. Applying a Log10 transformation to LI provided a much better fit, since LI encompasses a wide range of values at UQL. However, the R<sup>2</sup> was still much lower for UQL than for other watersheds (Table 15). Furthermore, elevation was not statistically significant (Table A20).

At the intensely harvested watershed ZIE, temperature and LA had the largest

effect sizes, followed by LI and species (Table A21). ET rate at ZIE was best described by temperature, LI, and LA (Table 15). All three terms were statistically significant and explained 65% of the variation in ET rate at ZIE (Table A22; Table 14).

## Ferns

Similarly to the sprouts, multiple regression modeling suggests that temperature and LI had a large effect on ET rate in ferns across watersheds. In contrast to the sprout group however, percent harvest and basal area had a large effect size on ET rate, while VWC was relatively unimportant (Table A23). Despite the relationship between percent harvest and ET rate, percent harvest was removed from the model since it was slightly correlated with basal area and elevation. Species was also removed from the model since it had the lowest effect size, and because both fern species were not present in every watershed. Using stepwise model selection, the best fit model chosen for predicting ET rate of ferns across watersheds was:

$$y_i = 0.000961*LI + 3.35*T + 0.438*VWC - 0.212*BA - 0.106*EL - 29.3 + \varepsilon_i \quad \text{Eqn. 6,}$$

where LI is light intensity (lux), T is temperature (°C), VWC is volumetric water content (%), BA is canopy basal area (ft<sup>2</sup>), EL is elevation (m),  $y_i$  is evapotranspiration rate for plant  $i$ , and  $\varepsilon_i$  is the random error.

Together, these variables described 77% of variation in fern ET rate across watersheds (Table 16). BA and elevation, however, were not statistically significant (Table 17, Table A24).

In WIL, temperature had the largest effect on ET rate of ferns. Biomass and LI

also had high effect sizes (Table A25). In contrast to the cross-watershed model, basal area and elevation at WIL were the least influential on ET rate. Temperature, biomass, and LI explained 85% of the variation in ET rate at WIL (Table 16). Biomass, however, was not statistically significant (Table A26).

As it did for the sprouts group, LI had a large effect on ET rate in ferns at TRE. In contrast to WIL, elevation and BA had a large effect on fern ET rate in TRE while temperature and biomass had little effect (Table A27). Elevation, BA, and LI described 83% of the variation in ET rate at TRE, but elevation was not statistically significant (Table A28).

Elevation, VWC, and temperature had equally large effect on fern ET rate in UQL (Table A29). These three variables, along with LI, were the most effective at predicting ET rate in UQL. LI, however, was not statistically significant (Table A30). As was the case for sprouts in UQL, the best fit model for fern ET in UQL demonstrated a poor fit compared to other watershed models ( $R^2 = 0.45$ ; Table 16).

As they did in TRE, elevation, BA, and LI had a large effect on ET rates of ferns in ZIE (Table A31). Temp, however, was the most influential variable. The effect size of VWC was extremely low, as it was for the sprout group. The top model at ZIE was based on BA, LI, temp, and elevation (Table A32). All terms were significant, and the model for ZIE demonstrated the best fit of the watershed models ( $R^2 = 0.93$ ; Table 16).

**Table 16: Best-Approximating Models for Fern Evapotranspiration Rate by Watershed**

The best-approximating models were those with the lowest AIC values. See Appendix B. VWC, volumetric water content (%); T, temperature (°C); BA, basal area (ft<sup>2</sup>); LI, light intensity (lux); EL, elevation (m); BM, biomass (g);  $y_i$ , evapotranspiration rate for plant  $i$  (mm/day);  $\varepsilon_i$ , random error.

Watershed	Best-approximating model	Adjusted R <sup>2</sup>	p-value
All	$y_i = 0.000961*LI + 3.35*T + 0.438*VWC - 0.212*BA - 0.106*EL - 29.3 + \varepsilon_i$	0.7716	< 2.2e-16
WIL	$y_i = 4.67*T + 0.00714*LI - 0.330*BM - 68.4 + \varepsilon_i$	0.8452	4.028e-06
TRE	$y_i = 0.00129*LI - 2.41*BA - 0.415*EL + 92.1 + \varepsilon_i$	0.8267	6.671e-10
UQL	$y_i = 0.000655*LI - 0.245*EL + 1.54*VWC + 2.07*T + 2.75 + \varepsilon_i$	0.4464	1.246e-3
ZIE	$y_i = 0.00160*LI + 3.68*T - 0.446*BA - 0.643*EL - 80.6 + \varepsilon_i$	0.9292	4.206e-08

**Table 17: Variables that were Significantly Correlated with Fern Evapotranspiration Rate within each Watershed**

Bolded variables indicate a positive relationship, while standard-type indicates a negative relationship. Significance threshold was set at  $\alpha = 0.05$ . VWC, volumetric water content (%); T, temperature (°C); BA, basal area (ft<sup>2</sup>); LI, light intensity (lux); EL, elevation (m).

Watershed	Significant variables
All	<b>T, LI, VWC</b>
WIL	<b>LI, T</b>
TRE	<b>LI, BA</b>
UQL	<b>VWC, EL, T</b>
ZIE	<b>EL, BA, T, LI</b>

In every watershed, fern ET rate demonstrated a positive relationship with LI. This correlation was significant in every watershed except UQL (Table 17). The nature of the relationship was similar across watersheds, but the slope of ET rate vs. LI was slightly higher in TRE (Figure 19A). TRE also had the widest range of LI values. While most watersheds also displayed a positive relationship in fern ET rate with temperature, this relationship was slightly negative in TRE (Figure 19B). ZIE saw much higher temperatures than other watersheds, sometimes upwards of 40°C.

In most watersheds, there is little correlation between fern ET rate and VWC. The most pronounced relationship is in UQL (Figure 19C). TRE also has a slight positive correlation, and has the largest range of VWC values. Biomass did a poor job of estimating fern ET rate all around and did not contribute significant variation to any model. Although it was selected as a variable in the best fit model for WIL, it was not statistically significant, and the nature of this relationship was actually negative (Figure 19D). Fern ET rate at all watersheds was negatively correlated with both elevation and basal area. The relationship of ET rate and basal area was much stronger in TRE and ZIE than in UQL and WIL (Figure 19E). Similarly, elevation had little to no effect on ET rate in WIL (Figure 19F).



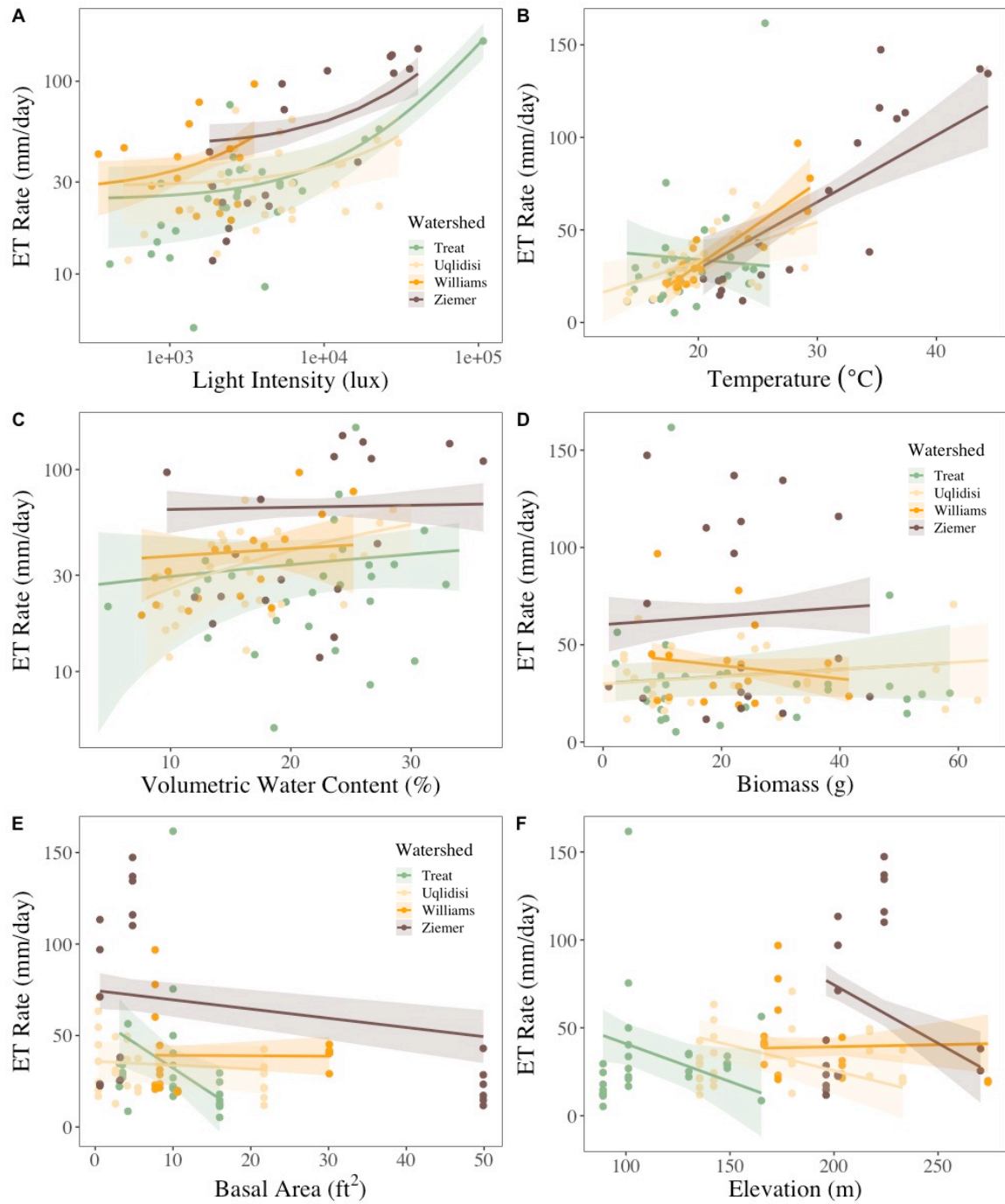


**Figure 19: Marginal Effects of Several Predictor Variables on Fern ET Rate**

Predictions were made from watershed-specific multiple regression models using ggeffects. Marginal effects of each variable were made by holding other variables at their

mean value. Lines denote model predictions with a 95% confidence interval while points denote observed data.

## DISCUSSION

### *Watershed Vegetation*

Although understory ET rates were highest in the intensively harvested watershed (ZIE), understory diversity was greatest in the thinned stands, TRE and UQL. Both ZIE and the control watershed, WIL, had much lower Shannon diversity indices than the thinned watersheds. The understory in ZIE consisted mainly of *V. ovatum*, *S. sempervirens*, and *L. densiflorus*, which are all tree species with a high propensity to sprout from stumps (Figure 9). TRE and UQL had the highest average number of species per plot, and the understory in these watersheds was rich in herbs and ferns (Figure 9). ZIE had the highest density of understory plants, followed closely by UQL (Figure 8). WIL had the lowest density, diversity, and richness (Table 4).

Soil water and light availability was virtually unlimited in the heavily harvested stands, allowing for enhanced growth of subcanopy vegetation and likely driving the high stem density at ZIE. At UQL, understory density was potentially high due to new colonizing plants, as well as the preservation of pre-harvest vegetation that was not as heavily disturbed by logging operations as the vegetation in ZIE. The heterogeneity in microhabitats caused by the harvesting operations also likely led to the higher species richness in TRE and UQL – leaving some canopy intact maintained favorable environments for already established shade tolerant species, while increased light and

water availability promoted the growth of overstory tree sprouts and early successional species.

These results are consistent with the intermediate disturbance hypothesis, which proposes that species diversity is enhanced by nonequilibria of an environment, and is greatest following a moderate disturbance (Huston, 1979). This has been demonstrated by the understory in forest stands following beetle kill (Stone & Wolfe, 1996; Yeager & Riordan, 1953), forest fires (Grandpré *et al.*, 1993; Hart and Chen, 2008), and logging (Atauri *et al.*, 2004; Hart and Chen, 2008). However, results are conflicting. Some studies have found no trend between harvesting intensity and subcanopy diversity post harvesting (Duguid and Ashton, 2013). Although understory density and diversity sampling was conducted within study plots alone, and may not be representative of the entire watershed, my data support the theory that understory diversity is greatest in moderately harvested stands.

This kind of competitive nonequilibria has also been shown to enhance sprout development. Studies have observed the highest sprout density in stands with the lowest residual canopy density following harvesting (Yanai, Twery and Stout, 1998), including studies conducted in coast redwood forests (O'Hara *et al.*, 2007). *S. sempervirens* is known for its ability to sprout from stumps and lignotubers, giving it a competitive advantage over other conifers (Del Tredici, 1998). Following disturbance, redwoods sprout prolifically (Olson Jr., Roy and Walters, 1990; O'Hara *et al.*, 2017). Thus, redwood stands that are managed for timber resources are often thinned to promote sprouting and growth of larger diameter trees (Boe, 1974; Hara *et al.*, 2015; O'Hara *et al.*, 2007; O'Hara *et al.*, 2017). Within established understory density sampling plots, we

observed a higher number of redwood sprouts in UQL and TRE than in ZIE. Redwoods often sprout vegetatively in clumps near a “mother tree” rather than via sexual reproduction (O’Hara *et al.*, 2017). Thus, it is likely that increased access to water and light in addition to ample redwood biomass for vegetative sprouting promoted sprout development in the thinned watersheds in the South Fork Caspar Creek. It is possible, however, that succession could impact this regeneration pattern. Redwoods tend to aggressively close small canopy gaps, which can slow regeneration in thinned or selectively logged forest stands (O’Hara *et al.*, 2017). With time, mature trees may shade out seedlings at TRE and UQL while seedlings at ZIE are able to grow into a member of the new canopy. On the other hand, understory sampling was not designed to specifically account for redwood sprouts, and heterogeneity due to redwood clumping could have biased these results.

### ***Evapotranspiration Rates across Watersheds***

As predicted, the mean understory ET rate in both June and July was highest in the ZIE watershed. Because ZIE had the highest harvest rate of the watersheds, VWC and LI were also highest. In contrast, WIL, the control watershed, had the lowest mean understory ET rate in both June and July. This corresponds to patterns in VWC and LI, which were also both lowest at WIL. UQL, the moderately harvested watershed, and TRE, the lightly harvested watershed, had similar mean ET rates.

Understory vegetation at ZIE had access to virtually unlimited water and energy to drive transpiration. At WIL, however, the closed canopy reduced incoming light, thus lowering both VPD and ET rates. Furthermore, although WIL and ZIE are geographically

close and receive similar rainfall, water in undisturbed stands was readily transpired by mature trees, leaving WIL's soils drier than ZIE. The similar mean ET rate at UQL and TRE is likely because post-harvest BA was similar between the two watersheds, for two reasons: 1) TRE had a lower pre-harvest BA than UQL in most plots and 2) the summit plot of TRE was harvested by almost 70%, instead of the planned BA reduction of 35%. Thus, environmental conditions between the two watersheds were somewhat similar. However, mean LI was higher at UQL while VWC was higher at TRE. UQL may have experienced an increase in understory ET rate sufficient to offset the increase in VWC expected with canopy removal. The understory vegetation density at UQL was higher than at TRE, so plants there may have faced more competition for water. Thus, while an individual plant at UQL may have had a lower ET rate than one at TRE, net transpiration from the plant community may have been higher in UQL.

Though there are few studies that have measured understory water use after timber harvesting, several studies imply that the understory may use a significant proportion of soil water or may compete with the overstory for resources. For instance, Greenwood *et al.* (1985) measured understory water use in an Australian Jarrah forest and speculated that increased water use by the understory after harvesting may significantly offset decreased water use by the canopy. In a northeastern Oregon forest, reducing Ponderosa pine root density increased understory biomass (Riegel *et al.*, 1992). Similarly, an increase in overstory ET rates was observed following plot-scale removal of the salal dominated understory in a Douglas fir forest (Kelliher *et al.*, 1986). In the South Fork Caspar Creek, understory ET rates were significantly higher in intensely harvested plots than in the control plots and thinned plots. However, more thorough sampling is

needed in order to fully quantify total ET from each watershed, particularly to determine if the effect of harvesting on ET rates is persistent across time.

### ***Topography, Basal Area, and Soil Water Relations***

Across the study watersheds, the influence of hillslope position on mean ET rate was only evident at the riparian sites which, on average, had much lower ET rates than the other plots. In the unharvested WIL, however, mean ET rate at the riparian plot was higher than the other hillslope plots (excluding the toeslope) in June and higher than all plots in July. Across watersheds, VWC was highest at the sideslope plots. While VWC was still relatively high at the sideslope of WIL, the lack of large variation in basal area among plots at WIL had an influence on soil moisture distribution. VWC remained comparatively high down to the toeslope, and then decreased slightly in the riparian zone of WIL, likely due to transpiration by several large conifers.

Topography and basal area may both impact transpiration on a landscape by influencing water availability. In this study, basal area was controlled by harvesting operations, which in turn may also be limited by topography. For example, since the riparian plots were within the WLPZ, they could not be harvested to meet the targeted basal area reduction without breaking California riparian management laws. Furthermore, merchantable trees that are at the top of the hillslope are much easier to fell than those at the bottom of the stream valley, and many were left undisturbed the last time South Fork Caspar Creek was clear-cut. Thus, even before harvesting outside the WLPZ, basal area across watersheds was generally higher in the riparian and toeslope plots. This means that even WIL, which was not disturbed, has much a higher basal area in the riparian plot than

at other positions along the hillslope. Thus, a plot's position on the hillslope influences soil water availability via both variation in canopy cover and lateral downslope water flow. In TRE, UQL, and ZIE, soil water was proportional to basal area. In WIL, however, topography and geomorphology were likely the main controls on VWC. Across watersheds, VWC was likely highest at the sideslope plots because this was the furthest downslope water could move before it was transpired in the WLPZ, where basal area is on average higher.

Studies have shown that geomorphology, topography, and soil thickness influence VWC along a hillslope profile (Famiglietti *et al.*, 1998; Tromp-van Meerveld and McDonnell, 2006; Dymond *et al.*, 2017). Soil water is likely to be higher below the mid-slope of a hill, as hillslope processes promote downslope movement of soil and water. However, vegetation may also influence this pattern. As a mature coast redwood tree may consume around 600 liters of water per day (Dawson, 1998), high basal area is likely to decrease soil VWC within a stand. Stand thinning has been shown to increase soil moisture in red pine forest stands (Sucoff and Hong, 1974) and reduce water stress in lodgepole pine (*Pinus contorta* var. *latifolia*) in Montana (Donner and Running, 1986). Similarly, one study which compiled data across water-stressed areas of the southwestern United States found a positive relationship between stand basal area and tree mortality (Bradford and Bell, 2017). In stands with reduced basal area, tree mortality was lower, which may be attributed to decreased moisture stress. Thus, both topography and basal area may influence the distribution of soil water within a watershed.

### ***Environmental and Climactic Controls on Evapotranspiration***

Multiple regression modeling suggests that environmental variables, particularly light, soil moisture, and temperature, vary in their impact on ET rate across watersheds. For example, an increase in soil moisture at the control watershed WIL or the moderately harvested watershed UQL was accompanied by an increase in sprout ET rate (Figure 18). However, an increase in VWC at the lightly harvested watershed TRE or the intensely harvested watershed ZIE had little effect on ET rate when other variables were held constant. This indicates that soil water is not limiting understory transpiration at TRE and ZIE, but it is at UQL and WIL. In the WIL watershed, VWC decreased by 39% from June to July, compared to the average decrease of 21%. This was accompanied by a decrease in ET rate of almost half, in comparison to the average 23% decrease across watersheds (Table 12). In all watersheds, a decrease in mean ET rate was observed from June to July. This change was not as large in UQL as it was in WIL, but ET rate in UQL did decrease proportionally to VWC between sampling periods. TRE displayed the smallest decrease across watersheds, which corresponded to what was also the smallest decrease in LI and VWC. Interestingly, while other watersheds saw an increase in LI from June to July, UQL saw a 26% decrease. At ZIE, LI increased by 334% between June and July measurements. However, even as transpiration rate and LI at ZIE are positively correlated, mean plant ET rate at ZIE decreased by 20%. Sprout and fern ET rate at ZIE was most strongly correlated with temperature. Temperature was also a significant factor at WIL for both sprouts and ferns.

Multiple regression modeling suggests that timber harvesting increases understory transpiration rate by altering environmental conditions and reducing water stress. In WIL,



where the forest had progressed farther via succession, ET was likely limited by VWC during the dry summer months. Since the canopy cover was higher in WIL, understory vegetation must compete for soil water with overstory trees and the mature mid-story. Water was thus in higher demand, and soil water was depleted. In ZIE, soil moisture was more abundant due to the loss of overstory trees as a flux of water back to the atmosphere. Thus, the understory was not stressed for water and ET rates remained high despite varying VWC at the time of ET measurements. Although ZIE did show a positive correlation with LI, the slope was small, indicating that light was also not a limiting factor in the heavily harvested watershed. Light intensity is positively correlated with photosynthesis, and thus with transpiration. However, at high light intensity, photosynthesis reaches a maximum, called the light saturation point. At this point, increasing light intensity no longer increases photosynthesis rate. Furthermore, under high light conditions, excess energy that cannot be converted into energy via photochemistry may damage plants by producing harmful reactive oxygen compounds (Taiz and Zeiger, 2002). Thus, photosynthesis is less efficient at high light, and may lead to decreased transpiration rates if stomatal closure occurs. This could partially explain the decrease in ET rate in ZIE from June to July. Temperature could also have impacted this decrease – the sideslope, shoulder, and summit plots of ZIE reached much higher temperatures than other plots across watersheds. Temperature increases transpiration by increasing the kinetic energy of water (Taiz and Zeiger, 2002). In high temperatures, plants are likely to keep their stomata open to allow for the cooling effect of transpiration. However, stomatal closure is likely to occur at high temperatures if the plant is also stressed for water (Schulze *et al.*, 1973). The several ET rate measurements taken over 40

°C in ZIE all fell below the regression line, suggesting a slight decrease in transpiration associated with high temperatures. However, temperature had a strong positive effect overall on sprout and fern ET rate in both ZIE and WIL (Figure 18 & 19). At ZIE, this was likely a result of the contrast in temperature between the shaded riparian plot and the sunny higher elevation plots. At WIL, where the understory is shaded, temperature may be considered a limiting factor and warm weather is likely to beneficially impact transpiration.

While it may be expected that ecophysiological processes at UQL would be similar to TRE or ZIE, sprouts and ferns at UQL were more similar to WIL in their response to abiotic factors. UQL and WIL are geographically near each other, but their proximity did not influence similarity in any measured variable. UQL is also near TRE, but both environmental variables and plant physiological response to those variables were much different between the two watersheds despite their similar mean ET rate. UQL had a more intense harvest rate than TRE, but plants at TRE and ZIE were more similar in their response to environmental factors. Harvesting at the summit plot of TRE may have been one reason why UQL and TRE were relatively dissimilar ecophysiological. Due to an almost 200% overharvest of this plot, the effect of VWC on ET rate may have been overwhelmed by the effect of LI. Like ZIE, VWC at TRE was quite high across topographic positions and throughout the summer. Thus, it was likely not limiting transpiration. On the other hand, the high understory stem count at UQL could increase competition for soil water between residual overstory trees and subcanopy vegetation. Another possible reason for the differences observed between UQL and TRE is VPD. UQL and TRE are the closest study catchments to the coast, and thus generally had more

fog cover than ZIE and WIL. This proximity to the coast may have provided a climactic buffer from the late summer sun and heat. The summit of UQL is at a much higher elevation than the summit of TRE, so UQL could possibly see more fog than TRE. The only day of sampling that had notable fog was on 7/26/19, when sampling was conducted at the riparian, toeslope, and shoulder plots of UQL. Fog lowers VPD by increasing absolute humidity of the air, which would slow transpiration. In contrast, sampling at UQL was also conducted on cooler, sunny, breezy days. This would increase VPD and transpiration rates. This gradient of VPD during sampling days may be responsible for the unexplained variance observed in the models developed for ET rate by UQL sprouts and ferns. Fog may also explain the decrease in mean LI at UQL from June to July.

Multiple studies have demonstrated an increase in ET rates of Mediterranean plants during autumn wet-up and spring warm-up, while drought in the summer and cool temperatures in the winter limit photosynthesis (and thus transpiration) seasonally (Flexas *et al.*, 2014). Though VWC in South Fork Caspar Creek watershed does not generally reach its minimum until fall, understory vegetation ET rate had already begun to decrease in late July. A decrease in transpiration and photosynthesis between early and late summer has also been demonstrated by several Mediterranean tree and shrub species in Cordoba, Spain (Quero *et al.*, 2011). This was associated with a decrease in stomatal aperture due to increased water stress. Another study conducted in Mendocino County, California, found that peak transpiration of several tree species occurred in June and July, and then steadily decreased as soils dried (Link *et al.*, 2014). More research is needed in order to determine the timing of peak understory transpiration in relation to canopy transpiration. Studies have shown that VWC may be the primary factor controlling

understory biomass production, and thus transpiration, in a seasonally dry climate (Riegel *et al.*, 1992). However, this may not be the case if the overstory is removed, which frees the understory from belowground competition for water. My data support that summer transpiration of sprouts and herbaceous vegetation is limited by soil water in an undisturbed forest stand, but not in a heavily harvested forest stand. Where soil and light were not limiting, temperature was the main influence on understory plant transpiration rate.

## **CONCLUSION**

A rapid ET chamber was developed for measuring ET rates of understory vegetation. This apparatus was adequate for comparing means of ET rate across watersheds, and the compact and lightweight construction made it ideal for portability in the field. Solo operation was manageable, but it was much easier with two people. Steep and heterogeneous catchments, such as those in this study, may be a more challenging environment for adopting this methodology without two sets of hands conducting measurements. However, this chamber is easily adaptable, and would be a simple, affordable option for measuring ET of small vegetation in any landscape.

In the South Fork Caspar Creek watershed, understory evapotranspiration was higher in logged catchments than in the undisturbed catchment. The highest ET rate was observed in the most intensely harvested watershed, which had been reduced in basal area by about 75%. However, increased understory ET rate was observed in the thinned watersheds as well. The higher understory ET rate seems to be caused by an increase in soil water, which is thought to limit productivity in Mediterranean climates. Multiple

regression modeling and marginal effect predictions indicate that VWC has a large impact on ET rates in the control watershed, but less impact on ET rates in harvested watersheds since it is virtually unlimited for shallow-rooted vegetation. In the intensely harvested watershed, where soil water and light were not limiting, temperature had the largest effect on ET rate.

These results imply that understory vegetation may represent a significant component of the hydrologic cycle in harvested forest stands and merits greater attention in both scientific studies and in forest management decisions. Quantifying understory and overstory ET at the landscape scale would provide better insight into how disturbance impacts soil water apportionment after disturbance.

## BIBLIOGRAPHY

- Akaike, H. (1974) 'A new look at the statistical model identification', *IEEE Transactions on Automatic Control*, 19(6), pp. 716–723. doi: 10.1109/TAC.1974.1100705.
- Allen, C. D. *et al.* (2010) 'A global overview of drought and heat-induced tree mortality reveals emerging climate change risks for forests', *Forest Ecology and Management*, 259(4), pp. 660–684. doi: 10.1016/j.foreco.2009.09.001.
- Allen, R. G., Pereira, L. S. and Smith, M. (1998) *Crop Evapotranspiration - Guidelines for Computing Crop Water Requirements*, *FAO Irrigation and Drainage Paper*. doi: 10.1017/CBO9781107415324.004.
- Allgood, T. L. (1996) *Comparison of Residual Structure, Recovery, and Diversity in Clearcut and 'New Forestry' Silvicultural Treatments at the Yurok Experimental Forest, a Coast Redwood Type*. Humboldt State University.
- Anapalli, S. S. *et al.* (2016) 'Simulation of crop evapotranspiration and crop coefficients with data in weighing lysimeters', *Agricultural Water Management*. Elsevier B.V., 177, pp. 274–283. doi: 10.1016/j.agwat.2016.08.009.
- Anapalli, S. S. *et al.* (2018) 'Quantifying soybean evapotranspiration using an eddy covariance approach', *Agricultural Water Management*. Elsevier, 209(July), pp. 228–239. doi: 10.1016/j.agwat.2018.07.023.
- Andreasson, F., Bergkvist, B. and Bååth, E. (2009) 'Bioavailability of DOC in leachates, soil matrix solutions and soil water extracts from beech forest floors', *Soil Biology and Biochemistry*, 41(8), pp. 1652–1658. doi: 10.1016/j.soilbio.2009.05.005.
- Arcilla, N., Holbech, L. H. and O'Donnell, S. (2015) 'Severe declines of understory birds follow illegal logging in Upper Guinea forests of Ghana, West Africa', *Biological Conservation*. Elsevier Ltd, 188, pp. 41–49. doi: 10.1016/j.biocon.2015.02.010.
- Atauri, J. A. *et al.* (2004) 'Effects of management on understory diversity in the forest ecosystems of northern Spain', *Environmental Management*, 34(6), pp. 819–828. doi: 10.1007/s00267-004-0180-0.
- Bailey, J. D. *et al.* (1998) 'Understory vegetation in old and young Douglas-fir forests of western Oregon', *Forest Ecology and Management*, 112(3), pp. 289–302. doi: 10.1016/S0378-1127(98)00408-3.
- Barrett, J. W. and Youngberg, C. T. (1965) 'Effect of Tree Spacing and Understory Vegetation on Water Use in a Pumice Soil', *Soil Science Society of America Journal*, 29(4), pp. 472–475. doi: 10.2136/sssaj1965.03615995002900040034x.
- Bates, C. G. and Henry, A. J. (1928) 'Second Phase of Streamflow Experiment At Wagon Wheel Gap, Colorado', *Monthly Weather Review*, 56(3), pp. 79–80. doi: 10.1175/1520-0493(1928)56<79:sposea>2.0.co;2.
- Beck, D. E. (1983) 'Thinning Increases Forage Production in Southern Appalachian Cove Hardwoods', *Southern Journal of Applied Forestry*, 7(1), pp. 53–57.
- Black, T. A. and Kelliher, F. M. (1989) 'Processes controlling understorey

- evapotranspiration', *Forest, Weather and Climate*, 324(1223), pp. 207–231.
- Boe, K. N. (1974) *Thinning Promotes Growth of Sprouts on Old-Growth Redwood Stumps*. Berkeley, CA.
- Boe, K. N. (1975) 'Forest and Range Experiment Station Natural Seedlings and Sprouts after Regeneration Cuttings in Old-Growth Redwood', *USDA Forest Service Research Paper*, pp. 1–17.
- Bosian, G. (1962) 'The Controlled Climate in the Plant Chamber and its Influence Upon Assimilation and Transpiration', in *Methodology of plant eco-physiology: proceedings of the Montpellier Symposium*, pp. 225–232.
- Bradford, J. B. and Bell, D. M. (2017) 'A window of opportunity for climate-change adaptation: easing tree mortality by reducing forest basal area', *Frontiers in Ecology and the Environment*, 15(1), pp. 11–17. doi: 10.1002/fee.1445.
- Burba, G. and Anderson, D. (2007) 'Introduction to the eddy covariance method', ... (2007). *Introduction to the eddy covariance method. LI- ...*, pp. 1–141. doi: 10.1016/j.ejpb.2007.03.022.
- Burgess, S. S. O. and Dawson, T. E. (2004) 'The contribution of fog to the water relations of *Sequoia sempervirens* (D. Don): Foliar uptake and prevention of dehydration', *Plant, Cell and Environment*, 27(8), pp. 1023–1034. doi: 10.1111/j.1365-3040.2004.01207.x.
- Bury, R. B. (1983) 'Differences in amphibian populations in logged and old growth redwood forest', *Northwest Science*, 57(3), pp. 167–178.
- Cafferata, P. H. and Reid, L. M. (2013) *Applications of Long-Term Watershed Research To Forest Management in California: 50 Years of Learning From the Caspar Creek Experimental Watersheds*.
- 'California Forest Practice Rules' (2015), 87(250), pp. 855–869.
- Connell, J. H. (1978) 'Diversity in Tropical Rain Forests and Coral Reefs', *Science*, 199(4335), pp. 1302–1310.
- Craig, A. and Macdonald, S. E. (2009) 'Threshold effects of variable retention harvesting on understory plant communities in the boreal mixedwood forest', *Forest Ecology and Management*, 258(12), pp. 2619–2627. doi: 10.1016/j.foreco.2009.09.019.
- Daley, M. J. and Phillips, N. G. (2006) 'Interspecific variation in nighttime transpiration and stomatal conductance in a mixed New England deciduous forest', *Tree Physiology*, 26(4), pp. 411–419. doi: 10.1093/treephys/26.4.411.
- Dawson, T. E. (1998) 'Fog in the California redwood forest: ecosystem inputs and use by plants', *Oecologia*, 117, pp. 476–485.
- Dech, J. P., Robinson, L. M. and Nosko, P. (2008) 'Understorey plant community characteristics and natural hardwood regeneration under three partial harvest treatments applied in a northern red oak (*Quercus rubra* L.) stand in the Great Lakes-St. Lawrence forest region of Canada', *Forest Ecology and Management*, 256(4), pp. 760–773. doi: 10.1016/j.foreco.2008.05.033.

- Delzon, S. and Loustau, D. (2005) 'Age-related decline in stand water use: Sap flow and transpiration in a pine forest chronosequence', *Agricultural and Forest Meteorology*, 129(3–4), pp. 105–119. doi: 10.1016/j.agrformet.2005.01.002.
- Donner, B. L. and Running, S. W. (1986) 'Water Stress Response After Thinning Pinus contorta Stands in Montana', *Forest Science*, 32(3), pp. 614–625. Available at: <https://doi.org/10.1093/forestscience/32.3.614>.
- Duguid, M. C. and Ashton, M. S. (2013) 'A meta-analysis of the effect of forest management for timber on understory plant species diversity in temperate forests', *Forest Ecology and Management*. Elsevier B.V., 303, pp. 81–90. doi: 10.1016/j.foreco.2013.04.009.
- Dymond, S. F. (2016) *Caspar Creek Experimental Watersheds Experiment Three Study Plan: The influence of forest stand density reduction on watershed processes in the South Fork, USDA Forest Service Pacific Southwest Research Station*.
- Dymond, S. F. *et al.* (2017) 'Topographic, edaphic, and vegetative controls on plant-available water', *Ecohydrology*, 10(8), pp. 1–12. doi: 10.1002/eco.1897.
- Ewers, B. E. *et al.* (2002) 'Tree species effects on stand transpiration in northern Wisconsin', *Water Resources Research*, 38(7), pp. 8-1-8–11. doi: 10.1029/2001wr000830.
- Ewers, B. E. *et al.* (2005) 'Effects of stand age and tree species on canopy transpiration and average stomatal conductance of boreal forests', *Plant, Cell and Environment*, 28(5), pp. 660–678. doi: 10.1111/j.1365-3040.2005.01312.x.
- Famiglietti, J. S., Rudnicki, J. W. and Rodell, M. (1998) 'Variability in surface moisture content along a hillslope transect: Rattlesnake Hill, Texas', *Journal of Hydrology*. Elsevier, 210(1–4), pp. 259–281. doi: 10.1016/S0022-1694(98)00187-5.
- Farber, M., Attia, Z. and Weiss, D. (2016) 'Cytokinin activity increases stomatal density and transpiration rate in tomato', *Journal of Experimental Botany*, 67(22), pp. 6351–6362. doi: 10.1093/jxb/erw398.
- Fisher, D. K. (2012) 'Simple weighing lysimeters for measuring evapotranspiration and developing crop coefficients', *International Journal of Agricultural and Biological Engineering*, 5(3). doi: 10.3965/j.ijabe.20120503.00?
- Fisher, J. B. *et al.* (2005) 'Evapotranspiration models compared on a Sierra Nevada forest ecosystem', *Environmental Modelling and Software*, 20(6), pp. 783–796. doi: 10.1016/j.envsoft.2004.04.009.
- Flexas, J. *et al.* (2014) 'Photosynthetic limitations in Mediterranean plants: A review', *Environmental and Experimental Botany*. Elsevier B.V., 103, pp. 12–23. doi: 10.1016/j.envexpbot.2013.09.002.
- Flumignan, D. L., de Faria, R. T. and Prete, C. E. C. (2011) 'Evapotranspiration components and dual crop coefficients of coffee trees during crop production', *Agricultural Water Management*. Elsevier B.V., 98(5), pp. 791–800. doi: 10.1016/j.agwat.2010.12.002.
- Garcia, C. A. *et al.* (2008) *Portable Chamber Measurements of Evapotranspiration at the*



*Amargosa Desert Research Site Near Beatty, Nye County, Nevada, Scientific Investigations Report 2008-5135.*

Gharsallah, O., Facchi, A. and Gandolfi, C. (2013) 'Comparison of six evapotranspiration models for a surface irrigated maize agro-ecosystem in Northern Italy', *Agricultural Water Management*. Elsevier B.V., 130, pp. 119–130. doi: 10.1016/j.agwat.2013.08.009.

Gholz, H. L. *et al.* (1979) *Equations for estimating biomass and leaf area of plants in the Pacific Northwest*, Forestry Research Laboratory, Oregon State University School of Forestry, Corvallis.

Giuggiola, A. *et al.* (2018) 'Competition for water in a xeric forest ecosystem – Effects of understory removal on soil micro-climate, growth and physiology of dominant Scots pine trees', *Forest Ecology and Management*. Elsevier, 409(December 2017), pp. 241–249. doi: 10.1016/j.foreco.2017.11.002.

Gordon, D. T. (1962) 'Growth response of east side pine poles to removal of low vegetation', *Research Notes, Pacific Southwest Forest and Range Experiment Station*, 209.

Grandpré, L., Gagnon, D. and Bergeron, Y. (1993) 'Changes in the understory of Canadian southern boreal forest after fire', *Journal of Vegetation Science*, 4(6), pp. 803–810. doi: 10.2307/3235618.

Graney, D. L. (1988) 'Growth of oak, ash, and cherry reproduction following overstory thinning and understory control in upland hardwood stands of northern Arkansas', in *Fifth Biennial Southern Silvicultural Research Conference*. Memphis, pp. 245–252.

Granier, A. (1985) 'Une nouvelle méthode pour la mesure du flux de sève brute dans le tronc des arbres', *Annales des Sciences forestières*, 42(2), pp. 193–200. doi: 10.1007/BF00117583.

Grant, G. E. and Jones, J. A. (1996) 'Peak flow responses to clear-cutting and roads in small and large basins, western Cascades, Oregon', *Water Resources Research*, 32(4), pp. 959–974. Available at: <http://dx.doi.org/10.1029/95WR03493>; doi:10.1029/95WR03493.

Greenwood, E. A. N. *et al.* (1985) 'Evaporation from the understorey in the Jarrah forest, southwestern Australia', *Journal of Hydrology*, 80, pp. 337–349.

Grieve, B. J. and Went, F. W. (1962) 'An Electric Hygrometer Apparatus for Measuring Water-Vapour Loss From Plants in the Field', in *Methodology of plant eco-physiology: proceedings of the Montpellier Symposium*, pp. 247–257.

Hara, K. L. O., Narayan, L. and Cahill, K. G. (2015) 'Twelve-Year Response of Coast Redwood to Precommercial Thinning Treatments', *Forest Science*, 61(4), pp. 780–789.

Harr, R. D., Fredriksen, R. L. and Rothacher, J. (1979) 'Changes in streamflow following timber harvest in southwestern Oregon', *Department of Agriculture, Forest Service, Pacific Northwest nad Range Experiment Station*, 249.

Hart, S. A. and Chen, H. Y. H. (2008) 'Fire, logging, and overstory affect understory abundance, diversity, and composition in boreal forest', *Ecological Monographs*, 78(1), pp. 123–140. doi: 10.1890/06-2140.1.

- Hartley, R. K. (2012) *Redwood forest conservation: Where do we go from here?*
- Heath, J., Kerstiens, G. and Tyree, M. T. (1997) 'Stem hydraulic conductance of European beech (*Fagus sylvatica* L.) and pedunculate oak (*Quercus robur* L.) grown in elevated CO<sub>2</sub>', *Journal of Experimental Botany*, 48(312), pp. 1487–1489. doi: 10.1093/jxb/48.7.1487.
- Henry, N. (1998) 'Overview of the Caspar Creek watershed study', *Proceedings of the Conference on Coastal Watersheds: The Caspar Creek Story*, pp. 1–9.
- Hibbert, A. R. (1967) 'Forest treatment effects on water yield', in *International Symposium for Hydrology*, pp. 527–543. doi: 10.1.1.545.6751.
- Holbrook, N. M. and Zwieniecki, M. A. (2005) *No Title*. doi: <https://doi.org/10.1016/B978-0-12-088457-5.X5000-X>.
- Huston, M. (1979) 'A General Hypothesis of Species Diversity', *The American Naturalist*, 113(1), pp. 81–101.
- Jasechko, S. *et al.* (2013) 'Terrestrial water fluxes dominated by transpiration', *Nature*, 496(7445), pp. 347–350. doi: 10.1038/nature11983.
- Johnson, E. A. and Kovner, J. L. (1956) 'Effect on Streamflow of Cutting a Forest Understory', *Forest Science*, 2(2), pp. 83–91.
- Kelliher, F. M. *et al.* (1990) 'Partitioning evapotranspiration into tree and understorey components in two young *Pinus radiata* D. Don Stands', *Agricultural and Forest Meteorology*, 50, pp. 211–227.
- Kelliher, F. M., Black, T. A. and Price, D. T. (1986) 'Estimating the effects of understory removal from a Douglas Fir forest using a two-layer canopy evapotranspiration model', *Water Resources Research*, 22(13), pp. 1891–1899. doi: 10.1029/WR022i013p01891.
- Keppeler, E. T. and Ziemer, R. R. (1990) 'Logging effects on streamflow: Water Yield and Summer Low Flows at Caspar Creek in Northwestern California', *Water Resources Research*, 26(7), pp. 1657–1667. doi: 10.1029/WR026i007p01657.
- Köstner, B. (2001) 'Evaporation and transpiration from forests in Central Europe - Relevance of patch-level studies for spatial scaling', *Meteorology and Atmospheric Physics*, 76(1–2), pp. 69–82. doi: 10.1007/s007030170040.
- Kramer, P. J. and Boyer, J. S. (1995) *Water Relations of Plants and Soils*. 2nd edn.
- Lewis, J. *et al.* (2001) 'Impacts of logging on storm peak flows, flow volumes and suspended sediment loads in Caspar Creek, California', *Water Science and Application*, 2, pp. 85–125. doi: 10.1029/ws002p0085.
- Li, S. *et al.* (2008) 'Evapotranspiration and crop coefficient of spring maize with plastic mulch using eddy covariance in northwest China', *Agricultural Water Management*, 95(11), pp. 1214–1222. doi: 10.1016/j.agwat.2008.04.014.
- Li, Y., He, L. and Zu, Y. (2010) 'Intraspecific variation in sensitivity to ultraviolet-B radiation in endogenous hormones and photosynthetic characteristics of 10 wheat cultivars grown under field conditions', *South African Journal of Botany*. Elsevier B.V., 76(3), pp. 493–498. doi: 10.1016/j.sajb.2010.03.005.

- Limm, E. B. *et al.* (2009) 'Foliar water uptake: A common water acquisition strategy for plants of the redwood forest', *Oecologia*, 161(3), pp. 449–459. doi: 10.1007/s00442-009-1400-3.
- Limm, E. B. and Dawson, T. E. (2010) 'Polystichum munitum (Dryopteridaceae) varies geographically in its capacity to absorb fog water by foliar uptake within the redwood forest ecosystem', *American Journal of Botany*, 97(7), pp. 1121–1128. doi: 10.3732/ajb.1000081.
- Lindquist, J. (2007) 'Precommercial Stocking Control of Coast Redwood at Caspar Creek, Jackson Demonstration State Forest', in *Proceedings of the redwood region For. Sci. symposium: What does the future hold?* Albany, CA, pp. 295–304.
- Link, P. *et al.* (2014) 'Species differences in the seasonality of evergreen tree transpiration in a Mediterranean climate: Analysis of multiyear, half-hourly sap flow observations', *Water Resources Research*, 50, pp. 1869–1894. doi: 10.1002/2013WR014979.Reply.
- Little, C. H. A. and Eidt, D. C. (1968) 'Effect of abscisic acid on budbreak and transpiration in woody species', *Nature*, 220(5166), pp. 498–499. doi: 10.1038/220498a0.
- Liu, X. *et al.* (2017) 'Comparison of 16 models for reference crop evapotranspiration against weighing lysimeter measurement', *Agricultural Water Management*. Elsevier B.V., 184, pp. 145–155. doi: 10.1016/j.agwat.2017.01.017.
- Lorimer, C. G. *et al.* (2009) 'Presettlement and modern disturbance regimes in coast redwood forests: Implications for the conservation of old-growth stands', *Forest Ecology and Management*, 258(7), pp. 1038–1054. doi: 10.1016/j.foreco.2009.07.008.
- Luo, C. *et al.* (2018) 'Portable canopy chamber measurements of evapotranspiration in corn, soybean, and reconstructed prairie', *Agricultural Water Management*. Elsevier B.V., 198, pp. 1–9. doi: 10.1016/j.agwat.2017.11.024.
- Maine, J. D. and Leuschner, W. A. (1980) 'Estimating the southern pine beetle's grazing impact', *Bulletin of the Entomological Society of America*, 26(2), pp. 117–120.
- Mallik, A. U. (2003) 'Conifer regeneration problems in boreal and temperate forests with ericaceous understory: Role of disturbance, seedbed limitation, and keystone species change', *Critical Reviews in Plant Sciences*, 22(3–4), pp. 341–366. doi: 10.1080/713610860.
- Medlyn, B. E. *et al.* (2005) 'On the validation of models of forest CO<sub>2</sub> exchange using eddy covariance data: Some perils and pitfalls', *Tree Physiology*, 25(7), pp. 839–857. doi: 10.1093/treephys/25.7.839.
- Meinzer, F. C. *et al.* (1995) 'Environmental and physiological regulation of transpiration in tropical forest gap species: the influence of boundary layer and hydraulic properties', *Oecologia*, 101(4), pp. 514–522. doi: 10.1007/BF00329432.
- Mohan, S. *et al.* (1996) 'Comparison of methods for estimating ref-et', *Journal of Irrigation and Drainage Engineering*, 122(6), pp. 361–364. doi: 10.1061/(ASCE)0733-9437(1996)122:6(361).
- Mollnau, C., Newton, M. and Stringham, T. (2014) 'Soil water dynamics and water use

- in a western juniper (*Juniperus occidentalis*) woodland', *Journal of Arid Environments*. Elsevier Ltd, 102, pp. 117–126. doi: 10.1016/j.jaridenv.2013.11.015.
- Müller, J. and Bolte, A. (2009) 'The use of lysimeters in forest hydrology research in north-east Germany', *Landbauforschung Volkenrode*, 59(1), pp. 1–10.
- Nelson, C. R., Halpern, C. B. and Agee, J. K. (2008) 'Thinning and burning result in low-level invasion by nonnative plants but neutral effects on natives', *Ecological Applications*, 18(3), pp. 762–770. doi: 10.1890/07-0474.1.
- Norris, R. F. and Bukovak, M. J. (1968) 'Structure of the Pear Leaf Cuticle with Special Reference to Cuticular Penetration', *American Journal of Botany*, 55(8), pp. 975–983.
- O'Hara, K. L. *et al.* (2017) 'Regeneration Dynamics of coast redwood, a sprouting conifer species: A review with implications for management and restoration', *Forests*, 8(5), pp. 1–19. doi: 10.3390/f8050144.
- O'Hara, K. L., Stancioiu, P. T. and Spencer, M. A. (2007) 'Understory stump sprout development under variable canopy density and leaf area in coast redwood', *Forest Ecology and Management*, 244(1–3), pp. 76–85. doi: 10.1016/j.foreco.2007.03.062.
- Olson Jr., D. F., Roy, D. F. and Walters, G. A. (1990) 'Sequoia sempervirens (D. Don) Endl.', *Silvics of North America*, 1, Conifer, pp. 541–551. Available at: [http://www.na.fs.fed.us/spfo/pubs/silvics\\_manual/Volume\\_1/sequoia/sempervirens.htm](http://www.na.fs.fed.us/spfo/pubs/silvics_manual/Volume_1/sequoia/sempervirens.htm).
- Oren, R. *et al.* (1998) 'Scaling xylem sap flux and soil water balance and calculating variance: A method for partitioning water flux in forests', *Annales des Sciences Forestieres*, 55(1–2), pp. 191–216. doi: 10.1051/forest:19980112.
- Parent, A. C. and Anctil, F. (2012) 'Quantifying evapotranspiration of a rainfed potato crop in South-eastern Canada using eddy covariance techniques', *Agricultural Water Management*, 113, pp. 45–56. doi: 10.1016/j.agwat.2012.06.014.
- Politi, N., Hunter, M. and Rivera, L. (2012) 'Assessing the effects of selective logging on birds in Neotropical piedmont and cloud montane forests', *Biodiversity and Conservation*, 21(12), pp. 3131–3155. doi: 10.1007/s10531-012-0358-3.
- Ponton, S. *et al.* (2006) 'Comparison of ecosystem water-use efficiency among Douglas-fir forest, aspen forest and grassland using eddy covariance and carbon isotope techniques', *Global Change Biology*, 12(2), pp. 294–310. doi: 10.1111/j.1365-2486.2005.01103.x.
- Price, K. *et al.* (2011) 'Effects of watershed land use and geomorphology on stream low flows during severe drought conditions in the southern Blue Ridge Mountains, Georgia and North Carolina, United States', *Water Resources Research*, 47(2). doi: 10.1029/2010WR009340.
- Quero, J. L. *et al.* (2011) 'Water-use strategies of six co-existing Mediterranean woody species during a summer drought', *Oecologia*, 166, pp. 45–57. doi: 10.1007/s00442-011-1922-3.
- Ramage, B. S., O'Hara, K. L. and Caldwell, B. T. (2010) 'The role of fire in the competitive dynamics of coast redwood forests', *Ecosphere*, 1(6). doi: 10.1890/ES10-00134.1.

- Ranger, J., Marques, R. and Jussy, J. H. (2001) 'Forest soil dynamics during stand development assessed by lysimeter and centrifuge solutions', *Forest Ecology and Management*, 144(1–3), pp. 129–145. doi: 10.1016/S0378-1127(00)00366-2.
- Reichstein, M. *et al.* (2013) 'Climate extremes and the carbon cycle', *Nature*. Nature Publishing Group, 500(7462), pp. 287–295. doi: 10.1038/nature12350.
- Reicosky, D. C. *et al.* (1983) 'Comparison of Alfalfa Evapotranspiration Measured by a Weighing Lysimeter and a Portable Chamber', *Agricultural Meteorology*, 28, pp. 205–211.
- Reicosky, D. C. and Peters, D. B. (1977) 'A Portable Chamber for Rapid Evapotranspiration Measurements on Field Plots', *Agronomy*, 69(4), pp. 729–732. doi: 10.2134/agronj1977.00021962006900040051x.
- Rice, R. M., Tilley, F. B. and Datzman, P. A. (1979) 'A watershed's response to logging and roads: South Fork of Caspar Creek, California, 1967-1976', *USDA Forest Service, Pacific Southwest Forest and Range Experiment Station, Berkeley, CA*, Research P.
- Riegel, G. M., Miller, R. F. and Krueger, W. C. (1992) 'Competition for Resources Between Understory Vegetation and Overstory Pinus Ponderosa in Northeastern Oregon', *Ecological Applications*, 2(1), pp. 71–85.
- Saigusa, N. *et al.* (2002) 'Gross primary production and net ecosystem exchange of a cool-temperate deciduous forest estimated by the eddy covariance method', *Agricultural and Forest Meteorology*, 112(3–4), pp. 203–215. doi: 10.1016/S0168-1923(02)00082-5.
- Schönherr, J. and Schmidt, H. W. (1979) 'Water permeability of plant cuticles', *Planta*, 144(4), pp. 391–400. doi: 10.1007/bf00391583.
- Schulze, E. D. *et al.* (1973) 'Stomatal responses to changes in temperature at increasing water stress', *Planta*, 110(1), pp. 29–42. doi: 10.1007/BF00386920.
- Scott, F. M. (1966) 'Cell wall surface of the higher plants', *Nature*, 210(5040), pp. 1015–1017. doi: 10.1038/2101015a0.
- Scott, R. L. (2010) 'Using watershed water balance to evaluate the accuracy of eddy covariance evaporation measurements for three semiarid ecosystems', *Agricultural and Forest Meteorology*, 150(2), pp. 219–225. doi: 10.1016/j.agrformet.2009.11.002.
- Shannon, C. E. and Weaver, W. (1949) *The Mathematical Theory of Communication*. Urbana, Illinois: University of Illinois Press.
- Simonin, K. A., Santiago, L. S. and Dawson, T. E. (2009) 'Fog interception by *Sequoia sempervirens* (D. Don) crowns decouples physiology from soil water deficit', *Plant, Cell and Environment*, 32(7), pp. 882–892. doi: 10.1111/j.1365-3040.2009.01967.x.
- Slavik, B. (1974) 'Methods of Studying Plant Water Relations', *Ecological Studies: Analysis and Synthesis*. Edited by J. Jacobs and J. S. Olson, 9.
- Smakhtin, V. U. (2001) 'Low Flow Hydrology: a Review', *Journal of Hydrology*, 240, pp. 147–186. doi: 10.1016/S0022-1694(00)00340-1.
- Stannard, D. I. (1988) *Use of a Hemispherical Chamber for Measurement of Evapotranspiration, U.S. Geological Survey Open-File Report*. doi:

10.1016/j.agwat.2003.12.006.

Stannard, D. I. and Wertz, M. A. (2006) 'Partitioning evapotranspiration in sparsely vegetated rangeland using a portable chamber', *Water Resources Research*, 42(2), pp. 1–13. doi: 10.1029/2005WR004251.

Starr, M. R. (1985) 'Variation in the quality of tension lysimeter soil water samples from a Finnish forest soil', *Soil Science*, 140(6), pp. 453–461.

Stednick, J. D. (1996) 'Monitoring the effects of timber harvest on annual water yield', *Journal of Hydrology*, 176, pp. 79–95.

Stone, E. C., Grah, R. F. and Zinke, P. J. (1969) *An Analysis of the Buffers and the Watershed Management Required to Preserve the Redwood Forest and Associated Streams in the Redwood National Park*.

Stone, W. E. and Wolfe, M. L. (1996) 'Response of understory vegetation to variable tree mortality following a mountain pine beetle epidemic in lodgepole pine stands in northern Utah', *Vegetatio*, 122, pp. 1–12. doi: 10.1152/ajpregu.00519.2002.

Sucoff, E. and Hong, S. G. (1974) 'Effects of Thinning on Needle Water Potential in Red Pine', *Forest Science*, 20(1), pp. 25–29. Available at: <https://doi.org/10.1093/forestscience/20.1.25>.

Surfleet, C. G. and Skaugset, A. E. (2013) 'The effect of timber harvest on summer low flows, hinkle creek, oregon', *Western Journal of Applied Forestry*, 28(1), pp. 13–21. doi: 10.5849/wjaf.11-038.

Sutherland, S. and Nelson, C. R. (2010) 'Nonnative plant response to silvicultural treatments: A model based on disturbance, propagule pressure, and competitive abilities', *Western Journal of Applied Forestry*, 25(1), pp. 27–33. doi: 10.1093/wjaf/25.1.27.

Taiz, L. and Zeiger, E. (2002) *Plant Physiology*. 3rd edn. Sinauer Associates. doi: 10.1093/aob/mcg079.

Del Tredici, P. (1998) 'Lignotubers in *Sequoia sempervirens*: development and ecological significance', *Madroña*, 45(3), pp. 255–260.

Tromp-van Meerveld, H. J. and McDonnell, J. J. (2006) 'On the interrelations between topography, soil depth, soil moisture, transpiration rates and species distribution at the hillslope scale', *Advances in Water Resources*, 29(2), pp. 293–310. doi: 10.1016/j.advwatres.2005.02.016.

Tukey, J. W. (1949) 'Comparing Individual Means in the Analysis of Variance', *Biometrics*, 5(2), pp. 99–114.

Ünlü, M., Kanber, R. and Kapur, B. (2010) 'Comparison of soybean evapotranspirations measured by weighing lysimeter and Bowen ratio-energy balance methods', *African Journal of Biotechnology*, 9(30), pp. 4700–4713. doi: 10.5897/AJB10.621.

Vertessy, R. A., Watson, F. G. R. and O'Sullivan, S. K. (2001) 'Factors determining relations between stand age and catchment water balance in mountain ash forests', *Forest Ecology and Management*, 143(1–3), pp. 13–26. doi: 10.1016/S0378-1127(00)00501-6.

Vincke, C. *et al.* (2005) 'Evapotranspiration of a Declining *Quercus robur* (L.) Stand

from 199 to 2001. Trees and Forest Floor Daily Transpiration', *Annals of Forest Science*, 62, pp. 503–512. doi: 10.1051/forest.

Wang, J. *et al.* (2018) 'Assessing the performance of two models on calculating maize actual evapotranspiration in a semi-humid and drought-prone region of China', *Theoretical and Applied Climatology*. *Theoretical and Applied Climatology*, 131(3–4), pp. 1147–1156. doi: 10.1007/s00704-016-2032-2.

Wegehenkel, M. and Gerke, H. H. (2013) 'Comparison of real evapotranspiration measured by weighing lysimeters with simulations based on the Penman formula and a crop growth model', *Journal of Hydrology and Hydromechanics*, 61(2), pp. 161–172. doi: 10.2478/johh-2013-0021.

Wilson, K. B. *et al.* (2001) 'A comparison of methods for determining forest evapotranspiration and its components: Sap-flow, soil water budget, eddy covariance and catchment water balance', *Agricultural and Forest Meteorology*, 106(2), pp. 153–168. doi: 10.1016/S0168-1923(00)00199-4.

Yanai, R. D., Twery, M. J. and Stout, S. L. (1998) 'Woody understory response to changes in overstory density: Thinning in Allegheny hardwoods', *Forest Ecology and Management*, 102(1), pp. 45–60. doi: 10.1016/S0378-1127(97)00117-5.

Yang, P. *et al.* (2016) 'Crop coefficient for cotton under plastic mulch and drip irrigation based on eddy covariance observation in an arid area of northwestern China', *Agricultural Water Management*. Elsevier B.V., 171, pp. 21–30. doi: 10.1016/j.agwat.2016.03.007.

Yeager, L. E. and Riordan, L. E. (1953) 'Effects of Beetle-Killed Timber on Range and Wildlife in Colorado', in *North American Wildlife & Natural Resources Conference*, pp. 596–616.

Zenner, E. K. *et al.* (2006) 'Responses of ground flora to a gradient of harvest intensity in the Missouri Ozarks', *Forest Ecology and Management*, 222(1–3), pp. 326–334. doi: 10.1016/j.foreco.2005.10.027.

Van Zyl, W. H. and De Jager, J. M. (1987) 'Accuracy of the Penman-Monteith equation adjusted for atmospheric stability', *Agricultural and Forest Meteorology*, 41, pp. 57–64.

## APPENDIX A: COMMON AND SCIENTIFIC SPECIES NAMES

### Herbs and Ferns

Common Name	Scientific Name
Northern maidenhair fern	<i>Adiantum aleuticum</i>
Western wild ginger	<i>Asarum caudatum</i>
Common lady fern	<i>Athyrium filix-femina</i>
Great horsetail	<i>Equisetum telmateia</i>
California honeysuckle	<i>Lonicera hispidula</i>
False solomon's seal	<i>Maianthemum racemosum</i>
Redwood sorrel	<i>Oxalis oregana</i>
Western sword fern	<i>Polystichum munitum</i>
Deer fern	<i>Struthiopteris spicant</i>
Pacific trillium	<i>Trillium ovatum</i>
Redwood violet	<i>Viola sempervirens</i>

### Trees and Shrubs

Common Name	Scientific Name
Grand fir	<i>Abies grandis</i>
Salal	<i>Gaultheria shallon</i>
Tanoak	<i>Notholithocarpus (formerly Lithocarpus) densiflorus</i>
Douglas fir	<i>Pseudotsuga menziesii</i>
Pacific rhododendron	<i>Rhododendron macrophyllum</i>
Trailing blackberry	<i>Rubus ursinus</i>
Coast redwood	<i>Sequoia sempervirens</i>
Western hemlock	<i>Tsuga heterophylla</i>
Evergreen huckleberry	<i>Vaccinium ovatum</i>



## APPENDIX B: SUPPLEMENTAL TABLES

**Table A1.** Tukey Comparison of Means for Plot Richness by Watershed

<b>comparison</b>	<b>estimate</b>	<b>lower</b>	<b>upper</b>	<b>p-value</b>
<b>UQL-TRE</b>	1.8	-0.7589739	4.35897392	0.22441343
<b>WIL-TRE</b>	-1.8	-4.3589739	0.75897392	0.22441343
<b>ZIE-TRE</b>	-0.8	-3.3589739	1.75897392	0.807826873
<b>WIL-UQL</b>	-3.6	-6.1589739	-1.04102608	0.004869428
<b>ZIE-UQL</b>	-2.6	-5.1589739	-0.04102608	0.045779412
<b>ZIE-WIL</b>	1	-1.5589739	3.55897392	0.684062286

**Table A2.** Tukey Comparison of Means for  $\log_{10}$ ET by Watershed

Tukey HSD confidence intervals and p-values are shown for the analysis of variance test comparing  $\log_{10}$  transformed ET rate across watersheds.

<b>Interaction</b>	<b>estimate</b>	<b>Lower</b>	<b>Upper</b>	<b>p-value</b>
<b>UQL-TRE</b>	0.08424616	-0.03079208	0.19928440	0.6066685
<b>WIL-TRE</b>	0.05207939	-0.07009963	0.17425841	0.9995454
<b>ZIE-TRE</b>	0.42682253	0.30945332	0.54419173	4.603e-11
<b>WIL-UQL</b>	-0.03216677	-0.14470138	0.08036783	0.5634177
<b>ZIE-UQL</b>	0.34257636	0.23528305	0.44986968	2.882e-09
<b>ZIE-WIL</b>	0.37474314	0.25982677	0.48965950	4.355e-11

**Table A3.** Tukey Comparison of Means for log<sub>10</sub>ET vs. Harvesting Intensity

Tukey HSD confidence intervals and p-values are shown for the analysis of variance test comparing log<sub>10</sub> transformed ET rate to harvesting intensity

<b>Interaction</b>	<b>estimate</b>	<b>Lower</b>	<b>Upper</b>	<b>p-value</b>
<b>Moderate:Low</b>	0.06698154	-0.07160461	0.2055677	0.5952713
<b>Moderate-High: Low</b>	0.16147774	0.04512634	0.2778291	0.0022560
<b>High:Low</b>	0.45363270	0.33550005	0.5717654	0.0000000
<b>Moderate-High: Moderate</b>	0.09449620	-0.05226959	0.2412620	0.3440384
<b>High:Moderate</b>	0.38665117	0.23846927	0.5348331	0.0000000
<b>High: Moderate-High</b>	0.29215496	0.16452502	0.4197849	0.0000001

**Table A4.** Confidence Intervals and p-values for Tukey HSD test of ET rate by topographic positions 1 (riparian zone), 2 (toeslope), 3 (sideslope), 4 (shoulder), and 5 (summit).

<b>Interaction</b>	<b>estimate</b>	<b>Lower</b>	<b>Upper</b>	<b>p-value</b>
<b>2-1</b>	0.16986468	-0.0070104	0.34673979	0.06649061
<b>3-1</b>	0.23095733	0.06140234	0.40051233	0.00210431
<b>4-1</b>	0.22118065	0.04912594	0.39323537	0.00445488
<b>5-1</b>	0.1608715	-0.0170839	0.33882694	0.09747635
<b>3-2</b>	0.06109265	-0.1133518	0.23553713	0.87147162
<b>4-2</b>	0.05131597	-0.1255591	0.22819108	0.9310879
<b>5-2</b>	-0.0089932	-0.1916133	0.17362697	0.99992388
<b>4-3</b>	-0.0097767	-0.1793317	0.15977832	0.99985738
<b>5-3</b>	-0.0700858	-0.2456256	0.10545394	0.80760946
<b>5-4</b>	-0.0603092	-0.2382646	0.11764629	0.8843214

**Table A5.** Confidence Intervals and p-values for Tukey HSD test of log10 transformed ET rate by topographic positions 1 (riparian zone), 2 (toeslope), 3 (sideslope), 4 (shoulder), and 5 (summit) within Ziemer watershed.

<b>Interaction</b>	<b>estimate</b>	<b>Lower</b>	<b>Upper</b>	<b>p-value</b>
2-1	0.23141239	-0.0943008	0.55712562	0.27941498
3-1	0.65184365	0.36253383	0.94115347	3.29E-07
4-1	0.55419355	0.26956484	0.83882225	8.78E-06
5-1	0.24701729	-0.0422925	0.53632711	0.12905641
3-2	0.42043126	0.09951211	0.74135042	0.00434529
4-2	0.32278116	0.00607557	0.63948675	0.04367672
5-2	0.0156049	-0.3053142	0.33652405	0.99991887
4-3	-0.0976501	-0.37678	0.18147978	0.8614984
5-3	-0.4048264	-0.688728	-0.1209247	0.00154794
5-4	-0.3071763	-0.5863061	-0.0280464	0.02401285

**Table A6.** Confidence Intervals and p-values for Tukey HSD test of log10 transformed ET rate by topographic positions 1 (riparian zone), 2 (toeslope), 3 (sideslope), 4 (shoulder), and 5 (summit) within Williams watershed.

<b>Interaction</b>	<b>estimate</b>	<b>Lower</b>	<b>Upper</b>	<b>p-value</b>
2-1	0.12544021	-0.1022848	0.35316523	0.52686672
3-1	-0.1191289	-0.3338831	0.09562533	0.51997568
4-1	-0.3176763	-0.5383618	-0.0969909	0.00157871
5-1	-0.1623284	-0.4224087	0.09775191	0.40129041
3-2	-0.2445691	-0.4841375	-0.0050007	0.04330266
4-2	-0.4431165	-0.6880159	-0.1982172	5.45E-05
5-2	-0.2877686	-0.5686874	-0.0068498	0.04225798
4-3	-0.1985474	-0.4314345	0.03433965	0.12795995
5-3	-0.0431995	-0.3137103	0.2273113	0.99095417
5-4	0.15534795	-0.1198952	0.43059106	0.50286836

**Table A7.** Confidence Intervals and p-values for Tukey HSD test of log10 transformed ET rate by topographic positions 1 (riparian zone), 2 (toeslope), 3 (sideslope), 4 (shoulder), and 5 (summit) within Treat watershed.

<b>Interaction</b>	<b>estimate</b>	<b>Lower</b>	<b>Upper</b>	<b>p-value</b>
2-1	0.36050545	0.07859156	0.64241934	0.00588474
3-1	0.31678891	0.02979508	0.60378274	0.02363139
4-1	0.23224607	-0.0496678	0.51415996	0.15252806
5-1	0.34823264	0.07449191	0.62197337	0.00622019
3-2	-0.0437165	-0.301535	0.21410194	0.98893572
4-2	-0.1282594	-0.3804108	0.12389207	0.60684229
5-2	-0.0122728	-0.255252	0.23070641	0.99990335
4-3	-0.0845428	-0.3423613	0.17327564	0.88529044
5-3	0.03144373	-0.2174115	0.28029894	0.99641213
5-4	0.11598657	-0.1269926	0.35896578	0.66234948

**Table A8.** Confidence Intervals and p-values for Tukey HSD test of log10 transformed ET rate by topographic positions 1 (riparian zone), 2 (toeslope), 3 (sideslope), 4 (shoulder), and 5 (summit) within Uqlidisi watershed.

<b>Interaction</b>	<b>estimate</b>	<b>Lower</b>	<b>Upper</b>	<b>p-value</b>
2-1	0.12598637	-0.0848298	0.33680254	0.45337341
3-1	0.11169728	-0.0924246	0.31581916	0.54174126
4-1	0.33968142	0.12025699	0.55910584	0.0004935
5-1	0.17595176	-0.0623524	0.4142559	0.24366219
3-2	-0.0142891	-0.218411	0.18983279	0.99965496
4-2	0.21369505	-0.0057294	0.43311948	0.05987246
5-2	0.04996539	-0.1883387	0.28826953	0.97612225
4-3	0.22798414	0.01498328	0.44098499	0.03011361
5-3	0.06425448	-0.1681485	0.29665746	0.936108
5-4	-0.1637297	-0.4096819	0.08222254	0.3432669

**Table A9.** Effect sizes of all possible predictor variables on sprout ET rate across watersheds

<b>Variable</b>	<b>SSR</b>	<b>df</b>	<b>pEta.sqr</b>	<b>dR.sqr</b>	<b>SSE</b>	<b>SST</b>
<b>(Intercept)</b>	2.18E+05	1	7.47E-01	NA	7.39E+04	3.16E+05
<b>as.factor(SP)</b>	2.30E+03	2	3.02E-02	7.29E-03	7.39E+04	3.16E+05
<b>scale(VWC)</b>	3.76E+03	1	4.85E-02	1.19E-02	7.39E+04	3.16E+05
<b>scale(EL)</b>	2.14E+02	1	2.89E-03	6.78E-04	7.39E+04	3.16E+05
<b>scale(PH)</b>	4.74E+01	1	6.42E-04	1.50E-04	7.39E+04	3.16E+05
<b>scale(BA)</b>	1.87E+02	1	2.52E-03	5.91E-04	7.39E+04	3.16E+05
<b>scale(T)</b>	5.09E+04	1	4.08E-01	1.61E-01	7.39E+04	3.16E+05
<b>scale(LI)</b>	1.52E+04	1	1.70E-01	4.81E-02	7.39E+04	3.16E+05
<b>scale(LA)</b>	2.56E+04	1	2.57E-01	8.10E-02	7.39E+04	3.16E+05

**Table A10.** Results of Best Fit Model for Predicting Sprout ET Rate across Watersheds

<b>Term</b>	<b>Estimate</b>	<b>Std error</b>	<b>T value</b>	<b>P value</b>
<b>Intercept - VAOV</b>	-7.13E+01	8.84E+00	-8.06E+00	3.21E-13
<b>Intercept - SESE</b>	-7.07E+00	5.12E+00	-1.38E+00	1.69E-01
<b>Intercept - LIDE</b>	-8.01E+00	4.53E+00	-1.77E+00	7.90E-02
<b>T</b>	3.98E+00	3.56E-01	1.12E+01	3.74E-21
<b>LI</b>	9.24E-04	1.64E-04	5.62E+00	9.84E-08
<b>VWC</b>	8.51E-01	3.12E-01	2.73E+00	7.14E-03
<b>LA</b>	6.92E-03	9.05E-04	7.65E+00	3.04E-12

Multiple R-squared: 0.7647                                  Adjusted R-squared: 0.7545  
 F-statistic: 75.29 on 6 and 139 DF                                  p-value: < 2.2e-16

Residual standard error: 23.12 on 139 degrees of freedom

**Table A11.** Effect sizes of predictor variables in Model 2 on sprout ET rate at WIL

<b>Variable</b>	<b>SSR</b>	<b>df</b>	<b>pEta.sqr</b>	<b>dR.sqr</b>	<b>SSE</b>	<b>SST</b>
<b>(Intercept)</b>	1.22E+04	1	8.46E-01	NA	2.21E+03	7.67E+03
<b>as.factor(SP)</b>	1.03E+01	1	4.64E-03	1.34E-03	2.21E+03	7.67E+03
<b>scale(LI)</b>	3.49E+01	1	1.55E-02	4.55E-03	2.21E+03	7.67E+03
<b>scale(VWC)</b>	2.03E+02	1	8.40E-02	2.64E-02	2.21E+03	7.67E+03
<b>scale(T)</b>	3.80E+03	1	6.32E-01	4.95E-01	2.21E+03	7.67E+03
<b>scale(LA)</b>	6.06E+01	1	2.67E-02	7.90E-03	2.21E+03	7.67E+03

**Table A12.** Effect sizes of predictor variables in Model 2 on sprout ET rate at TRE

<b>Variable</b>	<b>SSR</b>	<b>df</b>	<b>pEta.sqr</b>	<b>dR.sqr</b>	<b>SSE</b>	<b>SST</b>
<b>(Intercept)</b>	1.24E+04	1	7.90E-01	<i>NA</i>	3.29E+03	9.70E+03
<b>as.factor(SP)</b>	2.52E+02	2	7.12E-02	2.60E-02	3.29E+03	9.70E+03
<b>scale(LI)</b>	2.56E+03	1	4.38E-01	2.64E-01	3.29E+03	9.70E+03
<b>scale(VWC)</b>	1.21E+01	1	3.66E-03	1.25E-03	3.29E+03	9.70E+03
<b>scale(T)</b>	1.25E+01	1	3.78E-03	1.29E-03	3.29E+03	9.70E+03
<b>scale(LA)</b>	8.88E-02	1	2.70E-05	9.15E-06	3.29E+03	9.70E+03

**Table A13.** Effect sizes of predictor variables in Model 2 on sprout ET rate at UQL.

<b>Variable</b>	<b>SSR</b>	<b>df</b>	<b>pEta.sqr</b>	<b>dR.sqr</b>	<b>SSE</b>	<b>SST</b>
<b>(Intercept)</b>	2.23E+04	1	7.72E-01	<i>NA</i>	6.59E+03	1.36E+04
<b>as.factor(SP)</b>	1.06E+03	2	1.39E-01	7.80E-02	6.59E+03	1.36E+04
<b>scale(LI)</b>	2.67E+03	1	2.89E-01	1.97E-01	6.59E+03	1.36E+04
<b>scale(VWC)</b>	6.21E+02	1	8.61E-02	4.57E-02	6.59E+03	1.36E+04
<b>scale(T)</b>	7.42E+02	1	1.01E-01	5.46E-02	6.59E+03	1.36E+04
<b>scale(LA)</b>	6.67E+02	1	9.19E-02	4.91E-02	6.59E+03	1.36E+04

**Table A14.** Effect sizes of predictor variables in Model 2 on sprout ET rate at ZIE.

<b>Variable</b>	<b>SSR</b>	<b>df</b>	<b>pEta.sqr</b>	<b>dR.sqr</b>	<b>SSE</b>	<b>SST</b>
<b>(Intercept)</b>	2.04E+05	1	8.18E-01	<i>NA</i>	4.53E+04	1.50E+05
<b>as.factor(SP)</b>	3.74E+03	2	7.64E-02	2.49E-02	4.53E+04	1.50E+05
<b>scale(LI)</b>	4.87E+03	1	9.72E-02	3.25E-02	4.53E+04	1.50E+05
<b>scale(VWC)</b>	2.17E+01	1	4.79E-04	1.44E-04	4.53E+04	1.50E+05
<b>scale(T)</b>	2.60E+04	1	3.65E-01	1.73E-01	4.53E+04	1.50E+05
<b>scale(LA)</b>	2.10E+04	1	3.17E-01	1.40E-01	4.53E+04	1.50E+05

**Table A15.** Effect sizes of all possible predictor variables on sprout ET rate at WIL.

Variable	SSR	df	pEta.sqr	dR.sqr	SSE	SST
<b>(Intercept)</b>	1.13E+04	1	8.49E-01	<i>NA</i>	2.00E+03	7.67E+03
<b>as.factor(SP)</b>	4.51E+00	1	2.26E-03	5.88E-04	2.00E+03	7.67E+03
<b>scale(EL)</b>	2.53E+00	1	1.27E-03	3.29E-04	2.00E+03	7.67E+03
<b>scale(BA)</b>	1.83E+02	1	8.39E-02	2.38E-02	2.00E+03	7.67E+03
<b>scale(T)</b>	2.38E+03	1	5.43E-01	3.10E-01	2.00E+03	7.67E+03
<b>scale(LI)</b>	1.73E+01	1	8.59E-03	2.25E-03	2.00E+03	7.67E+03
<b>scale(VWC)</b>	3.06E+01	1	1.51E-02	3.98E-03	2.00E+03	7.67E+03
<b>scale(LA)</b>	5.35E+01	1	2.61E-02	6.97E-03	2.00E+03	7.67E+03

**Table A16.** Results of Best Fit Model for Sprout ET Rate at WIL

Term	Estimate	Std error	T value	P value
<b>(Intercept)</b>	-4.34E+01	8.54E+00	-5.08E+00	1.88E-05
<b>T</b>	3.90E+00	4.44E-01	8.79E+00	8.44E-10
<b>BA</b>	-4.47E-01	1.77E-01	-2.53E+00	1.70E-02

Multiple R-squared: 0.7203  
Adjusted R-squared: 0.7017  
F-statistic: 38.63 on 2 and 30 DF  
p-value: 5.013e-09

Residual standard error: 8.459 on 30 degrees of freedom

**Table A17.** Effect sizes of all possible predictor variables on sprout ET rate at TRE.

Variable	SSR	df	pEta.sqr	dR.sqr	SSE	SST
<b>(Intercept)</b>	1.09E+04	1	8.15E-01	<i>NA</i>	2.46E+03	9.70E+03
<b>as.factor(SP)</b>	1.04E+02	2	4.06E-02	1.07E-02	2.46E+03	9.70E+03
<b>scale(VWC)</b>	6.47E+01	1	2.56E-02	6.67E-03	2.46E+03	9.70E+03
<b>scale(EL)</b>	7.50E+02	1	2.34E-01	7.73E-02	2.46E+03	9.70E+03
<b>scale(BA)</b>	1.65E+02	1	6.28E-02	1.70E-02	2.46E+03	9.70E+03
<b>scale(T)</b>	8.37E+00	1	3.39E-03	8.63E-04	2.46E+03	9.70E+03
<b>scale(LI)</b>	3.09E+03	1	5.57E-01	3.19E-01	2.46E+03	9.70E+03
<b>scale(LA)</b>	2.75E+01	1	1.10E-02	2.83E-03	2.46E+03	9.70E+03

**Table A18.** Results of Best Fit Model for Sprout ET Rate at TRE

<b>Term</b>	<b>Estimate</b>	<b>Std error</b>	<b>T value</b>	<b>P value</b>
<b>(Intercept)</b>	7.90E+01	2.42E+01	3.26E+00	3.20E-03
<b>LI</b>	2.10E-03	2.73E-04	7.68E+00	4.95E-08
<b>EL</b>	-3.92E-01	1.47E-01	-2.67E+00	1.32E-02
<b>BA</b>	-1.65E+00	1.22E+00	-1.35E+00	1.88E-01
Multiple R-squared: 0.7171			Adjusted R-squared: 0.6832	
F-statistic: 21.12 on 3 and 25 DF			p-value: 4.93e-07	
Residual standard error: 10.48 on 25 degrees of freedom				

**Table A19.** Effect sizes of all possible predictor variables on sprout ET rate at UQL.

<b>Variable</b>	<b>SSR</b>	<b>df</b>	<b>pEta.sqr</b>	<b>dR.sqr</b>	<b>SSE</b>	<b>SST</b>
<b>(Intercept)</b>	2.14E+04	1	7.77E-01	<i>NA</i>	6.13E+03	1.36E+04
<b>as.factor(SP)</b>	3.05E+02	2	4.74E-02	2.24E-02	6.13E+03	1.36E+04
<b>scale(VWC)</b>	1.69E+02	1	2.68E-02	1.24E-02	6.13E+03	1.36E+04
<b>scale(EL)</b>	1.55E+02	1	2.47E-02	1.14E-02	6.13E+03	1.36E+04
<b>scale(BA)</b>	5.18E+01	1	8.38E-03	3.81E-03	6.13E+03	1.36E+04
<b>scale(T)</b>	2.98E+02	1	4.64E-02	2.19E-02	6.13E+03	1.36E+04
<b>scale(LI)</b>	1.57E+03	1	2.04E-01	1.16E-01	6.13E+03	1.36E+04
<b>scale(LA)</b>	1.37E+02	1	2.18E-02	1.01E-02	6.13E+03	1.36E+04

**Table A20.** Results of Best Fit Model for Sprout ET Rate at UQL

<b>Term</b>	<b>Estimate</b>	<b>Std error</b>	<b>T value</b>	<b>P value</b>
<b>(Intercept)</b>	-8.66E+01	1.93E+01	-4.50E+00	7.60E-05
<b>log10(LI)</b>	2.68E+01	6.94E+00	3.87E+00	4.74E-04
<b>EL</b>	1.21E-01	8.38E-02	1.44E+00	1.58E-01
Multiple R-squared: 0.5806			Adjusted R-squared: 0.5559	
F-statistic: 23.53 on 2 and 34 DF			p-value: 3.848e-07	
Residual standard error: 12.95 on 34 degrees of freedom				



**Table A21.** Effect sizes of all possible predictor variables on sprout ET rate at ZIE.

Variable	SSR	df	pEta.sqr	dR.sqr	SSE	SST
<b>(Intercept)</b>	1.64E+05	1	7.85E-01	<i>NA</i>	4.50E+04	1.50E+05
<b>as.factor(SP)</b>	2.59E+03	2	5.45E-02	1.73E-02	4.50E+04	1.50E+05
<b>scale(EL)</b>	2.04E+01	1	4.54E-04	1.36E-04	4.50E+04	1.50E+05
<b>scale(BA)</b>	5.48E+01	1	1.22E-03	3.65E-04	4.50E+04	1.50E+05
<b>scale(T)</b>	2.06E+04	1	3.14E-01	1.37E-01	4.50E+04	1.50E+05
<b>scale(LI)</b>	5.10E+03	1	1.02E-01	3.39E-02	4.50E+04	1.50E+05
<b>scale(VWC)</b>	2.41E+01	1	5.37E-04	1.61E-04	4.50E+04	1.50E+05
<b>scale(LA)</b>	1.49E+04	1	2.49E-01	9.94E-02	4.50E+04	1.50E+05

**Table A22.** Results of Best Fit Model for Sprout ET Rate at ZIE

Term	Estimate	Std error	T value	P value
<b>(Intercept)</b>	-9.99E+01	2.76E+01	-3.62E+00	7.66E-04
<b>LI</b>	7.43E-04	3.28E-04	2.26E+00	2.88E-02
<b>T</b>	5.56E+00	9.39E-01	5.92E+00	4.77E-07
<b>LA</b>	7.16E-03	1.37E-03	5.22E+00	4.95E-06

Multiple R-squared: 0.6735  
Adjusted R-squared: 0.6507  
F-statistic: 29.57 on 3 and 43 DF  
p-value: 1.561e-10

Residual standard error: 33.77 on 43 degrees of freedom

**Table A23.** Effect sizes of all possible predictor variables on fern ET rate across watersheds.

Variable	SSR	pEta.sqr	dR.sqr	SSE	SST
<b>(Intercept)</b>	1.91E+04	5.09E-01	<i>NA</i>	1.85E+04	9.37E+04
<b>as.factor(SP)</b>	7.64E+01	4.12E-03	8.15E-04	1.85E+04	9.37E+04
<b>scale(EL)</b>	6.64E+02	3.47E-02	7.08E-03	1.85E+04	9.37E+04
<b>scale(PH)</b>	1.70E+03	8.42E-02	1.81E-02	1.85E+04	9.37E+04
<b>scale(BA)</b>	2.13E+03	1.03E-01	2.27E-02	1.85E+04	9.37E+04
<b>scale(T)</b>	2.30E+04	5.54E-01	2.45E-01	1.85E+04	9.37E+04
<b>scale(LI)</b>	1.23E+04	3.99E-01	1.31E-01	1.85E+04	9.37E+04
<b>scale(VWC)</b>	9.51E+02	4.89E-02	1.01E-02	1.85E+04	9.37E+04
<b>scale(mass_g)</b>	1.15E+02	6.18E-03	1.23E-03	1.85E+04	9.37E+04

**Table A24.** Results of Best Fit Model for Predicting Fern ET Rate Across Watersheds

<b>Term</b>	<b>Estimate</b>	<b>Std error</b>	<b>T value</b>	<b>P value</b>
<b>(Intercept)</b>	-2.93E+01	8.32E+00	-3.51E+00	7.09E-04
<b>VWC</b>	4.38E-01	2.61E-01	1.68E+00	9.72E-02
<b>EL</b>	-1.06E-01	3.99E-02	-2.65E+00	9.65E-03
<b>BA</b>	-2.12E-01	1.28E-01	-1.65E+00	1.02E-01
<b>T</b>	3.35E+00	3.48E-01	9.61E+00	3.13E-15
<b>LI</b>	9.61E-04	1.35E-04	7.10E+00	3.52E-10
Multiple R-squared: 0.7842			Adjusted R-squared: 0.7716	
F-statistic: 61.79 on 5 and 85 DF			p-value: < 2.2e-16	
Residual standard error: 15.42 on 85 degrees of freedom				

**Table A25.** Effect sizes of all possible predictor variables on fern ET rate at WIL.

<b>Variable</b>	<b>SSR</b>	<b>pEta.sqr</b>	<b>dR.sqr</b>	<b>SSE</b>	<b>SST</b>
<b>(Intercept)</b>	2.59E+04	0.965636	<i>NA</i>	922.5198	7548.214
<b>scale(VWC)</b>	1.28E+01	0.01367	1.69E-03	922.5198	7548.214
<b>scale(EL)</b>	4.88E+00	0.005263	6.47E-04	922.5198	7548.214
<b>scale(BA)</b>	4.91E-01	0.000532	6.50E-05	922.5198	7548.214
<b>scale(T)</b>	1.75E+03	0.654341	2.31E-01	922.5198	7548.214
<b>scale(LI)</b>	5.26E+02	0.363038	6.97E-02	922.5198	7548.214
<b>scale(mass_g)</b>	1.49E+02	0.138829	1.97E-02	922.5198	7548.214

**Table A26.** Results of Best Fit Model for Predicting Fern ET Rate at WIL

<b>Term</b>	<b>Estimate</b>	<b>Std error</b>	<b>T value</b>	<b>P value</b>
<b>(Intercept)</b>	-6.84E+01	1.38E+01	-4.95E+00	2.65E-04
<b>T</b>	4.67E+00	5.13E-01	9.11E+00	5.25E-07
<b>LI</b>	7.14E-03	2.47E-03	2.89E+00	1.27E-02
<b>mass_g</b>	-3.30E-01	2.29E-01	-1.44E+00	1.74E-01
Multiple R-squared: 0.8742			Adjusted R-squared: 0.8452	
F-statistic: 30.12 on 3 and 13 DF			p-value: 4.028e-06	
Residual standard error: 8.546 on 13 degrees of freedom				

**Table A27.** Effect sizes of all possible predictor variables on fern ET rate at TRE.

<b>Variable</b>	<b>SSR</b>	<b>pEta.sqr</b>	<b>dR.sqr</b>	<b>SSE</b>	<b>SST</b>
<b>Intercept)</b>	29410.01	0.901257	<i>NA</i>	3222.19	23405.07
<b>scale(VWC)</b>	142.278	0.042288	0.006079	3222.19	23405.07
<b>scale(EL)</b>	643.5541	0.166476	0.027496	3222.19	23405.07
<b>scale(BA)</b>	851.4122	0.209007	0.036377	3222.19	23405.07
<b>scale(T)</b>	22.59082	0.006962	0.000965	3222.19	23405.07
<b>scale(LI)</b>	9399.039	0.744701	0.401581	3222.19	23405.07
<b>scale(mass_g)</b>	123.1372	0.036809	0.005261	3222.19	23405.07

**Table A28.** Results of Best Fit Model for Predicting Fern ET Rate at TRE

<b>Term</b>	<b>Estimate</b>	<b>Std error</b>	<b>T value</b>	<b>P value</b>
<b>(Intercept)</b>	9.21E+01	3.28E+01	2.81E+00	9.74E-03
<b>EL</b>	-4.15E-01	2.07E-01	-2.01E+00	5.61E-02
<b>BA</b>	-2.41E+00	1.04E+00	-2.31E+00	3.00E-02
<b>LI</b>	1.29E-03	1.18E-04	1.09E+01	8.42E-11
Multiple R-squared: 0.8459			Adjusted R-squared: 0.8267	
F-statistic: 43.93 on 3 and 24 DF			p-value: 6.671e-10	
Residual standard error: 12.26 on 24 degrees of freedom				

**Table A29.** Effect sizes of all possible predictor variables on fern ET rate at UQL.

<b>Variable</b>	<b>SSR</b>	<b>pEta.sqr</b>	<b>dR.sqr</b>	<b>SSE</b>	<b>SST</b>
<b>(Intercept)</b>	29921.83	0.916265	<i>NA</i>	2734.492	6361.556
<b>scale(VWC)</b>	1202.739	0.305478	0.189064	2734.492	6361.556
<b>scale(EL)</b>	1482.894	0.351614	0.233102	2734.492	6361.556
<b>scale(BA)</b>	60.96645	0.021809	0.009584	2734.492	6361.556
<b>scale(T)</b>	1079.886	0.283109	0.169752	2734.492	6361.556
<b>scale(LI)</b>	581.7484	0.175424	0.091447	2734.492	6361.556
<b>scale(mass_g)</b>	184.9179	0.063341	0.029068	2734.492	6361.556

**Table A30.** Results of Best Fit Model for Predicting Fern ET Rate at UQL

<b>Term</b>	<b>Estimate</b>	<b>Std error</b>	<b>T value</b>	<b>P value</b>
<b>(Intercept)</b>	2.75E+00	1.39E+01	1.98E-01	8.45E-01
<b>VWC</b>	1.54E+00	4.50E-01	3.42E+00	2.33E-03
<b>EL</b>	-2.45E-01	7.99E-02	-3.07E+00	5.42E-03
<b>T</b>	2.07E+00	6.62E-01	3.13E+00	4.74E-03
<b>LI</b>	6.55E-04	3.54E-04	1.85E+00	7.72E-02
Multiple R-squared: 0.5284			Adjusted R-squared: 0.4464	
F-statistic: 6.444 on 4 and 23 DF			p-value: 0.001246	
Residual standard error: 11.42 on 23 degrees of freedom				

**Table A31.** Effect sizes of all possible predictor variables on fern ET rate at ZIE.

<b>Variable</b>	<b>SSR</b>	<b>pEta.sqr</b>	<b>dR.sqr</b>	<b>SSE</b>	<b>SST</b>
<b>(Intercept)</b>	76650.98	0.97275	<i>NA</i>	2147.277	41805.22
<b>scale(VWC)</b>	13.0984	0.006063	0.000313	2147.277	41805.22
<b>scale(EL)</b>	2872.128	0.572205	0.068703	2147.277	41805.22
<b>scale(BA)</b>	1127.294	0.344257	0.026965	2147.277	41805.22
<b>scale(T)</b>	4458.216	0.674926	0.106643	2147.277	41805.22
<b>scale(LI)</b>	2654.054	0.552775	0.063486	2147.277	41805.22
<b>scale(mass_g)</b>	105.5664	0.046859	0.002525	2147.277	41805.22

**Table A32:** Results of Best Fit Model for Predicting Fern ET Rate at ZIE

<b>Term</b>	<b>Estimate</b>	<b>Std error</b>	<b>T value</b>	<b>P value</b>
<b>(Intercept)</b>	8.06E+01	4.04E+01	2.00E+00	6.72E-02
<b>EL</b>	-6.43E-01	1.61E-01	-3.98E+00	1.56E-03
<b>BA</b>	-4.46E-01	1.83E-01	-2.44E+00	2.98E-02
<b>T</b>	3.68E+00	6.79E-01	5.42E+00	1.17E-04
<b>LI</b>	1.60E-03	3.85E-04	4.16E+00	1.12E-03
Multiple R-squared: 0.9458			Adjusted R-squared: 0.9292	
F-statistic: 56.74 on 4 and 13 DF			p-value: 4.206e-08	
Residual standard error: 13.2 on 13 degrees of freedom				